TECHNISCHE UNIVERSITÄT MÜNCHEN
Lehrstuhl für Humanbiologie

High fat diet increases tumor incidence in the intestine due to alterations in microbial communities and immune system

Manon Dominique Schulz

Vollständiger Abdruck der von der Fakultät Wissenschaftszentrum Weihenstephan für Ernährung, Landnutzung und Umwelt der Technischen Universität München zur Erlangung des akademischen Grades eines

Doktors der Naturwissenschaften

genehmigte Dissertation.

Vorsitzender: Univ.-Prof. Dr. D. Haller

Prüfer der Dissertation:

1. Univ.-Prof. Dr. M. Schemann
2. Univ.-Prof. Dr. R. M. Schmid
3. Priv.-Doz. M. C. Arkan-Greten, Ph.D.

Die Dissertation wurde am 26.09.2012 bei der Technischen Universität München eingereicht und durch die Fakultät Wissenschaftszentrum Weihenstephan für Ernährung, Landnutzung und Umwelt am 10.09.2013 angenommen.

Table of Contents

1. Introduction

1.1. Epidemiology and aetiology of cancer

Although the knowledge on how to prevent and to treat cancer improved in the recent years, however the cancer-associated death continue to increase worldwide. In the European Union (EU) cancer incidence was increased by 12 % in men and 9 % in women between year 1985 and 2000 [1]. The reason might be that life expectancy has increased and people reach later ages than before. Compared to 2000, the expected number of people in world population over the age of 65 will increase by 22 %, over the age of 80 by 50 % until 2015 [2]. Therefore also the cancer associated deaths are estimated to reach 1.405.000 in 2015, while in 2000 1.122.000 were recorded [2]. Indeed, cancer is the most common leading cause of death affecting around 8 million individuals worldwide.

Colon cancer with 207.400 deaths in 2006 is the second most common cause of cancer-associated death in Europe [2] and represents the major type of cancer in the digestive system with an incidence of around 52 %. On the contrary the small intestinal cancer is quite rare with less than 3 % incidence [3]. 30 – 50 % of all small bowel tumors are defined as adenocarcinoma that are located most frequently in the duodenum [4]. The survival rate is quite poor with around 6 to 8 months due to difficulties in detection of the tumor by conventional methods [5].

Risk factors include chronic inflammatory bowel disease (IBD), Crohn´s disease, familial adenomatous polyposis (FAP) and Helicobacter pylori infection [6]. Importantly patients with colorectal cancer have an increased risk to develop small bowel adenoma or vice versa [7]. Another risk for small intestinal adenocarcinoma development appears to be diet rich in fat [8] [9]. Overweight, obesity or physical inactivity alone account for about 274.000 cancer associated deaths per year and for one third of cancers of the colon, breast, kidney and digestive tract (WHO). For colorectal cancer it has been shown in several studies that there is a risk in the range of more than 1 for overweight and obese individuals [10].

1.2. Inflammation and cancer

Inflammation is one of the hallmarks of cancer. About 15 % of the worldwide cancer cases are connected to inflammation [11]. There are two inflammatory pathways described to have an important role in cancer development. The extrinsic pathway, which leads to chronic inflammation, represents an increased cancer risk. On the other hand, the intrinsic pathway results in changes in the genome such as mutations in oncogenes or tumor suppressor, which are necessary to promote tumor development and maintain cancer progression [12].

One explanation how inflammation can increase cancer risk is through induction of oxidative/nitrosative stress the increased production of reactive species by inflammatory cells. Elevated stress can then induce DNA mutations in cells [13, 14]. Indeed free radicals not only damage DNA but also induce alterations that can disrupt processes like DNA repair, cell-cycle checkpoints and apoptosis [14].

Chronic inflammation is a major risk factor for cancer development especially in the intestine. In Europe, 2,2 million people are affected by IBD [15]. The most common types of IBD are Crohn´s Disease and Ulcerative Colitis. The main difference between these two forms of IBD is that Crohn´s disease can affect the whole gastrointestinal tract while ulcerative colitis is limited to the colonic mucosa. The exact mechanism how the disease develops is still not yet completely understood however decreased goblet cell numbers that are important for the mucin secretion that protect epithelial cells as well as inhibition of the function of Paneth cells, which also play a major role in protection of the intestine are suggested to play a significant role. Furthermore endoplasmatic reticulum (ER) stress is suggested to be linked to IBD. Indeed, IBD patients show an increase in members of the endoplasmatic reticulum (ER) stress-signaling pathway. Moreover, alterations in pattern recognition receptor (PRR) signaling, which is crucial for the recognition of pathogens, the imbalance in microbial communities and the activation of the immune system are suggested to be associated with disease development [16].

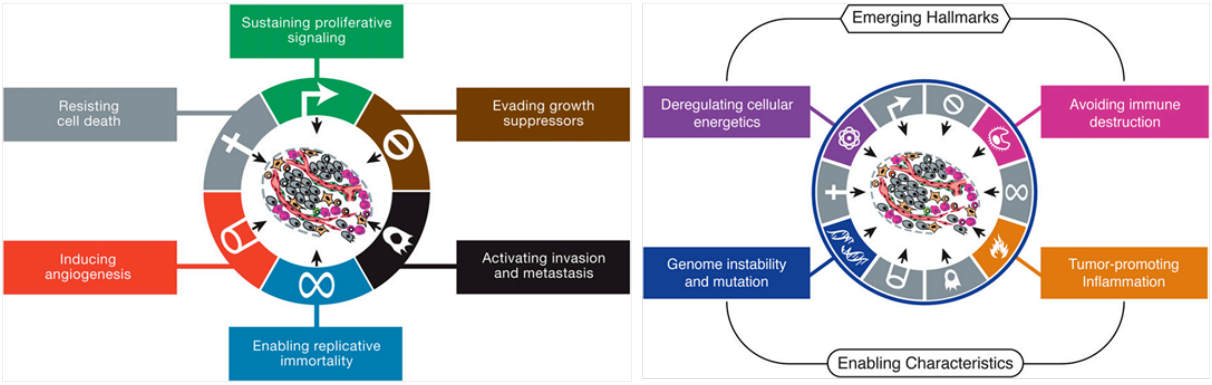

Figure 1.1: Hallmarks of cancer [17]

1.3. Obesity and influence of obesity on health and disease

1.3.1. Epidemiology of obesity and diabetes

The incidence of obesity increased dramatically worldwide in the last decades. Obesity is defined as excessive fat accumulation in the whole body and is defined with Body Mass Index (BMI) in kg/m^2, such that individuals with BMI ≥ 25 are defined as overweight and BMI ≥ 30 are obese. At present, approximately 1.6 billion adults are classified as overweight and at least 400 million as obese. The major reason for this dramatic increase in incidence is consumption of diet that is high in sugar and fat but low in vitamins, minerals and other micronutrients. On the other hand, there is a trend towards decreased physical activity due to sedentary life style such as working behavior, advancement in transport and increasing urbanisation.

It is well known that obese people are at a higher risk for developing many chronic illnesses such as diabetes, cardiovascular diseases and cancer. Indeed, 14 – 20 % of all cancers have been attributed to obesity and 35 % to diet [18]. There are several hypotheses on how obesity can promote tumor development such as decreased intake of vegetables and fruits that may play a protective role. Further during increased adiposity fat cells produce proteins like adiponectin, resistin and visfatin and importantly pro-inflammatory cytokines, such as tumor necrosis factor-α (TNF-α) and interleukin- (IL-) 6. In addition to cytokines especially adiponectin can protect cancer development because it inhibits several mitogenic growth factors and is found

to be decreased in obese individuals [19]. Another factor suggested is increased insulin levels due to elevated free insulin-like growth factors (IGF), which can induce cell proliferation [20].

The link between obesity induced insulin resistance (IR) and the development of diabetes is well known. At the present time more than 220 million people are affected by diabetes (WHO). Until 2030 the number of individuals with diabetes is estimated to reach 366 million. The prevalence of this disease is increased in elder people above the age of 64 [21]. The disease is predominantly found in the developed countries with the majority in U.S. and China and affects more women than men [22].

1.3.2. Type 2 Diabetes

Diabetes is a metabolic disease where the body either fails to produce enough insulin or is not responsive to it. Over 90 % of the diabetes patients have type 2 diabetes that arises from insulin resistance. Insulin resistance is a condition in which the cells are unable to respond to insulin properly resulting in a hyperinsulinemia often followed by a hyperglycemia.

Diabetes is defined by three pathophysiological key defects: increase of hepatic glucose production, reduced insulin secretion and decreased effect of insulin. Diabetes is a multiorgan disease, which is distinguished by impaired function of adipocytes, hepatocytes, ß-cells and muscle [23]. However, which of these defects come first is not clear.

Insulin sensitivity can alternate during life such as decreases during puberty and pregnancy and increases due to increased physical activity and decreased carbohydrate intake [24]. However, the specific mechanisms that lead to diabetes mellitus are still unclear although it is known that free fatty acids together with adipocytokines play an important role in the development of the disease [25]. The most critical factor that leads to development of insulin resistance and diabetes is obesity. Adipose tissue is known to release non-esterified fatty acids, glycerol, hormones and pro-inflammatory cytokines.

Indeed, during obesity the adipose tissue produces more of these substances, especially TNF-α and IL-6, which induces insulin resistance. Importantly, both of these cytokines lead to the activation of the NF-$_k$B-pathway and to enhanced

inflammation. Furthermore elevated non-esterified fatty acid levels employ significant impact on the development of IR [24] since free fatty acids are shown to inhibit the transport and phosphorylation of glucose which reduces the muscle glycogen synthesis and glucose oxidation by around 50 % [26].

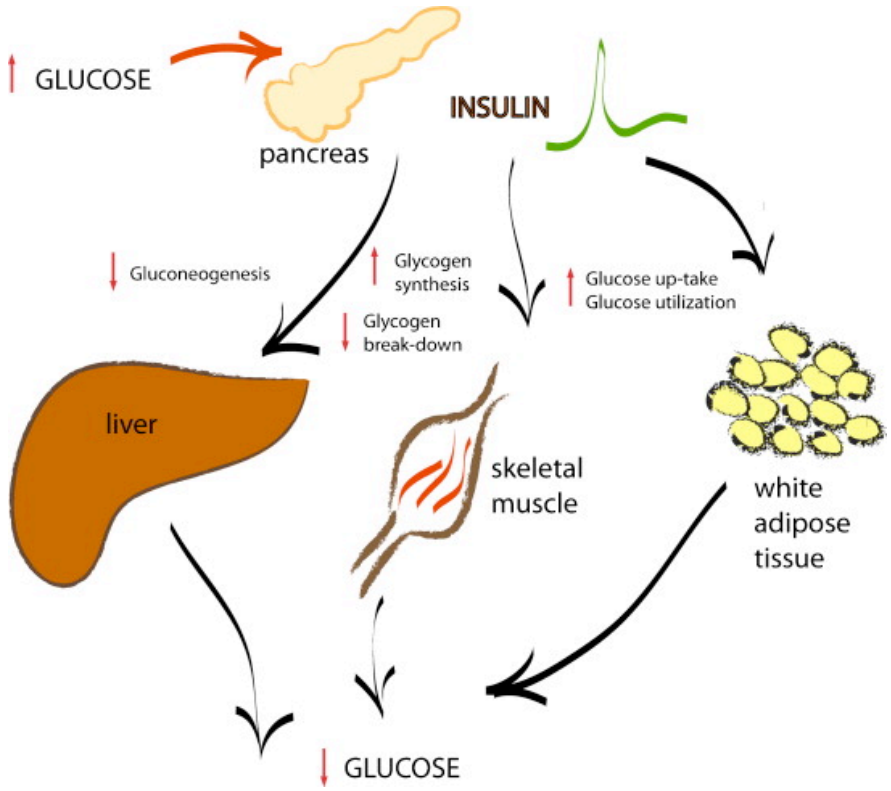

Figure 1.2: Crosstalk between insulin sensitive organs. The illustration shows the effect insulin produced by the pancreas after increased glucose levels in the blood. The insulin enhances the glucose uptake and utilization in skeletal muscle and adipose tissue. In the liver and muscle the glycogen synthesis is increased while glycogen break-down is decreased. Further gluconeogenesis in the liver is inhibited. All these circumstances triggered by insulin lead to a decrease in glucose levels in the blood. [27]

1.3.3. The insulin signaling pathway

Following binding of insulin to the insulin receptor thereby activated insulin receptor tyrosine kinase recruits and phosphorylates substrates of the insulin receptor, the insulin receptor substrates IRS-1 and IRS-2. Through this phosphorylation, the substrates open their binding sites. One of the most important binding partners in this pathway is phosphatidylinositol 3-kinase (PI 3-kinase), which activates the Akt

cascade. Akt itself is important for protein synthesis, glycogen and fatty acid synthesis. Akt phosphorylation leads to translocation of glucose transporter 4 (GLUT4) vesicles from the cytoplasm to the plasma membrane. GLUT4 is necessary for glucose uptake in muscle and adipose tissue.

Additionally the phosphorylation and recruitment of the IRS leads to the activation of the ERK/MAPK pathway that results in the transcription of genes involved in cell growth. [28-30]

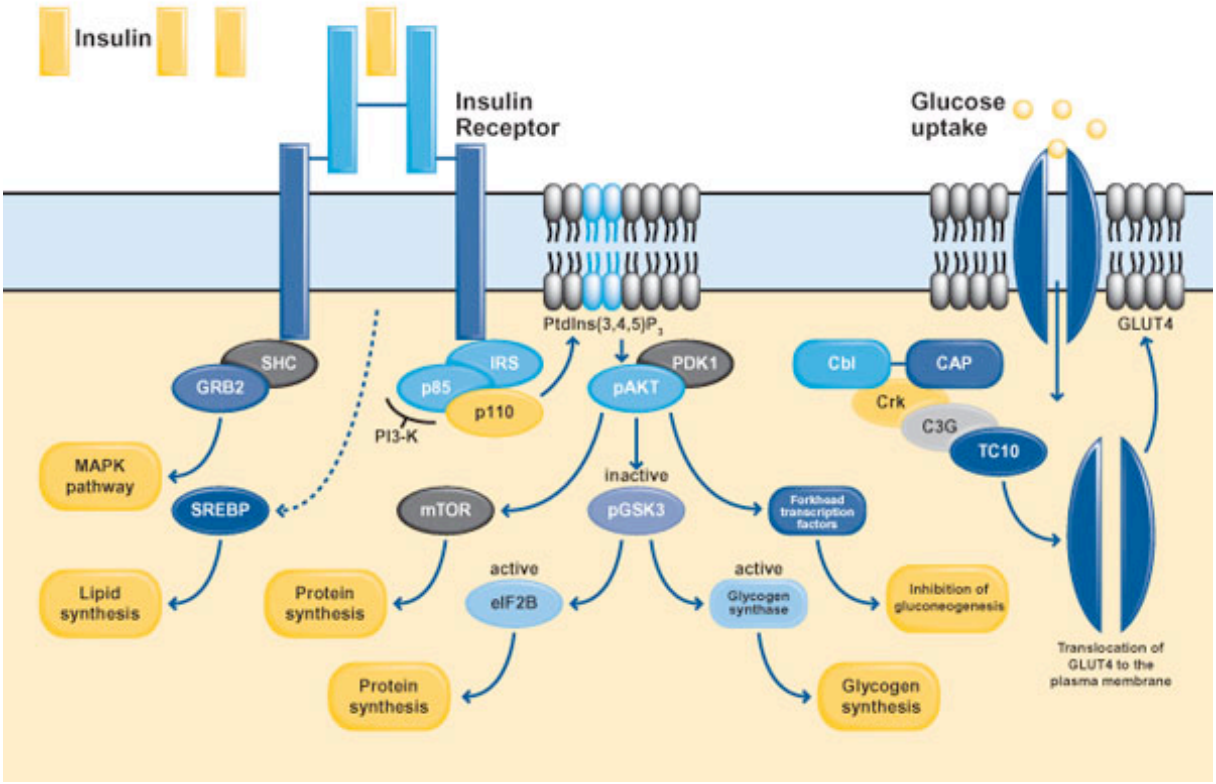

Figure 1.3: Scheme of the insulin signaling pathway. Following activation of the insulin receptor through binding of insulin, SREBP for lipid synthesis is produced and IRS, SHC and Cbl are phosphorylated. The phosphorylation open their binding sites and SHC bound to GRB2 activate the MAPK pathway. The binding of PI 3-kinase to IRS activates the enzyme to phosphorylate PDK1/2, which activates AKT. The activation of AKT pathway results in protein synthesis, cell growth and, besides the Cbl-CAP-complex, is involved in the translocation of GLUT4 to the cell membrane, which is necessary for the glucose uptake in the cell.

1.3.4. Obesity and inflammation

Obesity is a well-known risk factor for the development of several diseases, among them cancer. In the past decade further detailed information on the pathophysiology of fat-laden adipose tissue was obtained. It has been shown in both mouse model and humans that cytokines and chemokines like TNF-α, IL-6, IL-1ß and chemokine (C-C motif) ligand 2 (CCL2) were increased in adipose tissue. Toll-like receptors (TLRs) were found to be activated in tissues of obese mice in comparison to lean animals. Inflammatory changes were observed not only in adipose tissue, but also in liver, pancreas, brain and possibly in muscle suggesting systemic effects. [31]

Further changes were detected in inflammatory cells themselves characterized by increased macrophage infiltration and activation as well as a modest increase in T cells, especially of pro-inflammatory $CD8^+$ T cells in adipose tissue of obese animals. In contrast a decrease in anti-inflammatory $CD4^+$ $Foxp3^+$ T regulatory (Treg) cells was detected [32].

Moreover, the major product of adipocytes, adiponectin, has an important role in the development of inflammation during obesity. In comparison to the high levels of adiponectin in lean people, its levels are dramatically decreased in obese individuals. It has been shown that adiponectin has anti-inflammatory effects such that it suppresses the expression of pro-inflammatory cytokines TNF-α, IL-6 and interferon gamma (IFN-γ) by macrophages. On the other hand it increases the expression of peroxisome proliferator-activated receptor γ2 (PPARγ2), which is known to control the NF-$_k$B pathway [33].

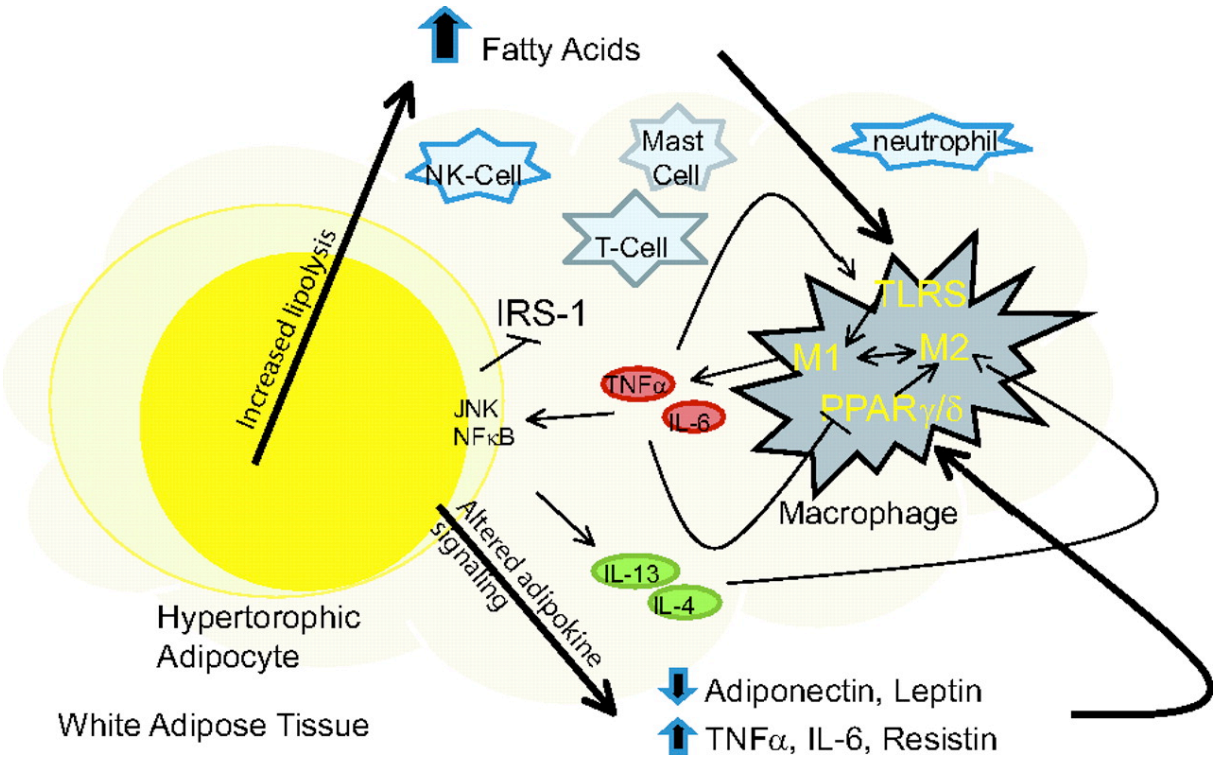

Figure 1.4: Role of adipocytes in inflammatory conditions during obesity. The adipocyte function is altered during the state of obesity. In addition to the increase in free fatty acid (FFA) release, adipokine production and signaling are shifted. Therefore levels of adiponectin are decreased and pro-inflammatory cytokines, like TNF-α and IL-6 are increased. These changes enhance an infiltration of immune cells, which further promotes inflammation by the release of cytokines and the followed activation of inflammatory signaling in adipocytes via c-Jun N-terminal kinase (JNK) and NF-$_k$B signaling. [34]

1.4. Intestine

1.4.1. Structure of the intestine

The intestine can be divided into 4 different parts: duodenum, jejunum, ileum, all together defined as the small intestine and colon as the large intestine. The small intestine and the large intestine are separated through the appendix. All parts consist of 3 layers: a variably thick muscle layer that is important for the peristalsis, a stromal tissue and the epithelial cell layer that has, in addition to the degradation and absorption of nutrients other various functions. While the small intestine consists of both villi - which are luminal projections - and crypts that are inversions of the epithelium, only crypts are found in the colon. The epithelial cells are steadily

renewing. Progenitor cells at the bottom of the crypts are dividing every 12-15 hours and cells migrate to the tip of the villi, which takes approximately 5 days [35]. The villi consist of three cell types: enterocytes, enteroendocrine cells and goblet cells while a fourth cell type, the Paneth cells, are found on the base in the crypt.

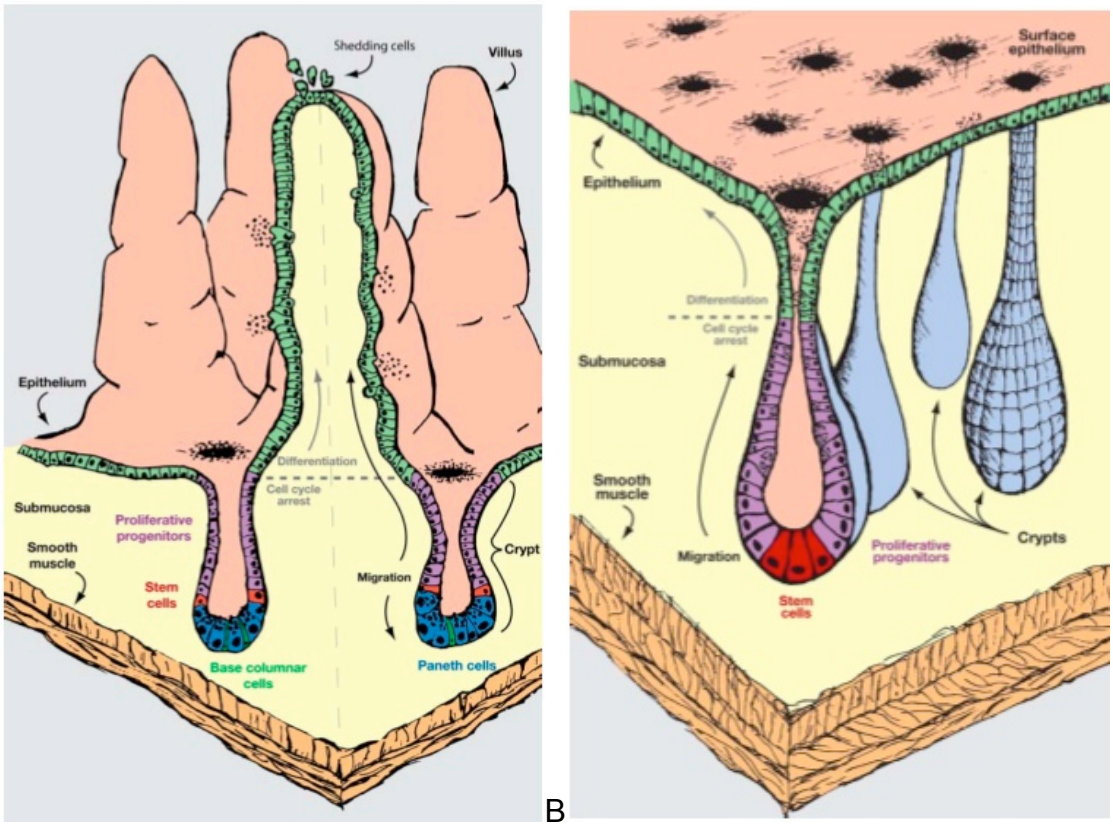

Figure 1.5: Structure of the intestine. A: Anatomy of the epithelium in the small intestine with the formation of stem cells in the crypt and the differentiation and migration of the cells to the top of the villi. **B:** Anatomy of the epithelium in the colon with the formation of stem cells in the base of the crypts and the migration and differentiation to the surface. [35]

1.4.2. Function of the intestine

The epithelial cells in the intestine have various functions including serving as a barrier as well as degrading and absorbing nutrients. The cell types enterocytes, enteroendocrines and goblet cells are found in the whole intestine while Paneth cells are restricted to the small intestine.

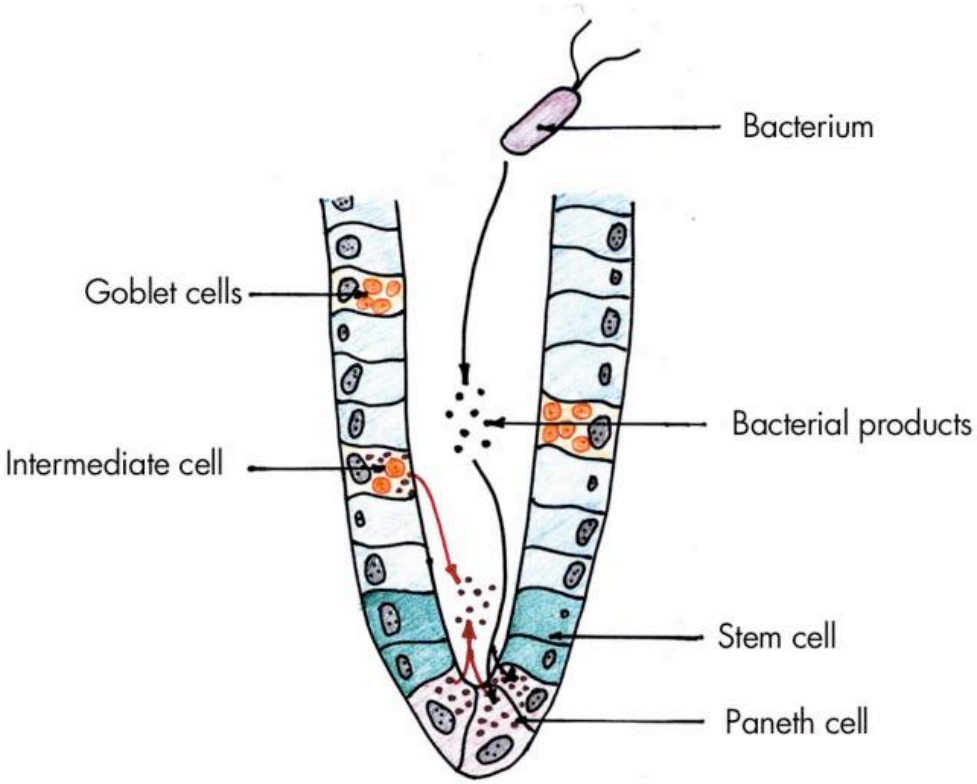

Figure 1.6: Scheme of a small intestinal crypt. Mucus secreting goblet cells and intermediate cells arising from stem cells are migrating to the top in direction of the villi while paneth cells that secrete antimicrobial peptides are located in the crypt base. [36]

Enterocytes are the most common cells and their main attribute is the uptake of nutrients and further to serve as an impermeable physical barrier [37]. Enteroendocrines are quite rare and are important for the secretion of hormones especially serotonin [38]. Goblet cells are secreting a mucus layer that protects the epithelial cells. Paneth cells, mainly localized in the ileum, are attributed to have multiple functions. Although their main function seem to be the control of the quantity of microbiobes in the small intestine they can produce cytokines themselves and seem to be important for crypt formation. In addition to TLRs Paneth cells express high levels of NOD2 (nucleotide-binding oligomerization domain containing 2) that detects microbiological particles and activates the NF-$_k$B pathway [39, 40]. Paneth cells are further able to react to increased concentration of bacteria with the release of antimicrobial peptides, which works as an important protection against bacterial invasion into the crypt environment and further regulates the bacterial density in the intestine [36]. The main antimicrobial peptides that are released by Paneth cells are lysozyme, secretory phospholipase A2 (sPLA2), defensins, RNases and C-type

lectins. Lysozyme and sPLA2 are both produced in large numbers by Paneth cells and enzymatically active antimicrobial proteins. They release enzymes, which kill bacteria by enzymatic reactions on microbial cell walls [37]. Defensins represent the most diverse and highly expressed protein family in the gut. They are classified in α, β and θ groups while α-defensins, which are termed as “cryptidins” in mice are strictly expressed in Paneth cells. Defensins kill bacteria in contrast to lysozyme and sPLA2 by binding to bacterial surfaces via electrostatic interaction followed by membrane disruption that lead to breakdown of membrane potential, loss of metabolites and ions and osmotic lysis [41]. The antimicrobial mechanism of RNases and C-type lectins remains poorly understood. C-type lectins like RegIIIγ are acting as directly antibacterial proteins. RegIIIγ is highly selective for gram positive bacteria and binds to peptidoglycan, disrupts the bacterial cell wall integrity and mediates direct killing of the microorganism [37].

Although the expression of most of the anti-bacterial compounds like lysozyme, RegIIIγ, phospholipase A are independent of NOD2, it has been shown in NOD2-deficient mice that there was still a significant rise in the amount of both gram-negative and gram-positive bacteria, like Bacteroides and Firmicutes [42].

1.4.3. Development of intestinal cancer

Gastric cancer is the second most common cancer type in the world but only less than 3 % of tumors in the digestive tract arise in the small bowel. Possible factors are the basic pH and the fluid condition, decreased immune reaction in the mucosa of the small intestine. Also the small bowel has less and shorter contact to bacteria because of the fast pass through and the decreased number of bacteria that are settled down, which results in decreased production of carcinogens. Other possible carcinogens that occur through the break down of the diet are metabolized and even decontaminated from the small intestinal mucosa. Another reason is the fast turnover of the epithelial cells, which disables time-dependent mutations. Furthermore the small intestine itself is steadily controlled by the highly developed immune system with an elaborated lymphoid tissue network [6].

The development of small intestinal cancer is similar to the pathology and molecular alterations in colorectal cancer [43]. There are two major types of colorectal cancer development: hereditary and sporadic. The hereditary types that include about 13 % of all colorectal cancer are again divided in familial adenomatous polyposis (FAP) and heriditary nonpolyposis colorectal cancer (HNPCC), which both arise through germline mutations [44]. The FAP gene is responsible for adenomatous poyposis coli (APC) [45] and a mutation or loss of this gene is found in the majority of colorectal tumor development, especially at early stages [46]. APC is a tumor suppressor gene that by binding to β-catenin is essential in regulating cell proliferation [47]. HNPCC is defined with a germline mutation in DNA mismatch repair genes. Around 80 % of the mutations arise in the mutS homolog 2 (MSH2) and mutL homolog1 (MLH1) genes, while mutations in postmeiotic segregation increased 1 and 2 (PMS1, PMS2) and mutS homolog 6 (MSH6) are not very common [48, 49]. The defect in these genes induce a genetic instability that results in secondary mutations in tumor suppressor genes and oncogenes, which then lead to tumor development [50].

However, most of the colorectal cancers have a sporadic background underlying a multistep model that was described by Fearon and Vogelstein 1990. It is based upon four characteristics. First, the development of tumors in the colon is the result of the inactivation of tumor suppressor genes coupled with the activation of oncogenes by mutations. Second, at least four genes must be mutated to develop a malignant tumor. Third, the order of genetic changes taking place can differ. Fourth, already heterozygous mutations in some tumor suppressor genes can lead to abnormal proliferation of cells. They also developed a model with certain tumor suppressor genes as well as oncogenes where mutations in a certain sequence took place and led step by step to the development of colorectal cancer. [51]

The first gene in the chain of mutations is APC at allele 5q, which is found in around 60 % colorectal carcinomas and 63 % adenomas and especially in the earliest stages of tumor development [46]. The next mutation in the chain is in the ras oncogene, which is found in around 50 % of colorectal tumors, also more in the earlier stages [52]. Further steps taking place in the development of cancer are allelic deletion on the chromosomes 18q and 17q. They are happening usually in later stages and occur in around 70 % of colorectal cancer [52]. The p53 gene on 17q plays a key role in the suppression of tumor and as cell regulator activated by DNA damage [53] while the DCC (deleted in colorectal cancer) gene is found on 18q. DCC is a trans-

membrane protein that binds to netrin-1, which itself is involved in axon guidance [54].

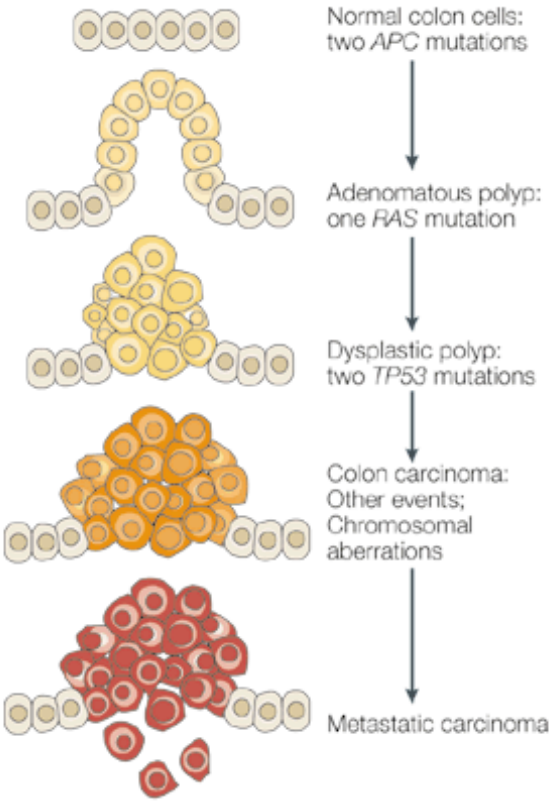

Figure 1.7: Possible processes of the development of colorectal cancer based on the Fearon and Vogelstein model. [55] According to the model, a chain of mutation cause in the formation of polyps and eventually colon carcinoma with metastatic carcinoma, beginning with APC, following RAS, TP53 and further chromosomal aberrations.

1.4.4. Classification of changes in the intestinal histology during tumor development through serrated pathway

Next to the hereditary and sporadic cancer development there is an alternative pathway, the serrated one. Up to 15 % of intestinal cancer have their seeds in hyperplastic polyps, initiating the serrated pathway. Hyperplastic polyps are considered to be benign, non-neoplastic lesions, though it has become more obvious that in some cases they can have a malignant potential [56]. Tumors developing through hyperplastic polyps are not following a certain chain of genetic changes like

described in the Fearon and Vogelstein model for sporadic cancer. They also are not arising because of hereditary events. Nevertheless it has been emphasized that the serrated pathway is accompanied by microsatellite instability (MSI) [57]. Two key events have been shown to initiate the serrated cancer development: hypermethylation of Cytosin-phosphatidyl-Guanin (CpG) islands and oncogenic BRAF mutation [58]. CpG islands are seen in approximately 50 % of the human gene and around 40 % of the genes have CpG islands in their promotor region. The methylation of one of these CpG islands implicates the stop of the gene expression. In context of intestinal cancer hypermethylation results in loss of expression of genes related to neoplastic development, like p16.

The second key event is the BRAF mutation. BRAF is known as proto-oncogene and mutated in 5 – 15 % of all intestinal carcinomas. It is a member of the RAF family of serin/threonine kinases and is able to send signals to cells that are directly involved in cell growth.

Furthermore it was shown that during the serrated pathway tumors can develop that differ in terms of histology [59]. They are mainly classified as sessile serrated adenoma, traditional serrated adenoma and serrated adenocarcinoma [60].

1.4.4.1. Hyperplastic polyp

A polyp is the description of a protuberance above the mucosa of the intestine. Crypts/villi are serrated but not branched. Usually they are quite small (< 5 mm) and are found in around 85 % of all polyps. These are often found in routine endoscopies [61]. They show no dysplastic nuclei and are said to be completely benign without malignant potential. Recently, however, genetic alterations were found in hyperplastic polyps, mainly for K-ras, but also for p53 mutations and DNA microsatellite instability. Furthermore they were associated with the development of malignant tumors suggesting hyperplastic polyps are neoplastic [62].

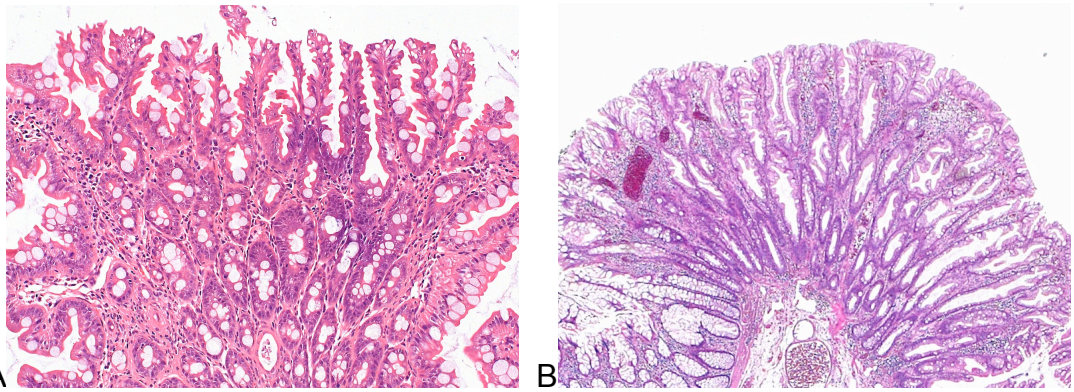

Figure 1.8: Histology of hyperplastic polyps. H&E staining of a hyperplastic polyp in mouse (A, 20x magnification) or human (B, 5x magnification).

1.4.4.2. Serrated adenoma

Serrated adenomas can be subdivided into traditional and sessile types. They measure up to 1,5 cm, are protuberant and have a tubular and/or villous structure showing lesions and atypical shapes of the nuclei. The tissue is highly serrated and branched [63]. Often serrated adenomas are related with microsatellite instability as well as mutations of oncogenes, tumor suppressor genes and genes repairing DNA mismatch, like K-ras, APC, p53, DCC, MLH1 and MSH2 [64].

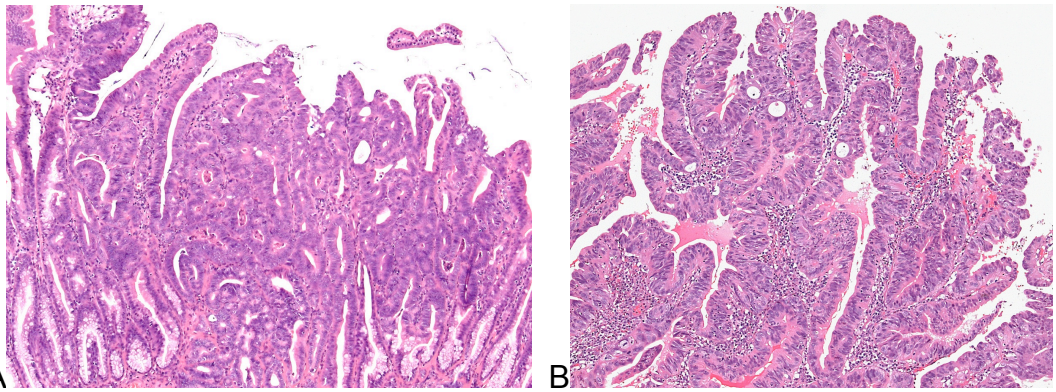

Figure 1.9: Histology of serrated adenoma. H&E staining of a serrated adenoma in mouse (A, 10x magnification) or human (B, 10x magnification).

1.4.4.3. Serrated adenocarcinoma

Around 95 % of all malignancies found in the colon are adenocarcinoma. As they develop from adenomas, their molecular properties are accordingly. These are malignant tumors that can reach up to several cm in diameter. Histologically they show a polyp-like extensive growth with tubular structure of the epithelial cells and flat infiltrating lesions, which are often ulcerated. What is often seen in adenocarcinoma (in around 10 – 20 %) is the accumulation of mucin. [62]

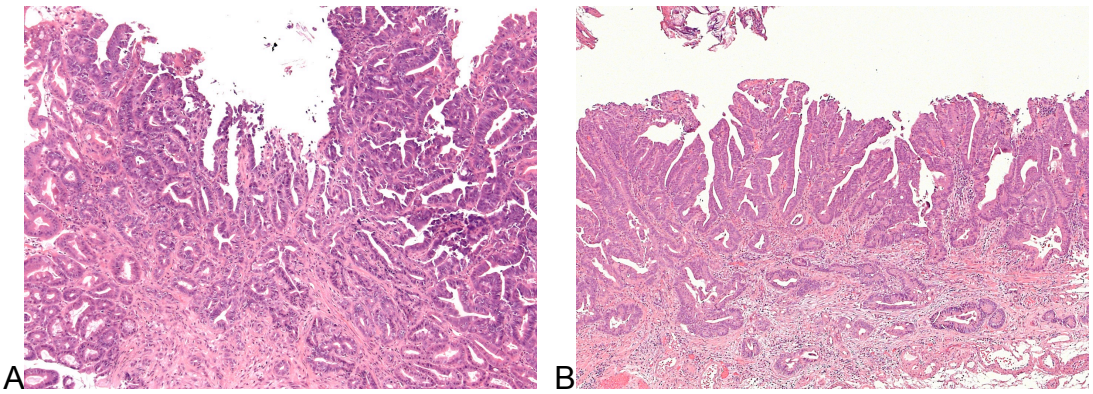

Figure 1.10: Histology of serrated adenocarcinoma. H&E staining of a serrated adenocarcinoma in mouse (A, 10x magnification) or human (B, 5x magnification).

1.4.5. Role of Ras signaling in terms of cancer development

1.4.5.1. Ras signaling pathway

Ras proteins are guanosin-triphosphatases (GTPases) that are involved in the activation of different pathways that control several cellular responses including proliferation, differentiation and cell survival.

The pathway initiates when a signal binds to a protein tyrosin kinase receptor. The best known receptors are epidermic growth factor receptor (EGFR) and platelet-derived growth factor receptor (PDGFR). The binding induces the oligomerization of the receptor, which in the end allows the activation of the kinase activity and transphosphorylation. Thereby adaptor proteins such as growth-factor-receptor bound protein 2 (GRB2) are able to recognize sequence homolog 2 (SH2) domains like SH2-containing protein (SHC). Hence it follows that guanine nucleotide exchange factors (GEFs), like son of sevenless homolog 1 (SOS-1), are recruited to

the cell membrane and promote the exchange of GDP for GTP [65]. Ras proteins cycle between inactive, guanosine diphosphate (GDP)-bound and active, guanosine triphosphate (GTP)-bound conformations [66]. The activation of the Ras proteins by GTP is caused by a conformational change in the regions named switch I and switch II and further regulated by GTPase activating proteins (GAPs), allowing the signaling to proceed for a relatively short interval [67].

Once activated, Ras can further activate several Ras effector pathways with the mitogen activated protein kinase (MAPK) pathway as the best-characterized one.

The MAPK, also named as MEK, is activated through phosphorylation of Raf. Raf itself is activated directly by binding to the activated Ras protein. MAPK further phosphorylates downstream proteins like ERK1 and ERK2, which activate themselves a wide range of nuclear transcription factors and kinases involved in cell proliferation. [65]

Ras-GTP further binds and thereby activates phosphatidylinositol 3-kinase (PI3K), which leads to the activation of downstream kinases such as 3-phosphoinositide-dependent protein kinase 1 (PDK1) and also Akt, which leads to cell survival by inactivating several pro-apoptotic proteins.

On the other hand PI3K activates Rac, a subfamily of the Rho GTPases, its levels are also increased through binding of tumor invasion and metastasis inducing protein 1 (TIAM1) to Ras-GTP.

Ras can further activate a family of exchange factors for the Ral small GTPases, activating Ral that can stimulate phospholipase D (PLD). Ras also can stimulate the release of calcium by the activation of protein kinase C, binding to Phospholipase Cε (PLCε).

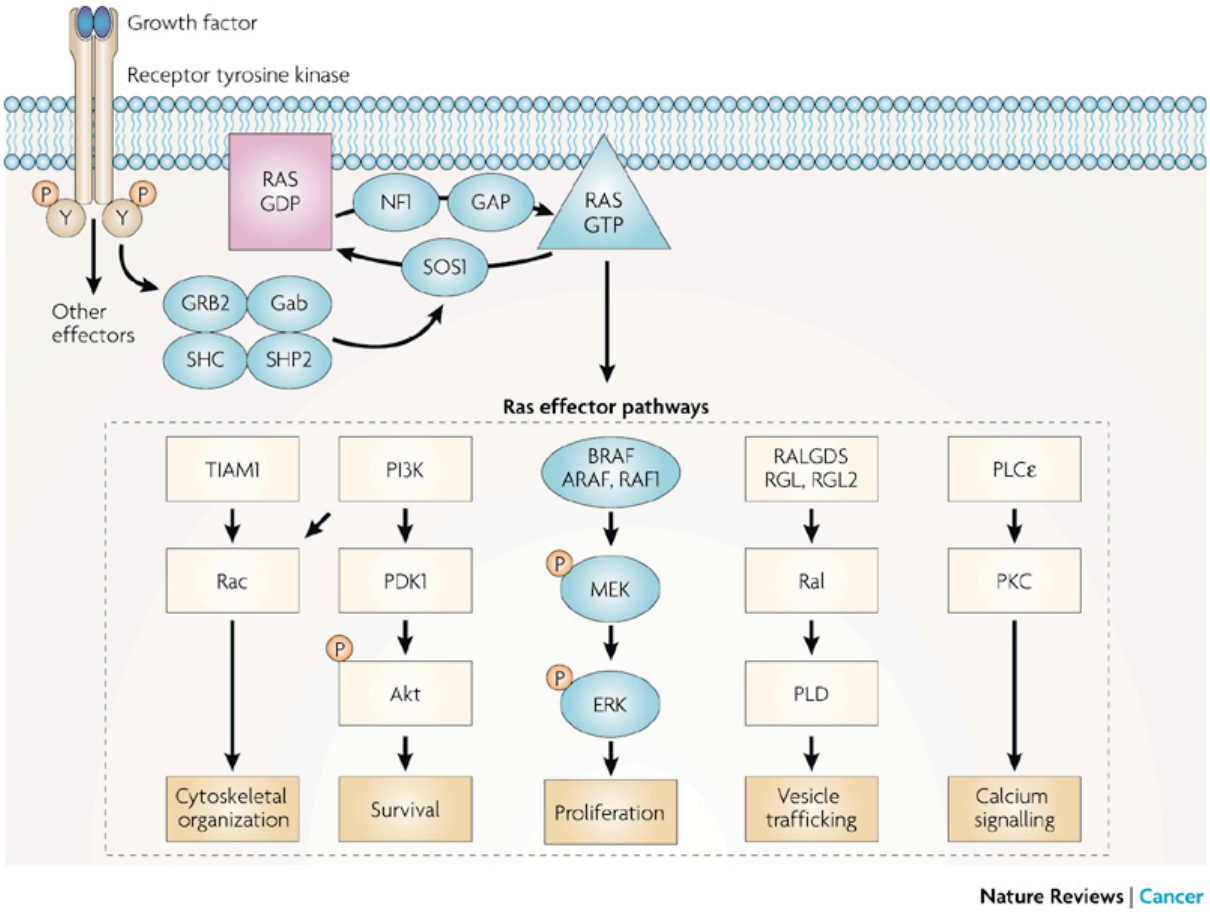

Figure 1.11: The Ras signaling pathway. By binding of a growth factor to the receptor tyrosine kinase, tansphosphorylation enables adaptor proteins, like GRB2 to recognize SH2 domains like SHC. This in turn activates GEFs, such as SOS1 to migrate to the cell membrane and to promote the exchange of GDP for GTP, resulting in an active Ras-GTP bound protein. Ras-GTP further activates a variety of effector pathways, most prominently the MAPK/Mek/Erk pathway, which results in cell proliferation. Activated Ras further enhances cell survival, cytoskeletal organization, vesicle trafficking and calcium release by stimulating further pathways through activating TIAM1, PI3K, PLCε and a family of exchange factors for the Ral small GTPases. [68]

1.4.5.2. Ras as an oncogene

Ras activation plays a prominent role in terms of cancer development as it is nearby described as second mutation step in the Fearon and Vogelstein model and is further mutated in around 30 % of all human cancer and up to 50 % of all colorectal tumors. The most common mutations resulting in Ras as oncogene are at codon 12,13 and 61, resulting in an inefficient acting of the GAPs, whereby Ras stays continuously in the GTP-bound active form [69]. There are three Ras genes, H-ras, N-ras and K-ras,

that encode for four gene products, as K-ras4a and K-ras4b arise through alternative splicing of the K-ras gene, K-ras 4b presenting the most prominent splice variant. K-ras mutation is the most prominent one in the majority of human cancer like breast, lung, pancreas and colon cancer [68]. H-ras mutation is for example found in around 11 % of bladder cancer, N-ras mutation in melanoma and myeloid leukemia.
To investigate the role of Ras mutation, overexpression was examined in cell culture and mice models. One outstanding mouse model is the K-ras^{G12D} model with an activating glycine to aspartic acid mutation at codon 12 (G12D) [70]. Mice carrying this mutation were highly susceptible for a variety of tumors, most prominently early onset lung cancer. To focus on special tissues, a K-ras^{G12D} mutant allele was generated in which loxP-stop-loxP elements were imported to the silent K-ras in the absence of cre recombinase expression. Especially in terms of lung, pancreatic and colon cancer this mutation in mice turned out to represent a convincing model for cancer research, as the data are generally consistent with genetic studies of human cancer.

1.5. Microbiota

1.5.1. Epidemiology and function

Around 1 x 10^{14} individual bacteria colonize the human intestine with a combined microbial genome estimated to be 100 times as large as that of their human host [71]. They reach the highest cell density recorded for any ecosystem [72]. Nevertheless the knowledge about microbiota is still limited although recent research on unraveling human microbiome genome [73, 74] is starting to uncover the role of bacterial communities under health and disease condition. The colon harbors the highest amount of bacteria while in the proximal gastrointestinal part hardly any bacteria are found. The stomach and duodenum have quite an acidic environment and also the increased peristaltic move makes it difficult for bacteria to colonize.
The microbiota in the intestine have multiple functions and effects: both beneficial and harmful. First and foremost they are necessary for the digestion of nutrients that are otherwise undigestible by the host. Further the commensal bacteria are necessary against the colonization of pathogenic bacteria. Along with its diverse

functions microbiota influence the proliferation and differentiation of epithelial cells and are necessary for the development of the immune system [75]. However, due to the quantity and diversity of bacteria it is not really possible to ascribe certain functions to individual bacterial strains.

What is known so far is that mammals are able to absorb simple sugars like glucose and galactose but fail in the digestion and utilizing of other polysaccharides. Thus, the intestine is well organized as the ingested carbohydrates first pass the proximal part of the small intestine where hardly any bacteria are colonized. Here the host itself absorbs sugars through monosaccharide transporters. Then undigested polysaccharides together with host-derived glycans are transported to the distal part of the small intestine and finally to the colon, where the highest amount of bacteria is located. Here the digestion of the polysaccharides and fermentation by the microbiota takes place and the host can absorb the produced short chain fatty acids (SCFA). [76].

The main SCFA, the bacterial fermentation end-products, are actetate, propionate and butyrate [77]. Apart from the function as energy source, especially butyrate is known to have several beneficial effects [78]. Butyrate is able to regulate trans-epithelial ion transport in the intestine such that it stimulates NaCl and inhibits Cl^- transport. As for its anti-carcinogenic effect, butyrate inhibits proliferation and induces apoptosis in tumor cells [79]. Further it has anti-inflammatory effects as it inhibits the pro-inflammatory NF-$_k$B pathway in human colonic epithelial cells [80]. Additionally it has influences on oxidative stress, visceral perception, intestinal motility and insulin resistance [81]. As butyrate has quite an unpleasant smell and taste, they are not considered for therapeutic use, instead often probiotics and prebiotics are used to indirectly boost the production of butyrate.

Probiotics are a mixture of living bacteria collected from human or animal intestinal tract, isolated and purified. The main ingredients are species of the bacterial strains Lactobacillus and Bifidobacterium. The beneficial effect of this bacterial composition is already well established and also produced as drugs or dietary supplements. [82]

Prebiotics are selectively fermented food ingredients that trigger the growth and increase of certain beneficial bacterial strains.

The composition of bacterial community colonized in an individual´s intestine is dependent on various aspects. The intestine is colonized from bacteria at birth and during the first year of life. Although the intestinal microbiota is quite similar between

family members however there are variations in the composition according to environmental conditions such as the diet [83]. One explanation for this variation is that changes in carbohydrates influence the pH in the gut lumen, which affects the bacteria in the intestine [84]. An obvious microbial change is observed in the case of obesity. Although the exact mechanisms are still not known, it was shown that there is a shift from Bacteroides to Firmicutes in obese animals and accordingly increased energy extraction of indigestible food components was observed [85]. Germ-free mice that got transplanted with the microbiota from obese mice had a significantly higher increase in body fat than those that received microbiota from lean mice [86]. Also a shift of gram positive to gram negative bacteria and a simultaneous increase of LPS in the plasma were detected [87] that could lead to systematic inflammation in organs such as liver, adipose tissue, hypothalamus and muscle. This condition indeed supports fully the low-grade inflammation during diet-induced obesity.

1.5.2. Microbiota and cancer

It is already well known that some pathogens can promote tumorigenesis, such as the hepatitis B and C viruses that lead to liver cancer. As for the bacteria only some species are found to be linked to cancer development. Helicobacter pylori has been shown to promote gastric cancer and was even classified as carcinogen from the World Health Organization in 1994 [88]. It also has been demonstrated that a human commensal colonic bacteria, Bacteroides fragilis, is associated with colon cancer through inducing colonic inflammation via $CD4^+$ T_H17 cells. Depleting $CD4^+$ T_H17 cells decreased significantly the tumor numbers in mice [89]. How exactly commensal bacteria in the intestine can promote tumorigesesis is not yet understood but is highly likely that the link includes the activation of the immune system and the resulting inflammation. One example for the link between microbiota, inflammation and cancer is the chronic inflammatory bowel diseases, Crohn´s disease and Ulcerative Colitis. Although the role of the bacteria is not yet clear, it has been detected in different studies that the diseases arise because of interactions of host genetic and immune factors, the intestinal microbiota and environmental triggers. Further it has been found out that patients with these diseases show an abnormal composition of intestinal microbiota, more precisely a depletion of members of the

phyla Firmicutes and Bacteroidetes [90]. However, it is still unclear if the whole microbial community or single bacteria strains are presenting an oncogenic risk factor. One hypothesis how one single bacteria strain can promote colon cancer is explained on the example of Bacteroides fragilis [91]. In vivo they showed that the bacteria have the ability to induce inflammation in colonic epithelial cells via activation of ß-catenin and stimulation of pro-inflammatory cytokine production through the NF-$_k$B pathway. Bacteroides fragilis also induces the activation of Stat3, which is required for the T_H17 response. Further it is suggested that the colonization of these tumor-inducing bacteria could promote the growth of more pro-oncogenic microbiota and inhibit the growth of anti-oncogenic microbiota [91]. Still the link between the commensal bacteria in the intestine and colonic cancer is nebulous and needs further research.

1.5.3. Recognition of microbiota

The epithelial cells in the intestine, enterocytes, enteroendocrine and goblet cells, express pattern recognition receptors (PRR) to detect the microbiota. They recognize so-called microbe-/pathogen-associated molecular patterns (MAMP/PAMP). There are three families of PRR known: Toll-like receptors (TLRs), which are the best-known so far, nucleotide oligomerisation domain (NOD) –like receptors (NLRs) and retinoic acid inducible gene I (RIG-I) –like receptors (RLRs) [92]. NLRs and RLRs are both cytoplasmic proteins. While RLRs recognizes viral RNA, the over 22 different NLRs in human and 34 in mice recognize a wide range of microbial products. Especially NOD1 and NOD2 are known to have an important role in the detection of bacteria. Both receptors bind intracellular microbial components: NOD1 recognizes products of gram negative bacteria and NOD2 a wide range of bacterial substances [93]. NOD2 is mainly found in dendritic cells, macrophages, Paneth cells and intestinal epithelial cells and is known to be essential for the regulation of the colonization of commensal bacteria in the intestine. It also leads to the activation of the immune system through the NF-$_k$B pathway. [42]

1.5.4. Toll-like receptor (TLR)

There are 11 human and 13 mouse TLRs known so far that are located not only at epithelial cells and lamina propria mononuclear cells, but also at T cells and antigen presenting cells, such as dendritic cells and macrophages [92]. They detect an immense number of PAMP/MAMPs from various microorganisms, not only bacteria, but also from viruses, fungi and protozoa. The expression, location and function of the individual receptors is still not completely understood but TLR-4 is shown to play a prominent role in the intestinal diseases [94]. TLR-2 and TLR-4 both recognize bacterial cell wall components: TLR-2 peptidoglycans from gram positive bacteria, TLR-4, lipopolysaccharide (LPS) from gram negative bacteria [95] that can lead to septic shock.

TLR-2 and -4 are in one group with TLR-1 and -6, cell membrane receptors, which detect lipids. Also located on the cell surface are human TLR-5 and -11, which recognize protein ligands. In contrast, TLR-3, -7, -8 and -9 are intracellular receptors that are able to recognize nucleic acids from bacteria and viruses.

The activation of the TLRs through the detection of PAMP/MAMPs leads to the stimulation of the recruitment of TIR-domains, which are located in the cytoplasm, via TIR-TIR interactions. TIR-domains involve MyD88, TIRAP, Trif and TRAM. The best known one is probably MyD88, which is shared by all TLRs apart from TLR-3. The recruitment of MyD88 is extremely important for the release of pro-inflammatory cytokines such as TNF-α, IL-6, IL-1β and IL-12, as it activates the MAP kinases, like ERK, JNK and p38, as well as the transcription factor NF-$_k$B [96].

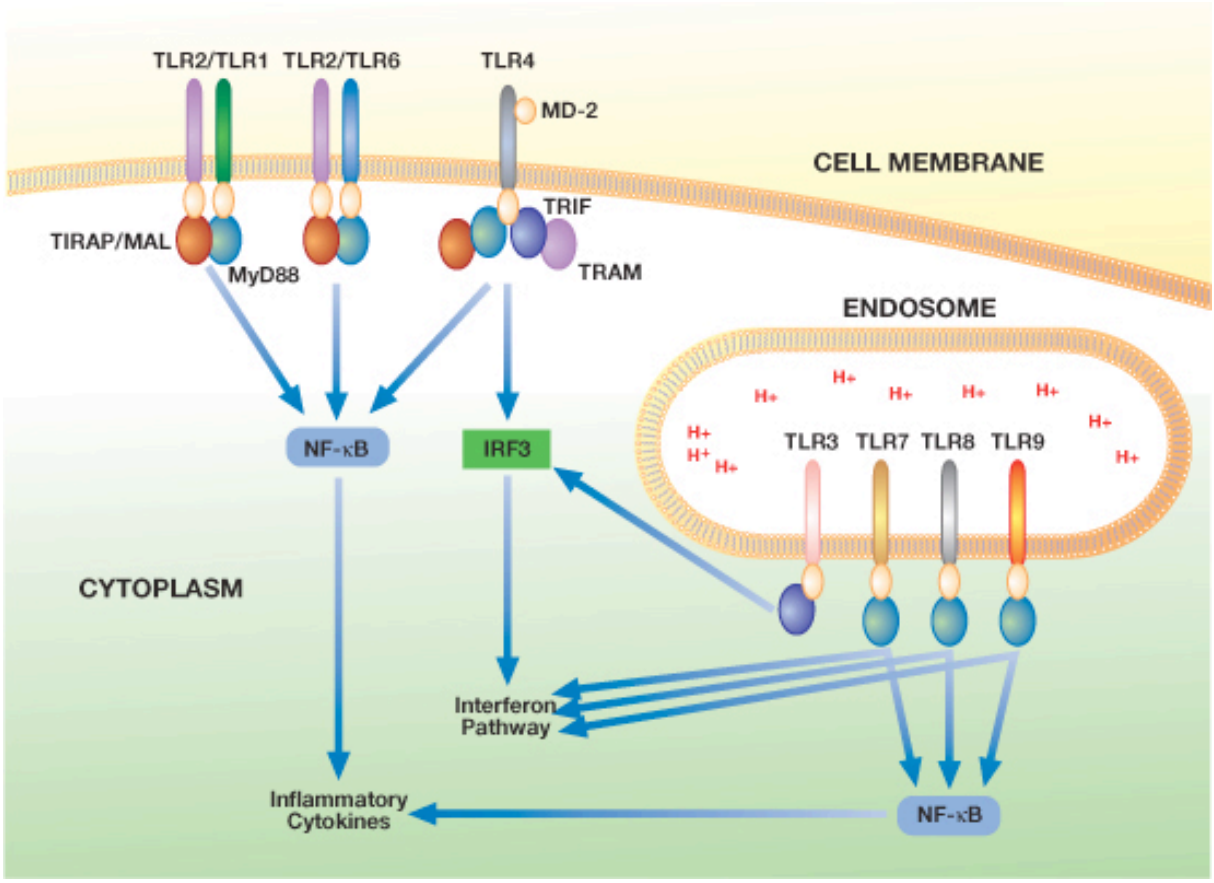

Figure 1.12: TLR signaling [97]. TLR-1, -2, -4 and -6 are located on the cell membrane, while TLR-3, -7, -8 and -9 are located intracellular. Apart from TL-3, all receptors have the adaptor molecule MyD88 in common. The activation of one of the TLRs activates the inflammatory immune response, either through the NF-$_k$B, or the IRF3 pathway.

1.6. The immune system

1.6.1. The NF-$_k$B pathway

Next to the IL-1 receptor, the NF-$_k$B pathway is mainly activated through the TLRs. There are 5 NF-$_k$B proteins, p50/p105, p52/p100, RelA, RelB and cRel, which have a Rel-homology domain in common. They form different homo- and hetero-dimer that are constituents of the pathway [98]. p105 and p100 have the same N-terminal regions like p50 and p52 and are the precursor of the smaller products. The exact function is still unknown but as p105 and p100 in comparison to the smaller products are not able to enter the nucleus, the amount of p50 and p52 is increasing through the activation of NF-$_k$B. [99]

The NF-$_k$B pathway is divided into the classical and the alternative pathway [98]. The classical pathway is mostly activated in state of acute inflammation as well as cell survival mechanisms thus seem to be related to the link of inflammation and cancer. Especially bacterial or viral components as well as pro-inflammatory cytokines lead to the activation of the IKK complex (I$_k$Bα kinase) that consists of IKKα, β and γ. IKKβ phosphorylates I$_k$Bs that are bound to NF-$_k$B proteins, which results in the degradation of the I$_k$Bs. The now unbound NF-$_k$B proteins are able to enter the nucleus and induce the transcription of target genes. The alternative pathway is independent of IKKβ and γ as IKKα homodimers are activated and lead to the phosphorylation and processing of p100. [100]

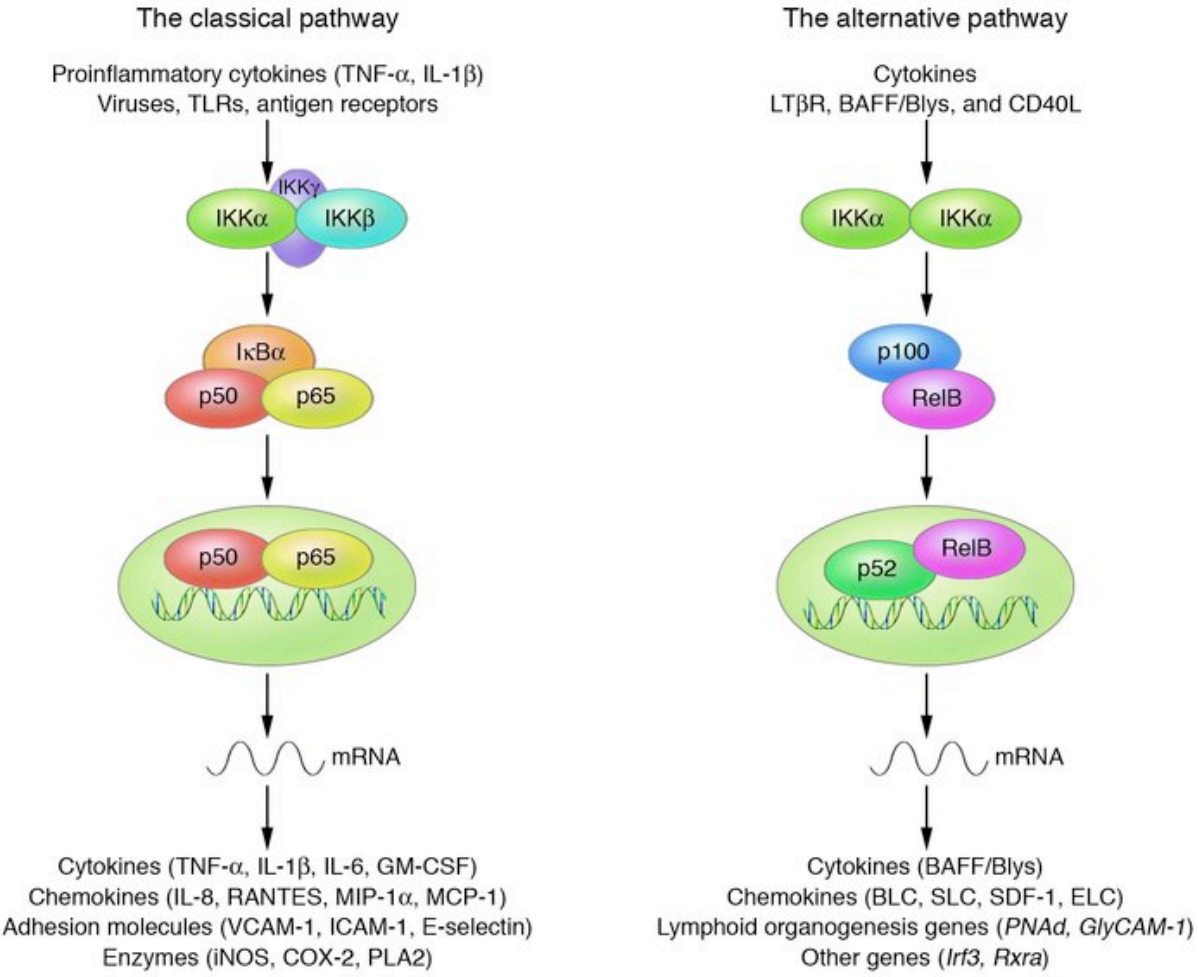

Figure 1.13: The NF-$_k$B pathway divided in alternative and classical pathway [101]. The alternative pathway is in contrast to the classical pathway, independent of IKKß and IKKγ. The activation of the NF-$_k$B pathway leads to a degradation of the proteins bound to each other, which makes them able to enter the nucleus and activate the transcription of certain immune response genes.

1.6.2. The NF-$_k$B pathway and the state of obesity

It has been shown that there is a link between the NF-$_k$B pathway and insulin resistance as overexpression of IKKß leads to a decrease in insulin sensitivity, while the inhibition of IKKß increased the sensitivity [102]. The mechanisms that interconnect inflammation, obesity and insulin resistance are still unclear, but it has been shown that the IKKß-NF-$_k$B pathway in cells that are directly involved in the insulin-regulated glucose metabolism, like hepatocytes, as well as cells that are not directly involved, such as myeloid cells, play an important role in obesity-induced insulin resistance. IKKß deletion in myeloid cells led to improved insulin sensitivity systemically, while the deletion in hepatocytes only had a local effect in the liver [103]. It is clear that HFD and obesity induce insulin resistance, however, how they can induce inflammation by activating the NF-$_k$B pathway is still unknown. One reason could be the upregulation of genes in adipose tissue, which are specific for inflammation and especially macrophages [104]. Thus the NF-$_k$B pathway could be activated and thereby express pro-inflammatory cytokines that could promote insulin resistance.

1.6.3. The NF-$_k$B pathway and cancer

It is well accepted that inflammation plays a critical role in the development of tumors and is a hallmark of cancer [105]. Large number of cancers show NF-$_k$B activation [106]. However, hardly in any cancer an oncogenic mutation related to the NF-$_k$B pathway was seen. So the activation of NF-$_k$B in cancer seems to be the result of an underlying inflammation or due to inflammatory microenvironment during malignant progression. Nevertheless it has been shown that the activation of NF-$_k$B plays a crucial role as a link between inflammation and cancer as it promotes the tumor development by the increased release of cytokines, such as IL-6 and TNF-α as well as the expression of survival gene Bcl-x. [107]

1.6.4. Immune system in the intestine

The immune system is divided in two: the innate and the adaptive immune system. The innate one uses pattern recognition receptor (PRR) to induce an immune response to pathogens, for example via the NF-$_k$B pathway. The two major groups of PRRs are TLRs and cytoplasmic nucleotide-binding domain, leucine-rich repeats (NLR) proteins. As the ligands of PRRs are not specific for pathogens, they can not differentiate between pathogenic and symbiotic microorganisms [108]. As a result, the distinction can fail and result in a dysregulated immune response, which is the basis of inflammatory diseases in the intestine [93].

In contrast, the adaptive immune system uses antigen receptors that are located on B- and T-cells. T cells are divided in T helper cells with the co-receptor CD4 and cytotoxic T cells with the co-receptor CD8. They recognize antigens that are presented from major histocompatibility complex (MHC) class I and class II molecules on the surface of antigen-presenting cells. B cells in contrast are able to recognize nearly any bound or unbound form of antigens that are present in the body. [108]

To monitor the barrier between the „inside“ and the „outside“ of the intestine, antigen-presenting cells such as dendritic cells are closely located to the epithelial cells.

Dendritic cells are able to absorb pathogens by phagocytosis and process these to antigenic peptides that are then transported back to the cell surface where they are presented to immune cells by MHC I and II.

Immune cells are mainly found in the mesenteric lymph nodes (MLN), the Peyer´s Patches (PP), specialized lymph nodes in the gut wall and lamina propria (LP).

In the intestine, the only physical barrier between the “inside” and the “outside” with all the commensal bacteria as well as pathogens is one layer of epithelial cells. A mucus layer is attached to these epithelial cells, which shows a protective role. The epithelial cells themselves play an important role. In addition to their role as barrier, they secrete IgA, an effective protector against microbes that is also important to limit the penetration of commensal bacteria and produce several antibacterial molecules such as defensins. The production and secretion is mainly activated through dendritic cells. Dendritic cells are located near the epithelial layer in the lamina propria until they are loaded with bacteria. Then they migrate to the PPs and MLNs, where they present the bacterial peptides via MHC I and II to B- and T-cells [109]. B-and T-cells

normally circulate through the lymph nodes until they face an antigen they are specific for. When they are activated, they migrate through the intestinal lymphatics, enter the blood stream at the level of the thoracic duct and go back to the intestinal lamina propria, where their immune response takes place. [110]

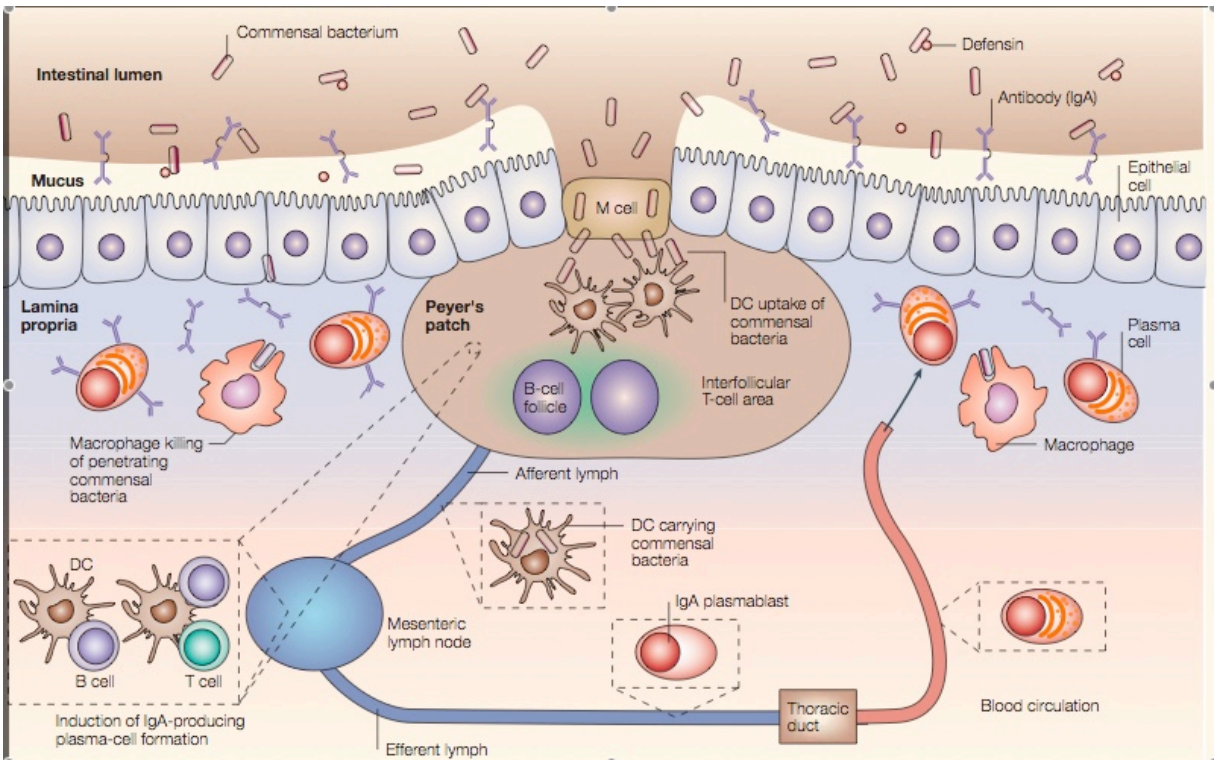

Figure 1.14: The immune system in the intestine [110]. Intestinal epithelial cells are able to produce antibacterial substances, like defensins that can kill bacteria in the intestinal lumen. Bacteria that penetrate the epithelial wall can be killed by macrophages in the lamina propria. Bacteria that survive can be uptaken by dendritic cells. In this way they can be presented to other immune cells, like T- and B-cells in Peyer´s Patches or mesenteric lymph nodes.

2. Aim of the study

Recent widespread “Western life style” with decreased physical activity, elevated uptake of fast food rich in fat and consequent increased incidence in obesity has been associated with elevated risk to develop gastrointestinal cancer, although the mechanisms remain still nebulous. In this study it was of our interest to examine the connection between diet-induced obesity and the development of intestinal cancer, using high fat diet that consists 60 % of the calories from fat. A mouse model with oncogenic K-ras mutation restricted to the intestinal epithelial cells (ViRas mouse) was chosen, as mutation in the K-ras oncogene is the most common mutation in 50 % of intestinal cancer in human.

The intestine harbors an extremely intricate system of microbiota with approximately 10^{13} microorganisms, including commensals and pathogens that have beneficial and harmful effects on the host respectively. Microbiota is important for the regulation of the energy balance by the fermentation of indigestible nutrients and the production of short chain fatty acids. Recent evidence suggests altered composition of microbiota is associated to obesity. In order to understand whether the microbiota is involved in diet-associated tumor development, the bacterial composition as well as endotoxin levels and short chain fatty acids were checked. To further proof microbiota influence the adaptor protein MyD88 of the NF-$_k$B pathway, representing the major pathway activated by bacteria and moreover related receptors were deleted in ViRas mice. Additionally, to elucidate the effect of beneficial alterations in the gut flora, mice were treated with probiotics, the fiber arabinogalactan and the short chain fatty acid butyrate that are known to exert several health-promoting properties. The direct influence of the microbiota was furthermore proven through the transfer of microbiota from ViRas mice on high fat diet to mice on normal diet.

It still remains unclear how changes in the microbiota affect the intestinal immunity but certainly the immune system plays a substantial role in the development of cancer. Therefore several parts of the immune system in ViRas mice were examined, amongst others the pro-inflammatory NF-$_k$B pathway important for the detection of bacteria, the antigen-presentation on dendritic cells necessary for immune response and the release of antimicrobial peptides essential for mucosal immunity.

Since the incidence of obesity and intestinal cancer are increasing year by year it is important to get a better understanding on how diet-induced obesity increases the risk to develop gastrointestinal cancer. Consequent diet-induced changes in microbiota and the immune system may represent potential therapeutic options during tumor development since modulation of gut bacteria through probiotics and short chain fatty acid supplementation is applicable.

3. Materials and Methods

3.1 Mice

Mice were housed in a pathogen-free facility with 12 h dark and 12 h light cycle. Animals were kept in 4 to 6 per cage, where they had free access to autoclaved and irradiated rodent food and autoclaved water. As normal diet, total pathogen free diet (Altromin # 1314) was used, containing of 22.5 gm% protein, 5.0 gm% fat and 4.5 gm% fibre. As high fat diet, a rodent diet with 60 kcal% fat (Research Diets, #D12492) was used. The fat enriched diet included 26.2 gm% protein, 26.3 gm% carbohydrate and 34.9 gm% fat.

3.1.1 Mouse Model

Villin-Cre [111], IL-1R$^{-/-}$ [112], MyD88^{fl} [113] mice were purchased from Jackson Laboratory. MyD88$^{-/-}$ [114], TLR-4$^{-/-}$ [115] and TLR-2$^{-/-}$ [116] were kindly provided by Dr. Shizuo Akira and Prof. Dr. Hermann Wagner, K-ras^{G12D} [117] by Dr. Dave Tuveson.

3.1.2 Genotyping

Mice were genotyped using DNA isolated from tail biopsies. The tails were lysed in 180 µl Lysis Buffer with 20 µl Proteinase K and incubated at 60 °C overnight. The reaction was inactivated by heating the samples up to 95 °C for 10 min, followed by centrifugation at 13200 rpm for 10 min. DNA was then dissolved in 100 µl distilled water (dH_2O) and a further 1:10 dilution was used for the Polymerase Chain Reaction (PCR).

Tail - Lysis Buffer:

1,5 M Tris-HCl

200 mM NaCl

0,2 % SDS

5 mM EDTA

500 ml dH_2O

PCR mix:

12 µl Taq PCR Master Mix

0,5 µl Primer (Forward/Reverse)

1,5 – 3 µl DNA

x µl dH_2O (add up to 25 µl in total)

PCR conditions for different mouse lines:
K-ras PCR:
94 °C 3´ 94 °C 30´´; 56 °C 1´; 72 °C 1´ (35 cycles) 72 °C 2´ 10 °C ∞
Cre PCR:
94 °C 5´ 94 °C 30´´; 58 °C 30´´; 72 °C 30´´ (35 cycles) 72 °C 7´ 4 °C ∞
MyD88 PCR:
94 °C 5´ 94 °C 1´; 62 °C 1´ 30´´; 74 °C 1´ (35 cycles) 74 °C 10´ 4 °C ∞
$MyD88^{fl}$ PCR (Primer 9481+9482):
94 °C 5´ 94 °C 30´´, 60 °C 1´, 72 °C 1´(35 cycles)

72 °C 7´ 4 °C ∞
TLR-4 CO PCR (Primer neu+mmt4):
95 °C 3´ 95 °C 30´´; 60 °C 30´´; 72 °C 3´ (35 cycles) 72 °C 2´ 4 °C ∞
TLR-4 KO PCR (Primer neu+mut):
95 °C 3´ 95 °C 30´´; 67 °C 1´; 74 °C 1´ (35 cycles) 72 °C 1´ 4 °C ∞
TLR-2 PCR:
94 °C 3´ 94 °C 10´´; 60 °C 30´´; 68 °C 1´ 30´´ (40 cycles) 68 °C 7´ 4°C ∞
IL-1R PCR:
94 °C 3´ 94 °C 20´´; 64 °C 30´´; 72 °C 35´´ (12 cycles) 94 °C 20´´; 58 °C 30´´; 72 °C 35´´ (25 cycles) 72 °C 2´ 10 °C ∞

3.1.3 Mouse treatment

Mice were supplemented with butyrate, probiotics or arabinogalactan. Sodium Butyrate (Aldrich, #303410) was orally gavaged three times a week (0,011 g/mouse in 100 µl water).

For probiotic treatment Symbiolact pur Pulver (SymbioPharm GmbH) was used. ½ package of bacteria (Lactobacillus acidophilus, Lactobacillus paracasei, Lactococcus

lactis, Bifidobacterium bifidum, Bifidobacterium lactis, one package contains 1 x 10^9 colony formimg units (cfu)) was provided in 250 ml drinking water.
Arabinogalactan (Fluka, A-09788) was orally gavaged three times a week (50 μg/g mouse diluted in 100 μl water).

3.1.4 Colonization with fecal samples

Mice at the age of six weeks were treated with a mixture of antibiotics for one week to deplete the bacteria in the intestine.
Antibiotic cocktail:
0,04285 g Ampicillin (Ratiopharm, F26162)
0,0215 g Vancomycin (Hikma, 43924TB21)
4,285 ml Neomycin (Sigma, N1142)
8,55 ml Metronidazol (Delta Select, 058071C)
in 200 ml water
Following antibiotic treatment mice received normal drinking water and were gavaged 3 times a week with fresh stool pellets from donor mice (approximately 9 x 10^6 bacteria).

3.1.5 Glucose Tolerance Test (GTT)

To evaluate hyperglycemia and insulin resistance in mice, Glucose Tolerance Test (GTT) was performed. Mice were fasted for 9 hours. 3 hours before the GTT, animals were transferred to a procedure room and separated in individual cages to acclimate. Following 9 hours of fasting, first basal glucose levels were measured using Blood Glucose Meter (Bayer, #3822850). Mice were then injected with 1,5 g/kg body weight of Glucose (Eitelfango) and blood glucose levels were recorded at 15´, 30´, 60´, 90´ and 120´. Simultaneously, plasma samples were collected to measure the insulin levels using Ultra Sensitive Rat Insulin ELISA Kit.

3.1.6 Blood Count

To perform blood count, 50 µl fresh blood, taken from the tail vein, was mixed directly with 8-10 µl EDTA K to avoid coagulation. From this sample a dilution was made with a Sysmex xt 2000i in dilution buffer to reach a minimal amount of 120 µl. Samples were directly measured by a Sysmex xt 2000i and calculated accordingly to the dilution.

3.1.7 Detection of endotoxin in circulation

Blood samples were assessed to measure the levels of endotoxin released from gram-negative bacteria using the kit Limulus Amebocyte Lysate (LAL) QCl-1000 (Lonza, #50-647U). Briefly, gram-negative infection of the horseshoe crab, Limulus polyphemus, results in intra-vascular coagulation, which is an enzymatic reaction between the endotoxin and a protein. The LAL kit uses the endotoxin reaction to activate an enzyme that produces a yellow colour. For the test, plasma samples were diluted 1:5 with LAL water and incubated for 10 min at 70 °C to inactivate plasma proteins. The test was performed according to the manufacturers instructions: all reactions were carried out at 37 °C. First, the samples were incubated with LAL for 10 min. The endotoxin in the samples hereby catalyzed the activation of a proenzyme in LAL. When in the next step a substrate solution was added, this activated proenzyme catalyzed the splitting of pNA of the substrate Ac-Ile-Glu-Ala-Arg-pNA. This release of pNA produced a yellow colour. The reaction was stopped after 6 min using a stop reagent and the absorbance was measured spectrophotometrically at 405 – 410 nm. As the intensity of the colour is dependent on the amount of endotoxin that is present in the sample, the concentration of endotoxin was hereby determined on the basis of a standard curve.

3.1.8 ELISA

ELISA was performed according to the manufacturers protocol. Briefly, the ELISA plate was coated with a capture antibody and incubated over night at 4 °C. After 3 washing steps wells were blocked with 1 x Assay Diluent. Standards and samples were incubated over night at 4 °C, followed by 5 washing steps. The detection antibody was incubated for 1 hour at room temperature, wells washed 5 times and for the enzyme reaction treated with Avidin-HRP for 30 min before wells were again washed 5 times. After the incubation of Substrate Solution for 15 min, the reaction was stopped with Stop Solution and read at 450 nm.

3.1.9 Animal sacrifice – Tissue harvesting and processing

Prior to sacrifice, mice were fasted overnight and injected intraperitoneally (IP) with 5´-Bromo-2´-deoxyuridine (BrdU) for 2 hours to visualize the proliferating cells. Mice were sacrificed by CO_2 inhalation followed by cervical dislocation. Tissues were harvested immediately and frozen in liquid nitrogen for further RNA and protein analysis. Furthermore one part of the tissues was fixed in 4 % Paraformaldehyde (PFA) overnight, then dehydrated (Leica, ASP 300 S) and embedded in paraffin for histological analysis. During the preparation of intestinal rolls, duodenum, jejunum, ileum and colon were flushed with cold PBS, cut longitudinally, rolled up on a stick from proximal to distal.

3.1.10 Cell isolation

3.1.10.1 Cell isolation from mesenteric lymph nodes and Peyer´s Patches

Mesenteric lymph nodes were collected and Peyer´s Patches were cut out of the intestine. Both were incubated at 37 °C for 20 min in a mixture of 3 ml RPMI, 15 µl Collagenase D (100 mg/ml) and 15 µl DNase I grade II (20 mg/ml). Tissue was passed through a filter and incubated at 37 °C for 10 min. The reaction was stopped

by the addition of 10 µl 0.5 M EDTA, and the volume was adjusted to 10 ml with RPMI. After centrifugation at 1700 rpm for 5 min, cells were resuspended in 500 µl FACS-/MACS-buffer and used either for FACS or dendritic cell isolation.

3.1.10.2 Cell isolation from lamina propria

The intestinal tissue was cut in 3 mm pieces, shaken vigorously in 25 ml RPMI and washed 3 times with PBS. Tissue pieces were then incubated in 50 ml PBS containing 0,015 g DTT and 500 µl 0,5 M EDTA with constant shaking at 37 °C for 20 min. With a cell strainer, the pieces were collected and transferred in 10 ml RPMI containing 50 µl DNase I grade II (100 mg/ml) and 50 µl Collagenase D (100 mg/ml), and incubated at 37 °C for 25 min in a rotating incubator. Cells were passed through a cell strainer and centrifuged at 1500 rpm for 5 min. The pellet was resuspended in 500 µl and either used for FACS or dendritic cell isolation.

3.1.10.3 T cell stimulation for Fluorescent activated cell sorting (FACS)

After the cell isolation from mesenteric lymph nodes, Peyer´s Patches and lamina propia, T cells were stimulated. Cells (about 2 x 10^6) were incubated in stimulation solution at 37 °C for 5 – 8 h. Afterwards dead cells were stained with 0,5 µg/ml Ethidium monoazide (EMA) for 15 min under light. After fixation with IC Fixation Buffer for 20 min on ice, cells were stained with fluorescent antibodies (1:200 dilution) plus Fc block (1:100 dilution) for another 20 min on ice and then directly used for FACS.

Stimulation solution:
RPMI
10 % FCS
1 % Penicillin/Streptavidin
20 ng/ml Phorbol 12-myristate 13-acetate (PMA)
1 µg/ml Ionomycin
1 µg/ml GogiPlug

3.1.10.4 Staining for FACS

Cells isolated from Peyer´s Patches, mesenteric lymph nodes and lamina propria were analysed by FACS. Approximately 1 x 10^6 cells were blocked with CD16/32 Fc Block for 10 min on ice, washed and centrifuged at 3000 rpm for 5 min. The first antibody was added and incubated for 20 min on ice. Cells were again washed and resuspended in FACS Buffer containing 0,05 µg/ml propidium iodide (PI) and used directly for the FACS. PI is used to identify dead cells, as it cannot enter live cells and becomes fluorescent when it binds to DNA.

FACS-buffer:
500 ml PBS
0,5 % FCS

3.1.10.5 Isolation of dendritic cells

Cells (10^7 cells/500 µl) were labelled using 2 µl of CD11c-FITC-antibody. The mixture was incubated at 4 °C under dark conditions. Then cells were washed with 1-2 ml MACS-buffer and centrifuged at 1800 rpm for 10 min. The pellet was resuspended in 450 µl MACS-buffer containing 50 µl anti-FITC-MicroBeads (Miltenyi Biotec, #120-000-293). The mixture was further incubated at 4 °C for 15 min, washed in 1 ml MACS-buffer and centrifuged 10 min at 1800 rpm. The pellet was diluted in 500 µl MACS-buffer. A column (Miltenyi Biotec, #130-042-201) was placed on a magnetic wall and washed 3 times with 500 µl MACS-buffer. Cells were transferred on the column and washed 3 times using 500 µl MACS-buffer. Then the column was removed from the magnetic wall and inserted in a falcon tube. 1 ml MACS-buffer was added and pressed with the plunge through the column into the falcon tube.

MACS-buffer:
500 ml PBS
2 % FCS
5 mM EDTA

3.1.11. Bone marrow transplantation (BMT) with T-cell depletion

For the bone marrow, a donor mouse was sacrificed and the bone of the hind leg was exposed from muscle and fat tissue. The bone was flushed with sterile PBS using a syringe. The bone marrow was collected in a falcon and stored on ice. Afterwards it was passed through a cell strainer in a new falcon and added up to 5 ml with sterile PBS. After centrifugation at 4 °C, 1500 rpm for 5 min, the pellet was resuspended in 500 µl MACS buffer. 12 µl CD3-FITC antibody was added and incubated for 20 min at 4 °C. Then it was centrifuged for 5 min at 1500 rpm and washed once with sterile PBS. The pellet was resuspended in 450 µl MACS buffer plus 50 µl FITC-MicroBeads and incubated again 20 min at 4 °C. After another washing step, the pellet was resuspended in 2 ml MACS-Buffer, applied on a prewashed MACS-column and washed three times with MACS-buffer. Cells that went through the column were counted, washed three times with sterile PBS and filtered through a 0,5 µm cell strainer. 2-4 x 10^6 cells in 100-150 µl PBS were used per mouse.
The recipient mice were irradiated at 9 Grey and the bone marrow was injected in the tail vein of the recipient mice. Mice were treated with 1 mg/ml of broad-spectrum antibiotic (Ciprobay, Bayer Vital GmbH) for two weeks to avoid donor-host rejection.

MACS-Buffer
PBS
0,5 % FCS
2 mM EDTA

Bone marrow transplantation was done in cooperation with the Institute of Molecular Immunology, Technical University of Munich.

3.2 Bacteria

3.2.1 Plating of bacteria

To check the composition of the microbiota, mouse feces were freshly collected. Briefly, 0,001 g feces were homogenized, and diluted in 1 ml sterile PBS. 100 µl from serial dilutions were plated on 4 different selective blood agar plates to distinguish the aerobic and anaerobic bacterial growth:

1 - MacConkey Agar for gram-negative, aerobic bacteria

2 - Columbia Agar for gram-positive, aerobic bacteria

3 - Schaedler Agar for anaerobic bacteria

4 - Schaedler-KV Agar for gram-negative, anaerobic bacteria

The plates for the detection of aerobic bacteria were incubated at 37 °C overnight. The plates for anaerobic bacteria were placed in a chamber under anaerobic conditions using AnaeroGen (Oxoid, #AN0025A) and incubated at 37 °C for about 48 hours. Single bacterial colonies were analysed by gram staining and Rapid ID and "colonies forming units (cfu´s) per ml" were calculated using following formula:

Cfu/ml = (n(colonies) x $10^{((n) \text{ of dilution})}$) / x ml (volume spread on the plate)

3.2.2 Gram Staining

Gram Stain Kit was used to stain and distinguish bacteria according to the property of their cell wall. Gram-positive bacteria have a thick layer (around 50 %) of peptidoglycan, while the gram-negative bacteria only have a thin (around 10 %) one. 1-2 bacterial colonies were smeared on microscope slides and heat-fixed. The slide was incubated for 1 min with each dilution of the kit and washed under tap water. First, all bacteria were stained with crystal violet, followed by the trapping agent iodine. In the third step, a decolourizer was used, which, due to the thin peptidoglycan layer, only removes the colour of the gram-negative bacteria. Last, slides were counterstained by Safranin.

3.2.3 Rapid ID

To identify anaerobic bacteria single colonies were picked and incubated further for 24 hours on Columbia-plates under anaerobic conditions. Then a solution was made with the bacteria and loaded on the Rapid ID 32 A (Biomérieux, #32300). The test was incubated 4 hours at 37 °C and then prepared for the reading according to the protocol.

3.2.4 Measurement of the short chain fatty acids (SCFA) in the stool samples

Fresh stool samples were collected from mice and immediately frozen in liquid nitrogen. To analyze the SCFA, the levels of acetate, propionate, butyrate, iso-valerate and valerate were measured with an HP 5890 series II gas chromatograph (Hewlett-Packard, Walbronn, Germany). This machine contains a HP-20 M column and a flame ionisation detector. The stool samples were diluted 1:5 with water. After centrifugation (5 min at 21000 g) 200 µl supernatant was added to the following ingredients:

23,6 µl Isobutyric acid (12 mM)

270 µl NaOH (1 M)

280 µl $HClO_4$ (0,36 M)

The mix was lyphilized over night and the remaining was diluted in 400 µl acetone containing 100 µl formic acid (5 M). After centrifugation 1 µl supernatant was used for the measurement.

Measurements were done in cooperation with Department of Gastrointestinal Microbiology, German Institute of Human Nutrition Potsdam-Rehbrücke, Nuthetal.

3.2.5 DNA Extraction from stool samples

Fresh stool samples from mice were collected and immediately frozen in liquid nitrogen. 200 mg stool was used for DNA extraction using the Qiagen Stool DNA Extraction Kit.

3.2.6 Pyrosequencing

To amplify the 16S rRNA from the stool samples, primers that span a highly conserved region were used, which yields approximately a 500 bp product (A-side and B-side). Fusion primers were designed for the sequencing (Primer A or Primer B) at the 5´-end and the A- or B-side at the 3´-end. To tag the different samples MIDs (multiplex identifier tags) were used in between.

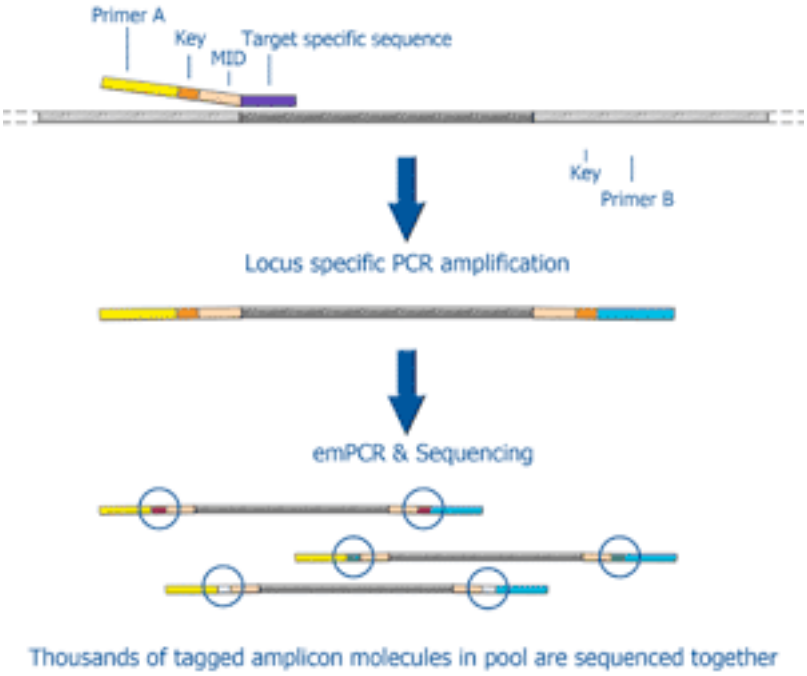

The PCR was made based on “Amplicon Library Preparation Method Manual” (Roche), using FastStart High Fidelity PCR System (Roche), 10 mM PCR Nucleotide Mix (Roche) and 10 ng stool DNA per reaction in 25 μl reaction volume.

The PCR program was as follows:
94 °C 3´
94 °C 15´´, 54 °C 45´´, 72 °C 1´ (30 cycles)
72 °C 8´
4 °C ∞

Negative control reactions were run using only one of the primers, respectively. Samples were purified on a 1,2 % agarose gel and amplicons were eluted from the gel slices. The further steps were performed according to Roche Protocols for the GS FLX Titanium Series (Library quantitation by fluorometry, Amplicon dilution and equimolar pooling, emPCR, Quality control, Amplicon sequencing).
Pyrosequenced amplicon libraries were screened for quality characteristics, chimeric sequences and PCR/pyrosequening-induced duplication artifacts using AmpiconNoise and Perseus software Version 1.25 [118, 119]. Cleaned data sets were the processed using the Qiime amplicon analysis pipeline version 1.5.0. Sequences were clustered into distance-based (97% similarity) operational taxonomic units (OTUs) using mothur version 1.25.0. Representatives of each OTU were aligned to GreenGenes core set alignment using PyNAST version1.1. Taxonomic assignments for each OTU were made using the Ribosomal Database Project (RDP) Classifier version 2.2. Relative abundance of each OTU served as input for the R PhylTemp function.
Bioinformatics were done in cooperation with Delaware Biotechnology Institute, University of Delaware.

3.3 Histology - Haematoxylin & Eosin (H&E) Staining

For stainings 3,5 μm sections were prepared from the paraffin blocks using a microtome (Mikrom, HM355S). Sections were laid in a 45 °C water bath, transferred to glass slides and dried at RT or 37 °C for at least 1 hour.
H&E staining was used to simply stain the nuclei and the cytoplasm. Sections were deparaffinized in Xylol and rehydrated in serial dilutions of ethanol. Sections were stained by incubating in Hematoxylin for 1 min, washed under tap water, followed by

incubation in Eosin Solution for about 10 seconds. Finally tissue was dehydrated again using serial ethanol-dilutions.

Rehydration:
10 min Xylol
2 min 100 % Ethanol
2 min 96 % Ethanol
2 min 80 % Ethanol
2 min 70 % Ethanol
2 min 50 % Ethanol
5 min PBS

Dehydration:
2 min 50 % Ethanol
2 min 70 % Ethanol
2 min 80 % Ethanol
2 min 96 % Ethanol
2 min 100 % Ethanol
10 min Xylol

Eosin Solution:
1 % Eosin Y Disodium Salt in dH_2O
15 drops acetic acid to 250 ml

Following the staining, the sections were dried at RT and covered with Mounting Medium and cover slips.
Histopathological evaluations were done in cooperation with Institute of Pathology, Ludwig Maximilian University.

3.4 Proteins

3.4.1 Protein extraction

Following harvesting, tissues were immediately frozen in liquid nitrogen and stored at -80 °C. The crushed tissue was homogenized in freshly prepared 1x Lysis Buffer with the phosphatase inhibitors and protease inhibitor 1 mM PMSF. After centrifuging full speed for 20 min at 4 °C, the supernatant was taken using a syringe and stored at -80 °C.

1x Lysis Buffer:
50 mM Tris HCl pH 7.5
250 mM NaCl
3 mM EDTA
3 mM EGTA
1 % Triton X-100
0,5 % NP40
10 % Glycerol
25 mM Na-pyrophosphate
1 Tablet Proteinase inhibitor per 50 ml

3.4.2 Determination of protein concentration and Western Blot

The protein concentration was detected using 2 µl of lysate in 1 ml of a 1:5 diluted BioRad protein assay, which contains a dye binding to basic and aromatic amino acid residues and causing a colour change of Coomassie Brillant Blue G-250 dye in the presence of different concentrations of protein. The intensity of the colour reaction was measured at 595 nm using a spectrometer (BioRad SmartSpec Plus). 10 µl of Laemmli Buffer with 5 % ß-mercaptoethanol was added to 40 µg of protein sample in 10 µl and proteins were denatured at 95 °C for 5 min. The samples were loaded on a 7-12 % SDS-polyacrylamide gel and run in 1x Running Buffer at 30 mA per gel using “BioRad Mini Protein Gel System”. The proteins in the gel were blotted onto a in methanol activated PVDF membrane (Zefa Laborservice, Immobilon-P,

#Z.IPVH00010) for 2 hours at 250 mA in 1x Transfer Buffer, using the Mini Trans-Blot Cell system (BioRad) under cool conditions. Gel and membrane were fixed on both sides in the sandwich using 2 layers of Whatman paper and one sponge. Following the transfer, the membrane was blocked for 30 min in 5 % Milk in PBS-Tween (0,1 % Tween 20) or 5 % BSA/PBS-Tween for phosphorylated antibodies. Then the first antibody in the same Milk/BSA solution was incubated on the membrane either overnight at 4 °C or for 3 hours at RT. The membrane was washed 3 times with PBS-Tween for 5 min each. The second antibody was diluted 1:3000 in 5 % Milk/PBS-Tween and incubated for 30 min. After 3 wash steps, the membrane was covered with ECL solution Super Signal West Pico for 5 min. The signal was detected by immediate exposure to an X-ray film (Thermo, #34089) for 10 sec to 10 min and the film developed using Hyperprocessor (Amersham Bioscience).

Laemmli Buffer:

3,55 ml dH_2O

1,25 ml 0,5M Tris-HCl pH 6,8

2,5 ml Glycerol

1 ml 20 % SDS

0,2 ml 0,5 % Bromophenol Blue

Gel, 7-12 %:

6,75-8,62 ml dH_2O

3,75 ml Main Gel Buffer

2,63-4,5 ml 40% Acrylamide

112,5 µl 10 % Ammoniumpersulfate

11,25 µl TEMED

Stacking Gel:

4,6 ml dH_2O

950 µl Stacking-Gel-Buffer

950 µl 40 % Acrylamide

62,5 µl 10 % Ammoniumpersufate

12,5 µl TEMED

Main Gel Buffer:

181,65 g Tris pH 8.8
20 ml 20 % SDS
adjust to 500 ml with dH_2O

Stacking-Gel-Buffer:
12,11 g Tris pH 7
5 ml 20 % SDS
adjust to 100 ml with dH_2O

10x Running Buffer:
15,15 g Tris
72 g Glycine
25 ml 20 % SDS
adjust to 500 ml with dH_2O

10x Transfer Buffer:
30 g Tris
144 g Glycine
adjust to 1 l with dH_2O

1x Transfer Buffer:
100 ml 10x Transfer Buffer
700 ml dH_2O
200 ml Methanol

3.4.3 EMSA (Electrophoretic mobility shift assay)

To study protein-DNA interaction, EMSA was performed. The principle is to incubate a radioactive labelled DNA sequence that contains consensus sequences for transcription factors, with proteins of interest. After loading on a gel, the DNA-protein complexes run in a reduced speed in comparison to the unbound DNA-fragments because of their molecular size and the radioactivity makes it possible to visualise these different complexes.

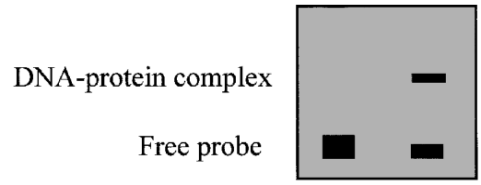

The oligonucleotide was first annealed by preparing a 1:10 dilution of forward and reverse stocks (40 nM) and incubating together at 80 °C for 10 min. Then it cooled down to RT and was stored at -20 °C.
The labelling of the oligonucleotide was carried out on ice as follows:

EMSA-mix:

2 µl oligonucleotide

39,5 µl dH_2O

5 µl 10x Polynucleotide kinase Buffer

1 µl T4 Polynucleotide kinase

2,5 µl (50 µCi) ^{32}P-γ-ATP

NF-$_{\kappa}$B Oligonucleotide

5´-AGT TGA GGG GAC TTT CCC AGG C-3´

3´-TCA ACT CCC CTG AAA GGG TCC G-5

The EMSA-mix was incubated at 37 °C for 30 min. During the incubation, a sepharose column for size exclusion was vortexed, the tip was broken off and spinned at 3000 rpm for 1 min. The mix was then transferred to the middle of the column and centrifuged at 3000 rpm for 1 min. The elution was stored at -20 °C for further use.

The samples were prepared as follows:

10 µg protein sample

2 µl 10 µg/µl BSA

2 µl 1 µg/µl dIdC

4 µl 5x Buffer F

2 µl Buffer D

0,5 -1 µl ^{32}P-γ-ATP labelled oligonucleotide

Buffer 5x F:
100 mM Hepes pH 7.9
20 % Glycerol
300 mM KCl
10 mM DTT
0,1 mM PMSF

Buffer D:
20 mM Hepes
20 % Glycerol
100 mM KCl
0,5 mM EDTA
0,25 % NP-40
2 mM DTT
0,1 mM PMSF

The samples were incubated at RT for 20 min. 4 % gel was prerun with the Loading Buffer at 150 V for about 20 min in 0.5x TBE. Samples were loaded on the gel and run at 200 V for about 1,5 h. The gel was transferred on 2 Whatman papers and dried at 80 °C for 1 h in a gel drier. The dried gel on the upper paper was exposed to a Kodak XAR5 film over night and developed using the Hyperprocessor.

4 % gel:
53,75 ml dH_2O
7,5 ml 5x TBE
10 ml 40 % Acrylamide
400 µl 10 % Ammoniumpersulfate
200 µl TEMED

5x TBE:
54 g Tris
27,5 g Boric Acid
20 ml 0.5 M EDTA pH 8.0

3.5 RNA

3.5.1 RNA Extraction

For RNA extraction, tissue was crashed in 1 ml Trizol. Samples were centrifuged for 10 min at 4 °C at 13200 rpm. The upper phase was collected and incubated at RT for 5 min. After adding 200 µl Chloroform and shaking for 15 sec, samples were further incubated at RT for 2-3 min and centrifuged for 15 min at 13200 rpm. The upper clear phase was collected carefully without touching the lower, organic phase. 400 µl Isopropyl alcohol and 400 µl High Salt Solution were added, incubated for 10-15 min at RT and then centrifuged for 10 min at 13200 rpm to precipitate the RNA. After discarding the supernatant, the pellet was washed with 75 % Ethanol and centrifuged for 5 min at 13200 rpm. The RNA pellet was dried at RT, dissolved in RNase free water and stored at -80 °C.

3.5.2 cDNA Synthesis

For the cDNA-synthesis a reaction mix was prepared as follows:

1 µg RNA
1 µl Oligo(dT) (500 µg/ml)
1 µl dNTP Mix (10 mM)
adjust to 12 µl with sterile dH_2O

The sample was heated up to 65 °C for 5 min, quickly transferred on ice and centrifuged. Then the enzyme-mix was added:

4 µl 5x First-Strand-Buffer
2 µl 0.1M DTT
1 µl RNase Out (40 units/µl)
1 µl SuperScript II RT

The sample was incubated for 50 min at 45 °C followed by the inactivation for 15 min at 70 °C. The cDNA was diluted with 80 µl dH_2O and stored at -20 °C.

3.5.3 Real-Time PCR

A Master Mix was prepared for each primer, pipetted into the wells of a 96 well-plate and 3 µl of cDNA was added.

Master Mix:
5 µl dH_2O
2 µl Primer
10 µl Syber Green MasterMix (ROX)

StepOnePlus Real Time PCR System (Applied Biosystems) was used for the Real-Time-PCR. The PCR conditions were as follows:

50 °C 2´
95 °C 10´
95 °C 15´´, 60 °C 1´ (40 cycles)

Cyclophilin was used as housekeeping gene. The Primers had a concentration of 100 pmol/µl. For the PCR they were diluted 1:10 and forward and reverse Primer used together in a mix.

3.5.4 Microarray

RNA samples were amplified and labeled using the Affymetrix One-Cycle Target Labeling Kit. The amplified and fragmented biotinylated cRNA was hybridized to Affymetrix MG 430A 2.0 arrays using standard procedures.
Data were processed and analyzed with R and Bioconductor [120] (R Development Core Team 2007*)*. Arrays were assessed for quality, RMA-normalized and filtered for

low and invariant expression. Differential gene expression between the groups was statistically assessed by SAM [121], which repeats permutations of the data to determine if the expressions of any genes are significantly related to the response. By SAM 36 differentially expressed genes between the groups were identified at the p-value (corrected for multiple testing FDR) cutoff of 0,0 %.
Data analysis was done in cooperation with Institute for Medical Microbiology, Immunology and Hygiene, Technical University of Munich.

3.6 Statistical analysis for multiple testing

Data were assessed for statistical significance. Mean values were compared by estimating a linear model for each sort of experiment. Relevant mean values were compared to each other in a hypothesis test (t-test) with the null hypothesis starting no difference in means. Test results were based on adjusted p values and reported as significant (*p value<0,05, **p value<0,01, ***p value<0,001). Adjusted p-values account for the number of test carried out (multiple test problem) and can therefore be used to control the group-wise error rate. The multiple testing adjustment is implemented in the glht (general linear hypothesis) function in packages multcom [122] in R (R Core Team 2012) [122, 123].
All data were proved for normal distribution. In some experiments it was not possible to confirm or to dismiss the normality assumption by statistical test due to the low number of replications in these experiments. Therefore samples were scanned for implausible values (outliers) and theoretical violation of the normality assumption, like measuring concentrations near the natural border zero. For tests involving groups where secure non-normality was found only the robust method was used (“robustbase”, Basic Robust Statistics. R package version 0.9-4) [124]. According to the robust method p values were only asymptotical valid and potentially too liberal.
Data analysis was performed in cooperation with Institute for Mathematical Statistics, Technical University of Munich.

3.7 Attachment Material and Methods

3.7.1 Bacterial plates

Columbia Agar (Biomérieux; #43049)
MacConkey Agar (Biomérieux; #43149)
Schaedler Agar (Biomérieux; #43279)
Schaedler-KV Agar (Biomérieux; #43223)

3.7.2 Commercial Kits

Gram Stain Kit (BD, #212539)
Limulus Amebocyte Lysate (LAL) QCl-1000 (Lonza, #50-647U)
Stool DNA Extraction Kit (Qiagen, #51504)
Mouse TNF alpha ELISA Ready-SET-Go! (eBioscience, #88-7324-22)
Ultra Sensitive Rat Insulin ELISA Kit (Crystal Chem. Inc., #90060) with Mouse Insulin Standard (Chrystal Chem. Inc., #90070)

3.7.3 Reagents and chemicals

(+)-Arabinogalactan (Fluka, #A-9788)
5´-Bromo-2´-deoxyuridine (Sigma, #B9285)
Acetic acid (Sigma, #45726)
Acrylamide (Merck, #1.00638.1000)
Ampicillin 2.0 (Ratiopharm, #F36162)
BioRad protein assay (BioRad, #500-0006)
Bovine serum albumin (Sigma, #A3059)
Collagenase D (Roche, #11088858001)
DNase I grade II (Roche, #10104159001)
EDTA (Fluka, #03609)
EDTA 0.5 M (Ambion, #AM9260G)

Eosin Y Disodium Salt (Sigma-Aldrich, #E4382)

Ethidium monoazide (Sigma, E2028)

Glycerol 2-phosphate disodium salt hydrate (Sigma, #221368)

Hematoxylin (Vector Laboratories, #H3401)

High Salt Solution (MRC, #PS161)

Hydrogen peroxide (Sigma, #H1009)

IC Fixation Buffer (eBioscience, #00-8222-49)

Ionomycin (Sigma, #10634)

Metronidazol (Delta Select, #058071C)

Mounting Medium (Vector Laboratories, #H5000)

NaCl (Fluka, #71376)

Neomycin Solution (Sigma, #N1142)

Paraformaldehyde (Electron Microskopy Sciences; #15710)

PCR Master Mix (Qiagen, #201445)

Permeabilisation Buffer (eBioscience, #88-8823)

Phorbol 12-myristate 13-acetate (PMA) (Sigma, #P8139)

Propidium Iodide (eBioscience, # BMS500PI)

Proteinase K (Qiagen, #1017738)

Proteinaseinhibitor (Roche, #11836170001)

Rodent Diet with 60kcal % Fat (Research Diets, #D12492)

Rodent Standard Diet (Altromin, #1314)

RPMI (GIBCO, #21875)

SDS (Roth, #2326.2)

Sodium Butyrate (Aldrich, #303410)

Sodium fluoride (Sigma, #S7920)

Sodium orthovanadata (Sigma, #S6508)

Sodium Pyrophosphate decarhydrate (Sigma, #221368)

Super Signal West Pico (Thermo, #1856135/36)

Syber Green MasterMix (ROX) (Roche, #14879600)

Symbio Lact (SymbioPharm GmbH, #243)

TEMED (Sigma, #T9281)

Tris/Hcl (Roth, #4855.2)

Trizol (TRI Reagent Soln., Ambion, #AM9738)

Vancomycin 1000mg (Hikma, #43924TB21)

3.7.4 Antibodies

APC-F4/80 (eBioscience, #17.4801.80)
CD16/32 Fc Block (BD Pharmingen, #553142)
CD3 FITC (BD Pharmingen, #555274)
CD3e Alexa Fluor 700 (eBioscience, #56-0033)
CD4 efluor 450 (eBioscience, #48-0041)
CD8a APC (eBioscience, #17-0081)
CD45 (BD Pharmingen, #553089)
CD45 Alexa Fluor 700 (eBioscience, #56-04151)
CD11b-FITC-antibody (eBiosciences, #557396)
CD11b APC eFluor 780 (eBioscience, #47-0112)
CD11c-FITC-antibody (BD Pharmingen, #557400)
cRel (Santa Cruz, #sc-71)
F4/80 FITC (eBioscience, #11-4801)
FoxP3 PE (eBioscience, #12-4774)
GolgiPlug (BD Bioscience, #51-2301KZ)
IFNγ PerCP Cy5.5 (eBioscience, #45-7311)
IL-4 PE Cy7 (eBioscience, #25-7042)
MHCII APC (eBioscience, #17-5321)
NFkB-p50 (Santa Cruz, #sc-7178)
NFkB-p65 (Santa Cruz, #sc-372)
NFkB-p100/p52 (Cell SIgnaling, #4882)

3.7.5 Primers

3.7.5.1 Primers for PCR

K-ras-5´: 5`-CCA TGG CTT GAG TAA GTC TGC G-3`
K-ras-3´: 5`-CGC AGA CTG TAG AGC AGC G-3`
Cre 370 FP: 5'- ACC TGA AGA TGT TCG CGA TTA TCT-3'
Cre 370 RP: 5'- ACC GTC AGT ACG TGA GAT ATC TT-3'
MyD88 F: 5´-TGG CAT GCC TCC ATC ATA GTT AAC C-3´
MyD88 R: 5´-GTC AGA AAC AAC CAC CAC CAT GC-3´

MyD88 neo: 5´-ATC GCC TTC TAT CGC CTT CTT GAC G-3´
9481: 5´-GTT GTG TGT GTC CGA CCG T-3´
9482: 5´-GTC AGA AAC AAC CAC CAT GC-3
TLR4 neu: 5´-GTT TAG AGA ATC TCG TGG CTG TGG AGA C-3´
TLR4 mmt4: 5´-TAT ATG CGG CCG CTC ATC TGC TGT ACT TTT TAC AGC C-3´
TLR4 mut: 5´-TGT TGG GTC GTT TGT TCG GAT CCG TCG-3´
TLR2 (1): 5´-CTT CCT GAA TTT GTC CAG TAC AGG G-3´
TLR2 (2): 5´-GGG CCA GCT CAT TCC TCC CAC TCA T-3´
TLR2 (3): 5´-TCG ACC TCG ATC AAC AGG AGA AGG G-3´
IL1R (1): 5´-CCA CAT ATT CTC CAT CAT CAT CTC TGC TGG TA-3´
IL1R (2): 5´-TTT CGA ATC TCA GTT GTC AAG TGT GTC CC-3´

3.7.5.2 Primers for Real-time PCR

Cyclophilin F: 5´-ATGGTCAACCCCACCGTGT-3´
Cyclophilin R: 5´-TTCTGCTGTCTTTGGAACTTTGTC-3´
TNF-α F: 5´-ACTCCAGGCGGTGCCTATG-3
TNF-α R: 5´-GAGCGTGGTGGCCCCT-3
IL-1β F: 5´-GTGGCTGTGGAGAAGCTGTG-3
IL-1β R: 5´-GAAGGTCCACGGGAAAGACAC-3
IL-6 F: 5´-ATGGTACTCCAGAAGACCAGAGGA-3
IL-6 R: 5´-GTATGAACAACGATGATGCACTTG-3
F4/80 F: 5´-CTTTGGCTATGGGCTTCCAGTC-3
F4/80 R: 5´-GCAAGGAGGACAGAGTTTATCGTG-3

3.7.5.3 Primers for sequencing

Sequencing primer:
Primer A: 5'-CGTATCGCCTCCCTCGCGCCA-3´
PrimerB: 5´-CTATGCGCCTTGCCAGCCCGC-3´

Key: 5´-TCAG-3

MIDs used:

MID-01: ACGAGTGCGT
MID-02: ACGCTCGACA
MID-03: AGACGCACTC
MID-04: AGCACTGTAG
MID-05: ATCAGACACG
MID-06: ATATCGCGAG
MID-07: CGTGTCTCTA
MID-08: CTCGCGTGTC
MID-10: TCTCTATGCG
MID-11: TGATACGTCT
MID-12 TCGTCGCTCG
MID-13: CATAGTAGTG
MID-14: CGAGAGATAC
MID-15: ATACGACGTA
MID-16: TCACGTACTA
MID-17: CGTCTAGTAC
MID-18: TCTACGTAGC
MID-19: TGTACTACTC
MID-20: ACGACTACAG
MID-21: CGTAGACTAG
MID-22: TACGAGTATG
MID-23: TACTCTCGTG
MID-24: TAGAGACGAG

3.7.5.4. Oligonucleotide used for EMSA

NF_kB: 5´-AGT TGA GGG GAC TTT CCC AGG C-3´
3´-TCA ACT CCC CTG AAA GGG TCC G-5´

4. Results

4.1. Mice with constitutive oncogenic K-ras-activation in the intestine

Intestinal cancer is the fourth leading cause of cancer associated deaths worldwide and mutations in the K-ras gene represent one of the most prominent events during the carcinogenic sequence in the gastrointestinal tract. To investigate the tumorigenic process in the intestine, K-ras^{G12D} mutants [117] were crossed to Villin-cre transgenics and fed on normal diet (ND). Villin is an actin-binding protein, which is mainly expressed in enterocytes. Thus, following recombination mice with oncogenic K-ras activation specifically in the intestinal epithelial cells were generated [125]. These mice showed normal birth and growth rates as the control (CO) littermates. Observing the weight curves over 24 weeks there was no difference between the K-ras$^{G12D\text{-}Villincre}$ (ViRas) mice in comparison to littermate COs (Figure 4.2 A). However there was macroscopically visible difference in the thickness as well as in the length of the whole intestine in ViRas mice (Figure 4.1 A). Further, the villi showed a distinct branching and serration (Figure 4.1 E), which was also observed in the crypts of the colon (Figure 4.1 F, G) that was missing in the CO animals (Figure 4.1 B, C, D).
Around 30 % of the ViRas mice displayed hyperplastic polyps after approximately 6 to 7 months on ND (Figure 4.1 H). However no adenoma, carcinoma or metastasis were detected in any of these animals. Furthermore no changes in blood count, more precisely red blood cells (RBC), hemoglobin (HGB), hematocrit (HCT) that could indicate anemia, as well as white blood cells (WBC) as an indication of inflammation were visible (Figure 4.1 I).
Thus, oncogenic K-ras activation in the intestinal epithelial cells led to changes in the architecture of the intestine and resulted in the development of hyperplastic polyps in both the small intestine and colon of the mice.

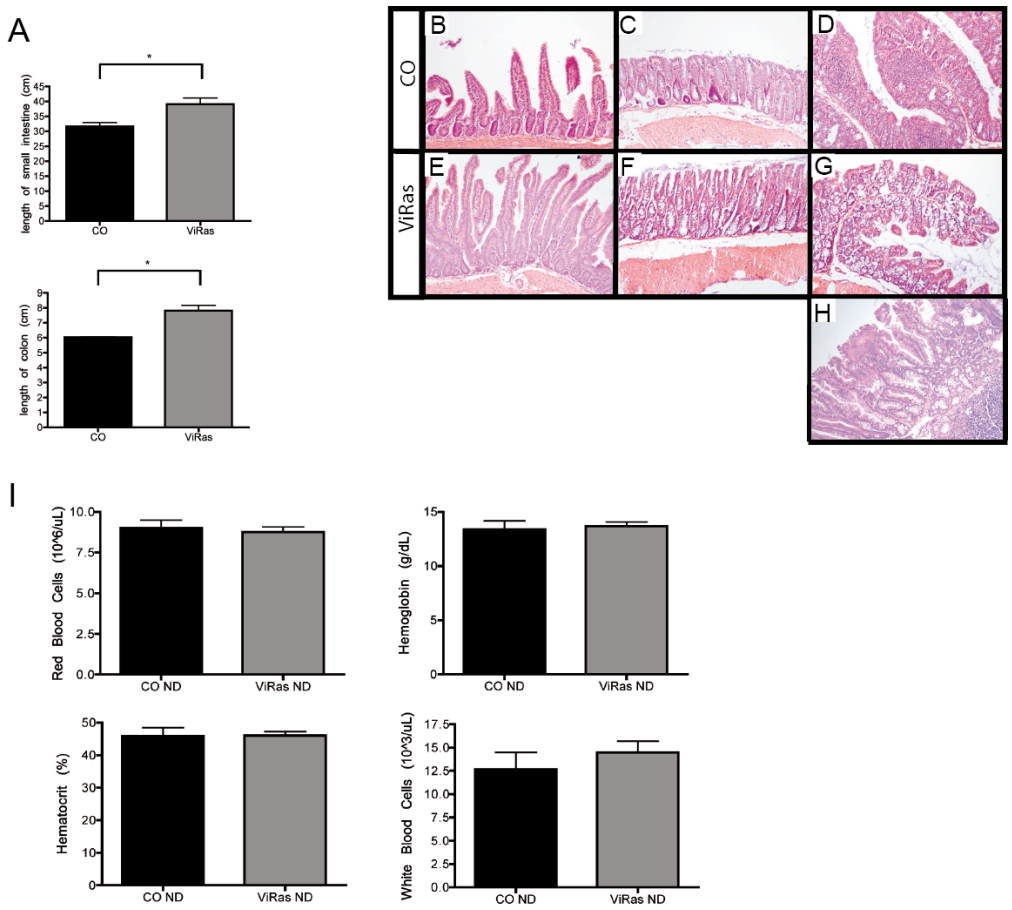

Figure 4.1: K-ras expression in the intestinal epithelial cells leads to histological changes but no changes in blood count. A: The length of the small intestine and colon of CO (n=3) and ViRas (n=6) mice after 24 weeks on ND (statistics made with t-test, *p<0,05). **B-G:** Representative picture of the histology of duodenum **(B)** and colon **(C, D)** of a CO mouse and duodenum **(E)** and colon **(F, G)** of a ViRas mouse on ND (10x magnification). **H:** Representative picture of a hyperplastic polyp in the duodenum of a ViRas mouse on ND (10x magnification). **I:** Blood count of CO (n=4) and ViRas (n=6) mice after 16 weeks on ND.

4.2. High fat diet accelerates adenocarcinoma sequence in the intestine

It has been shown that obesity is one of the major risk factors for gastrointestinal cancer. To investigate the role of diet-induced obesity in intestinal cancer development, mice were fed with a high fat diet (HFD) (60 % kcal obtained from fat). Since ViRas mice only show histological differences but no tumor development on ND, it provided an appropriate mouse model to investigate the effect of diet-induced obesity on tumorigenesis.

In contrast to the ViRas mice that were kept on ND, which showed similar weight gain as their littermate COs, mice fed on HFD displayed significant weight differences

(Figure 4.2 A). Meanwhile CO mice showed a steady increase until they reached 55 – 60 g, ViRas mice stayed at a median weight of approximately 35 g following 24 weeks on the diet regimen. After 16 weeks on diet, blood counts were checked (Figure 4.2 B). While the mice on ND did not show any changes between the genotypes (Figure 4.1 I) however on HFD there was a significant decrease in RBC, HBG and HCT, which indicates a state of anemia. Furthermore a trend towards an increase in the WBC was observed that could suggest increased infection in these animals, although this difference did not reach statistical significance.

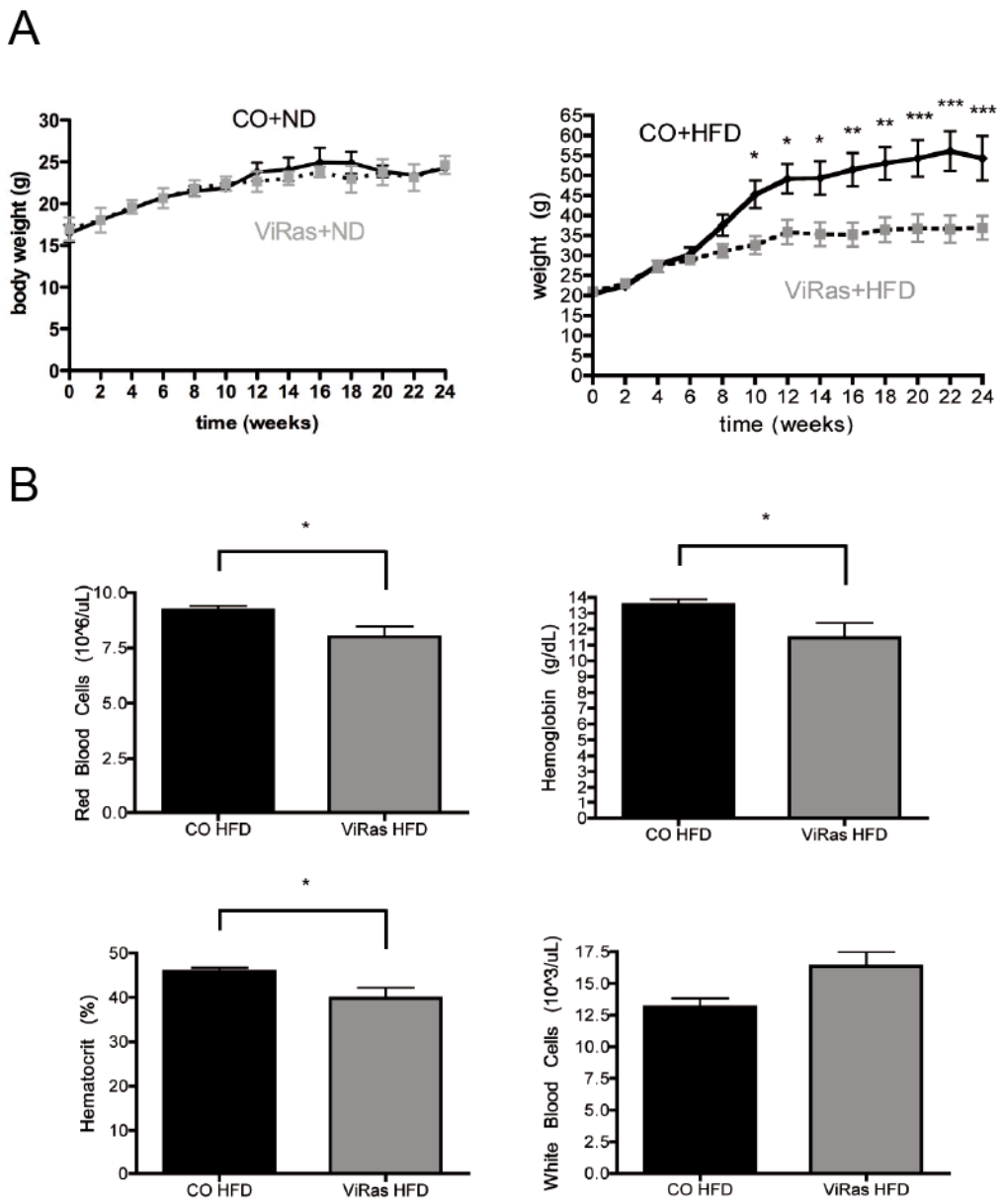

Figure 4.2: Mice with K-ras expression showed significant changes in weight gain and blood cell count when fed on HFD. A: Weight curve of CO and ViRas mice on ND (CO: n=4, ViRas: n=6) and HFD (CO: n=5, ViRas: n=7) monitored over 24 weeks (statistical analysis made for multiple testing, *p<0,05, **p<0,01,

***<0,001). **B:** Blood count of CO and ViRas mice (n=15) after 16 weeks on HFD (statistics done with t-test, p-values adjusted for multiple testing, *p<0,05).

Importantly 60 % of the ViRas mice fed on HFD developed tumors in the proximal part of the small intestine (majorly in the duodenum and jejunum), but not in the colon. Up to 5 tumors per mouse were detected that were classified as typical serrated adenoma and adenocarcinoma (Figure 4.3 A, B). Further two mice showed metastasis in liver, pancreas and spleen (Figure 4.3 C, D, E) only when they were fed on HFD for over 47 weeks. This stands in contrast to the ViRas mice on ND, which showed neither adenomas nor adenocarcinoma or metastasis in other organs. These results suggest that HFD strongly impairs health in mice and increases tumor incidence in the small intestine.

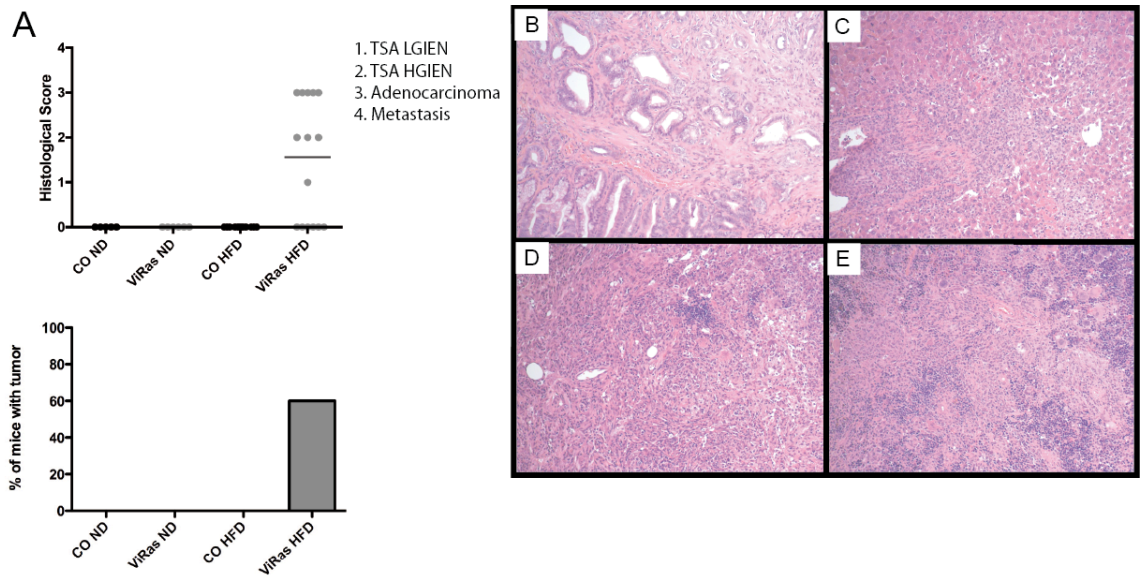

Figure 4.3: HFD increases tumor incidence in the small intestine and metastases in other organs in ViRas mice. A: Histological score and percentage of tumors in mice after 24 weeks on either ND (CO: n=5, ViRas: n=6) or HFD (CO: n=13, ViRas: n=15). **B:** Representative picture of an adenocarcinoma in the duodenum of ViRas mouse on HFD with metastasis to **C:** liver, **D:** pancreas and **E:** spleen (all 20x magnification)

4.3. High fat diet increases tumor incidence independent of insulin resistance

Obesity appears to be a major risk factor in the development of diseases, such as diabetes, cardiovascular diseases and cancer. Indeed obese individuals have an

increased risk to develop insulin resistance [24]. Importantly however insulin resistance is also suggested to be associated with tumor development. To elucidate whether HFD induced insulin resistance is linked to carcinogenesis in ViRas mice, we tested insulin sensitivity by performing a Glucose Tolerance Test (GTT). To do so, mice were fasted and injected with 1.5 g/kg body weight of glucose. Blood glucose levels were measured in certain time interval as well as blood samples were withdrawn to check for glucose-stimulated insulin secretion by ELISA. ViRas mice on ND showed a trend towards higher insulin sensitivity than their CO littermates as they had lower fasting blood glucose levels and showed a faster glucose clearance following injection (Figure 4.4 A). Additionally fasting insulin levels were lower in ViRas mice (Figure 4.4 B). In agreement with increased weight gain, CO mice on HFD showed high fasting blood glucose levels (140 mg/dl). However fasting glucose values in ViRas mice remained around 90 mg/dl (Figure 4.4 C). Although the curves remained overall lower in ViRas mice, it took both groups nearly 2 hours to reach their initial blood glucose level after the injection. Interestingly, however there was a significant difference in the insulin levels of the HFD mice (Figure 4.4 D). While CO mice on ND had relatively higher insulin secretion than ViRas mice, the difference on HFD between the genotypes was more evident.

Overall, HFD induced hyperglycemia and consequent hyperinsulinemia in mice. Although under ND conditions both groups of mice were equally glucose tolerant, however ViRas animals remained significantly insulin sensitive during HFD suggesting enhanced carcinogenesis was not associated to insulin resistance in the animals.

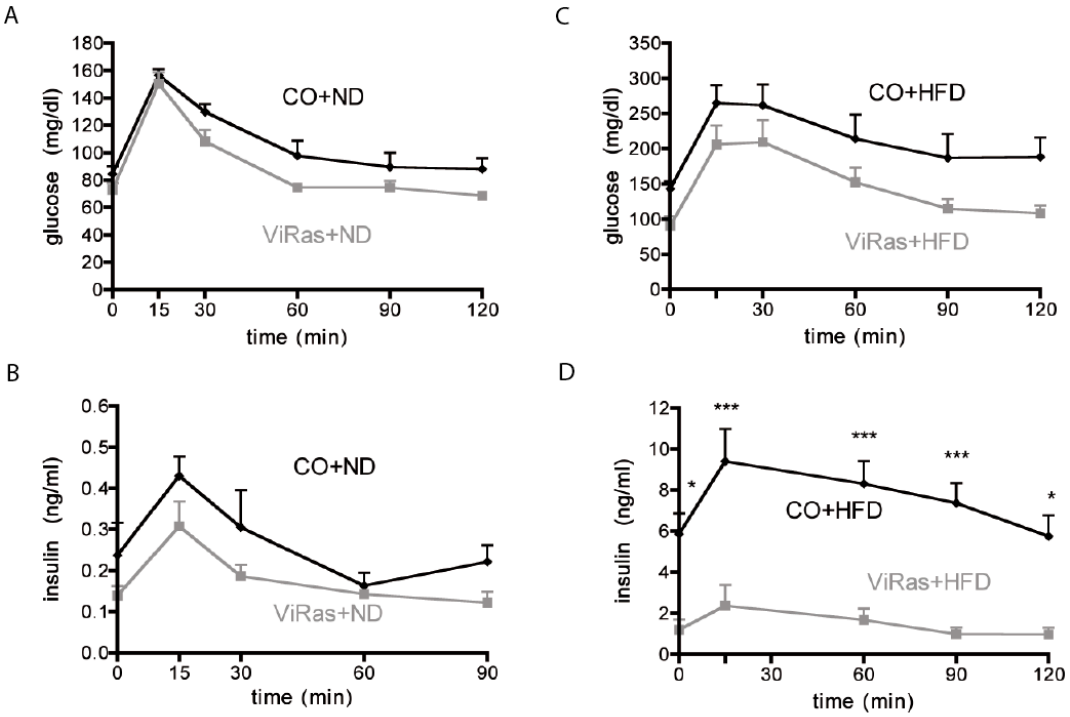

Figure 4.4: Control mice on HFD develop insulin resistance and hyperglycemia while ViRas mice remain insulin sensitive. A-B: Glucose **(A)** and insulin **(B)** levels during GTT in mice fed on ND (CO: n=3, ViRas: n=5). **C-D:** Glucose **(C)** and insulin **(D)** levels during GTT in mice fed on HFD (CO: n=8, ViRas: n=5). (Statistical analysis made for multiple testing, *p<0,05, ***p<0,001)

4.4. ViRas mice show activation of the NF-$_k$B pathway but no increase in related inflammatory cytokines

It is now widely accepted that obesity is an inflammatory condition and that adipocytes can produce pro-inflammatory cytokines such as TNF-α and IL-1β in addition to many other adipokines that can recruit inflammatory cells. Importantly inflammation appears to be a major component of tumorigenesis. It is known that while on one hand inflammatory responses have the ability to promote tumor development, on the other hand increased immune response is important for cancer cell killing [105]. To elucidate whether the HFD-enhanced tumor development is linked to increased inflammation, the NF-$_k$B pathway was observed. To check DNA-protein interaction, NF-$_k$B EMSA was performed using small intestinal samples from CO and ViRas mice (Figure 4.5 A). Interestingly there was an increased NF-$_k$B DNA binding in ViRas intestine in comparison to the COs. Further, when different members of both the classical and alternative pathway were compared between the

genotypes and diets by Western Blot (Figure 4.5 A), increased RelA, RelB, c-Rel and p105 were observed in ViRas small intestinal samples in comparison to CO mice. As the activation of the NF-$_k$B pathway results in pro-inflammatory cytokine production, the expression of TNF-α, IL-1β and IL-6 levels were analyzed by RT-PCR in duodenum as well as in colonic samples (Figure 4.5 B). Furthermore, using the surface marker F4/80, macrophage recruitment was observed, which represent the dominant cell type for NF-$_k$B activation during tumorigenesis (Figure 4.5 B). No difference was observed for the cytokine expression in ViRas mice, although there was a tendency towards a decrease, which is contradictory to the increase in the NF-$_k$B pathway. Moreover, we saw a significant decrease in F4/80 expression in ViRas mice and further a significant reduction in TNF-α levels visible in the blood plasma of ViRas HFD mice in comparison to their CO littermates (Figure 4.5. C). Collectively, these results suggest that increased NF-$_k$B signaling may be restricted to the epithelial cell compartment since the macrophage activation as well as consequent pro-inflammatory cytokine expression seemed to be decreased during tumorigenesis in ViRas mice.

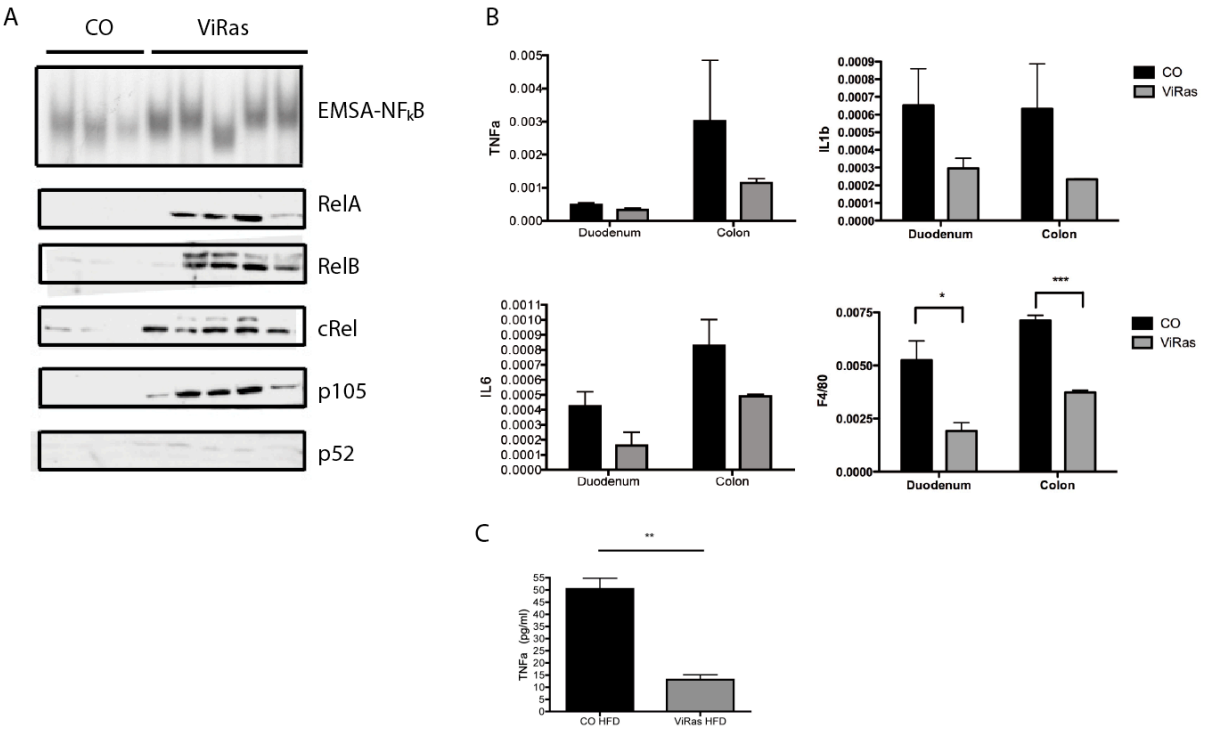

Figure 4.5: ViRas mice show an up-regulation in members of the NF-$_k$B pathway but a decrease in downstream pro-inflammatory cytokines. A: NF-$_k$B-EMSA and Western Blot with NF-$_k$B subunits (RelA, RelB, c-Rel, p105, p52) using proteins from duodenum of CO and ViRas mice after 23 weeks on HFD. **B**: TNF-α, IL-1β, IL-6 and F4/80 mRNA levels in duodenum and colon samples from CO and

ViRas mice after 23 weeks on ND **C:** TNF-α levels in the blood plasma samples of CO and ViRas mice after 23 weeks on HFD. (B and C: n=3, statistics made with t-test, *p<0,05, **p<0,01, ***p<0,001).

4.5. ViRas mice show down-modulation of the host immune response

As the pro-inflammatory cytokine expression was slightly down-regulated in the ViRas mice during tumor development in the small intestine we investigated immune response in these animals in further detail. In order to do so, gene expression was checked by microarray using RNA from the duodenum of CO and ViRas mice under both ND and HFD condition. Genes involved in pathogenic antigen recognition such as C-type lectin domain family were down-regulated, while angiopoetin-like 4, which is secreted by tumor cells that is known to promote tumorigenesis [126] was up-regulated in ViRas mice, especially after HFD. Furthermore, expression of genes related to immune response, such as T-cell specific GTPase and immunoglobulin lambda chain, as well as interferon related genes were reduced in ViRas mice in comparison to CO animals. In addition to the decrease observed in mice with oncogenic K-ras activation, there was a further decrease after HFD in genes involved in immune response. Especially expression of genes related to Fc receptor and histocompatibility class II involved in the binding and presentation of antigens to immune cells, such as macrophages and dendritic cells, were down-regulated. Further, defensin related cryptidin, Reg3a, that is active against bacteria, fungi and viruses was decreased in ViRas mice, suggesting an overall down-modulation of immunity due to K-ras activation, which is further suppressed following high fat feeding. Thus not only the cytokine expression, but also the recognition and presentation of antigens seemed to be down-regulated following oncogenic K-ras activation that was further repressed after HFD, suggesting a possible mechanism for the tumor cells to escape from host immunity.

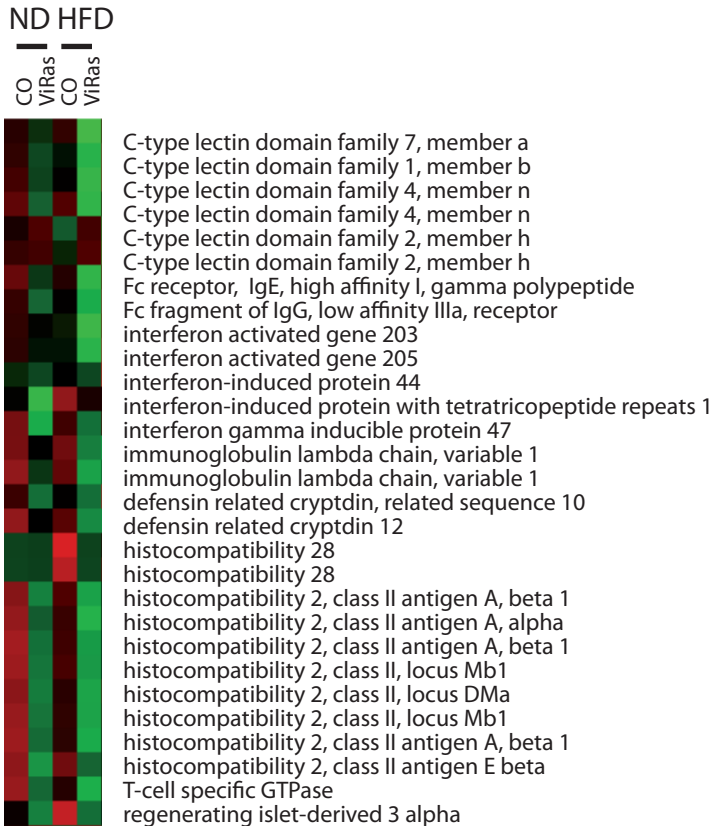

Figure 4.6: Genes that are important for the immune system are down-regulated in ViRas mice in comparison to CO mice on ND that are further altered after HFD. Microarray using RNA from the duodenum of CO and ViRas mice after 23 weeks on ND (CO: n=2, ViRas: n=3) and HFD (CO: n=2, ViRas: n=2), showing alterations in genes involved in pathogen recognition and host immune response.

4.6. ViRas mice show decreased antigen-presentation in dendritic cells

As suppressed host immunity may favor tumor development, we checked immune cells from the small intestine by FACS analysis. Therefore cells extracted from mesenteric lymph node (MLN), Peyer´s Patches (PP) and lamina propria (LP) from the small intestine of CO and ViRas mice under ND or HFD condition were sorted. Importantly MHC II - $CD11c^+$ double positive dendritic cells were decreased especially in the LP of ViRas mice (Figure 4.7 A). As for the activation of $CD11c^+$ cells, no change in CD86 was observed (Figure 4.7 B). Furthermore, MHC II - $CD11b^+$ double positive cells were also slightly decreased (Figure 4.7 C). When

$CD11c^+$ dendritic cells from the LP were gated on MHC II there was an obvious decrease in ViRas mice in comparison to their COs (Figure 4.7 D).

Moreover, MHC II on $CD11c^+$ cells (Figure 4.7 E and H), CD86 on $CD11c^+$ cells (Figure 4.7 F and I) and MHC II on $CD11b^+$ cells (Figure 4.7 G and J) were checked in PP and MLN from ViRas mice in comparison to COs (Figure 4.7 H-J). However the decrease was only observed in PP but not in MLN (Figure 4.7 E-G) in mice fed with high fat food.

These results suggest decreased antigen presentation in the dendritic cells of the LP both under ND and HFD condition thereby, confirming our previous finding that oncogene activation in combination with high fat feeding masks immune response by altering recognition of bacteria and perhaps tumor antigens therefore allowing tumor cells to escape from host immunity.

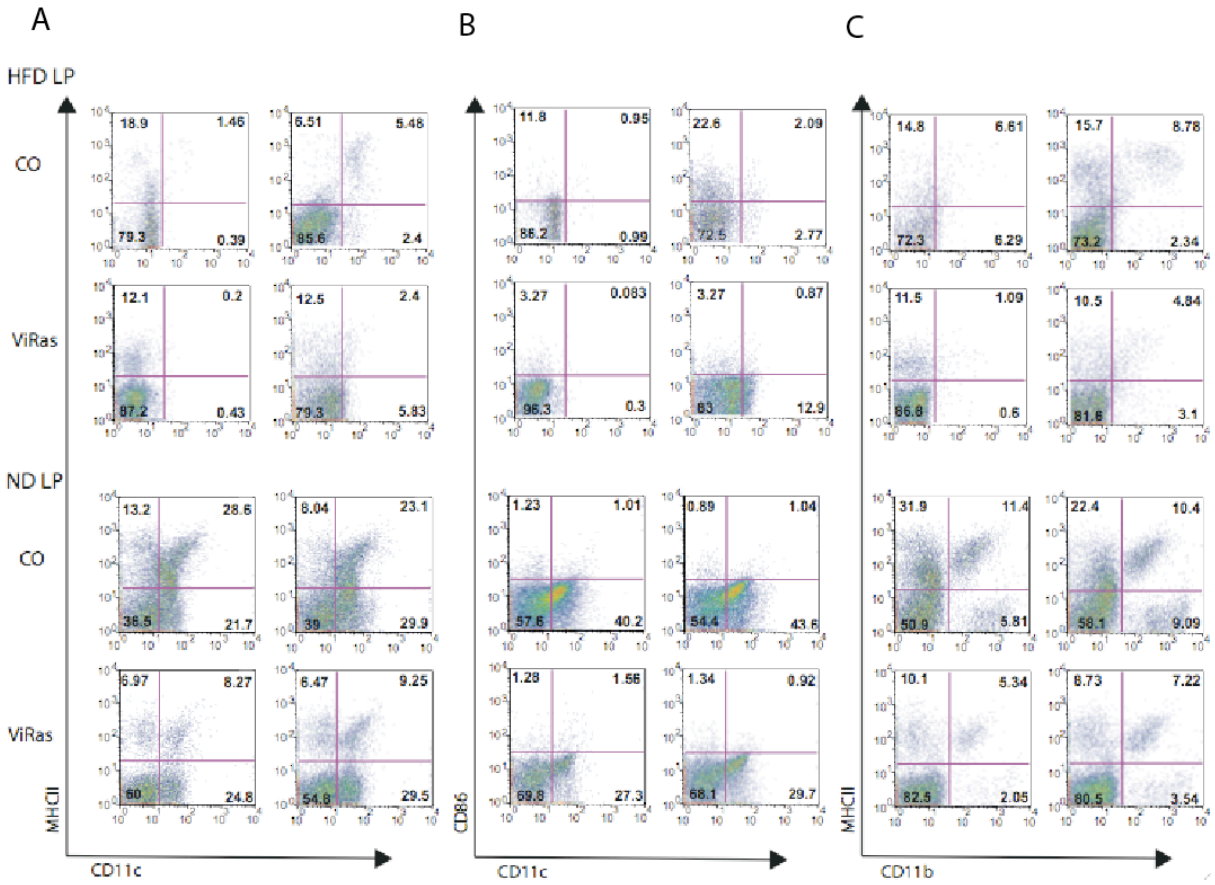
A
B
C
HFD LP
CO
ViRas
ND LP
CO
ViRas
MHCII
CD11c
CD86
CD11c
MHCII
CD11b
18.9
1.46
79.3
0.39
5.51
5.48
85.6
2.4
12.1
0.2
87.2
0.43
12.5
2.4
79.3
5.83
13.2
28.6
36.5
21.7
8.04
23.1
39
29.9
6.97
8.27
60
24.8
8.47
9.25
54.8
29.5
11.8
0.95
86.2
0.99
22.6
2.09
72.5
2.77
3.27
0.083
96.3
0.3
3.27
0.87
83
12.9
1.23
1.01
57.6
40.2
0.89
1.04
54.4
43.6
1.28
1.56
69.8
27.3
1.34
0.92
68.1
29.7
14.8
6.81
72.3
6.29
15.7
8.78
73.2
2.34
11.5
1.09
86.8
0.6
10.5
4.84
81.6
3.1
31.9
11.4
50.9
5.81
22.4
10.4
58.1
9.09
10.1
5.34
82.5
2.05
8.73
7.22
80.5
3.54

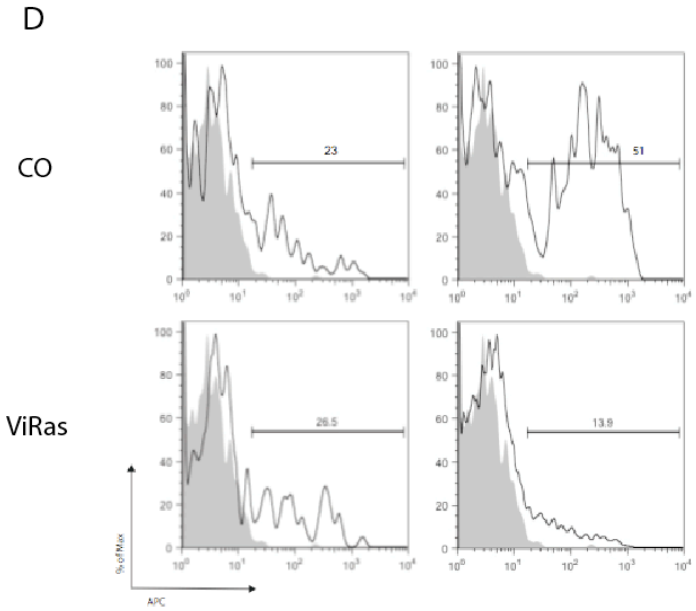
D
CO
ViRas
23
51
26.5
13.9
% of Max
APC

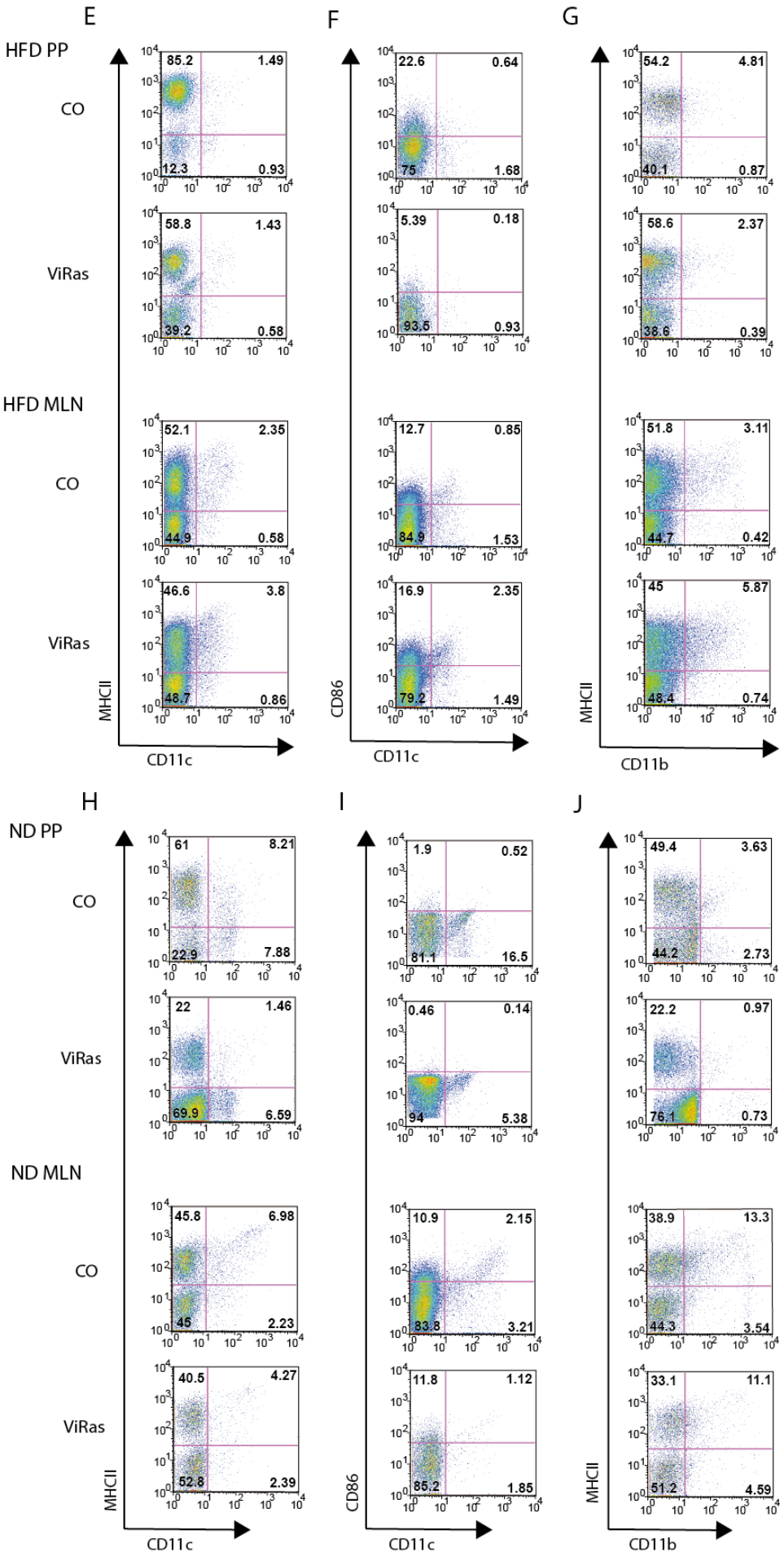
E
F
G
HFD PP
CO
ViRas
HFD MLN
CO
ViRas
MHCII
CD11c
CD86
CD11c
MHCII
CD11b
85.2
1.49
12.3
0.93
58.8
1.43
39.2
0.58
52.1
2.35
44.9
0.58
46.6
3.8
48.7
0.86
22.6
0.64
75
1.68
5.39
0.18
93.5
0.93
12.7
0.85
84.9
1.53
16.9
2.35
79.2
1.49
54.2
4.81
40.1
0.87
58.6
2.37
38.6
0.39
51.8
3.11
44.7
0.42
45
5.87
48.4
0.74
H
I
J
ND PP
CO
ViRas
ND MLN
CO
ViRas
MHCII
CD11c
CD86
CD11c
MHCII
CD11b
61
8.21
22.9
7.88
22
1.46
69.9
6.59
45.8
6.98
45
2.23
40.5
4.27
52.8
2.39
1.9
0.52
81.1
16.5
0.46
0.14
94
5.38
10.9
2.15
83.8
3.21
11.8
1.12
85.2
1.85
49.4
3.63
44.2
2.73
22.2
0.97
76.1
0.73
38.9
13.3
44.3
3.54
33.1
11.1
51.2
4.59

Figure 4.7: ViRas mice show decreased antigen presenting CD11c$^+$ cells and MHC II on CD11c$^+$ cells. A-C: FACS analysis using LP from CO and ViRas mice for CD11c-MHC II **(A)**, CD11c-CD86 **(B)** and CD11b-MHC II **(C). D:** CD11c$^+$ LP cells from CO and ViRas mice on HFD gated on MHC II. **E-G:** FACS analysis using PP and MLN from CO and ViRas mice on HFD for CD11c-MHC II **(E)**, CD11c-CD86 **(F)** and CD11b-MHC II **(G)**. **H-J:** FACS analysis using PP and MLN from CO and ViRas mice on ND for CD11c-MHC II **(H)**, CD11c-CD86 **(I)** and CD11b-MHC II **(J)**.

4.7. ViRas mice on HFD show no increase of T cells in LP

T cells play a crucial role in adaptive immunity. CD4$^+$ cells produce cytokines when they are activated via detection of antigens presented by MHC II on dendritic cells. CD8$^+$ cells have the ability to destroy tumor cells. On the other hand regulatory T cells (FOXP3$^+$) are important for the immunological tolerance. As there was a down-regulation of the immune system in ViRas mice we wanted to evaluate whether decreased MHC II on dendritic cells led to a decreased antigen presentation to T-cells. Cells of LP were isolated from the small intestine of CO and ViRas mice after 24 weeks on HFD. Cells were stimulated and then checked for T cell population, as well as cytokine (IFN-γ and IL-4) release via FACS analyses. In cells of LP no difference in T cell population or cytokine release between CO and ViRas mice was detected (Figure 4.8).

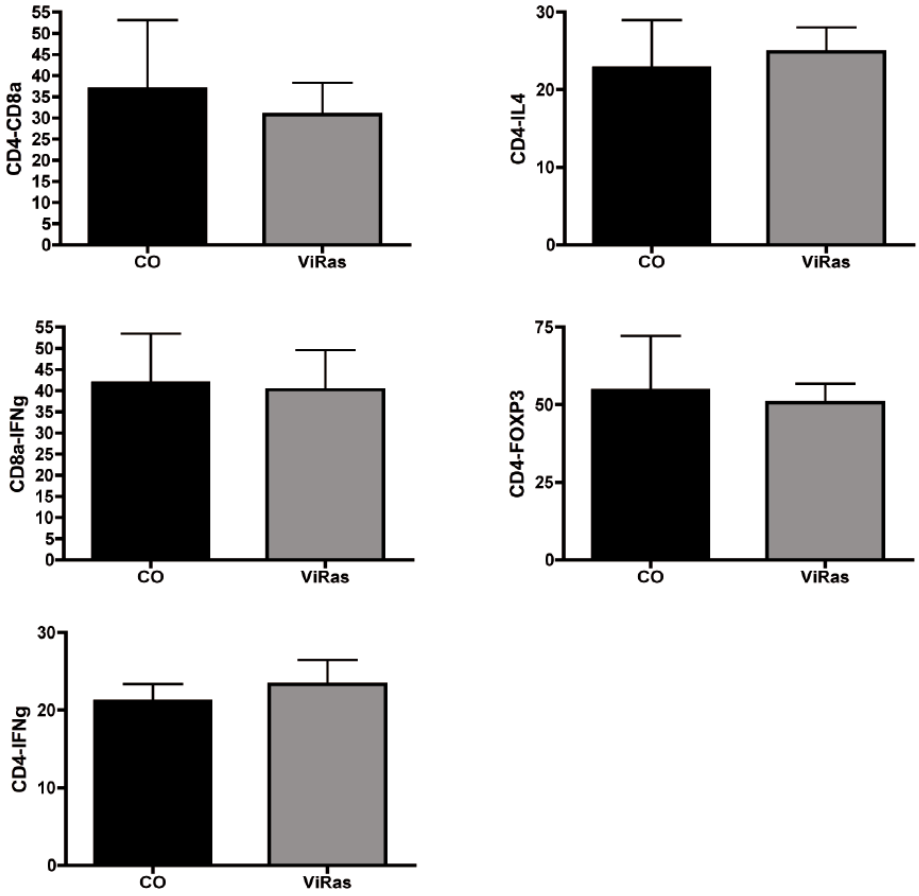

Figure 4.8: ViRas mice after 24 weeks on HFD show no change in T cell population in LP. FACS for CD4-CD8a, CD8a-IFN-γ, CD4-IFN-γ, CD4-IL-4 and CD4-FOXP3 with cells isolated from LP from CO and ViRas mice after 23 weeks on HFD (n=3).

4.8. Oncogenic K-ras activation in combination with diet causes a shift in the microbial communitiy

Although the composition of microbiota in the intestine is defined very early in life and remains more or less stable during adulthood, it has been recently shown that the flora can change under certain disease states [71] and diet conditions. Furthermore the microbiota is strongly related to the immune system in the intestine where we saw a down-regulation in the mice that developed tumors. In order to determine the influence of the diet on the intestinal microbiota and to check whether there is a correlation between altered microbial community and tumor development in the intestine, we analyzed the colonic and the small intestinal stool samples by both

culturing *in vitro* on selective agar plates and analyzing by RapidID32A as well as by pyrosequencing.

Bacterial colonization of the gut increases gradually from the stomach to the colon, the latter harboring the richest community. Indeed analysis of fecal samples in the proximal and distal parts of the small intestine showed similar bacterial counts under different direct regimen (Fig. 4.9 A), which remained lower in comparison to the colon (Fig. 4.9 B). Among the major phylums, Firmicutes (Clostridium) and Proteobacteria (E.coli) showed a trend towards an increase after HFD, which is in accordance with previous findings in literature [127].

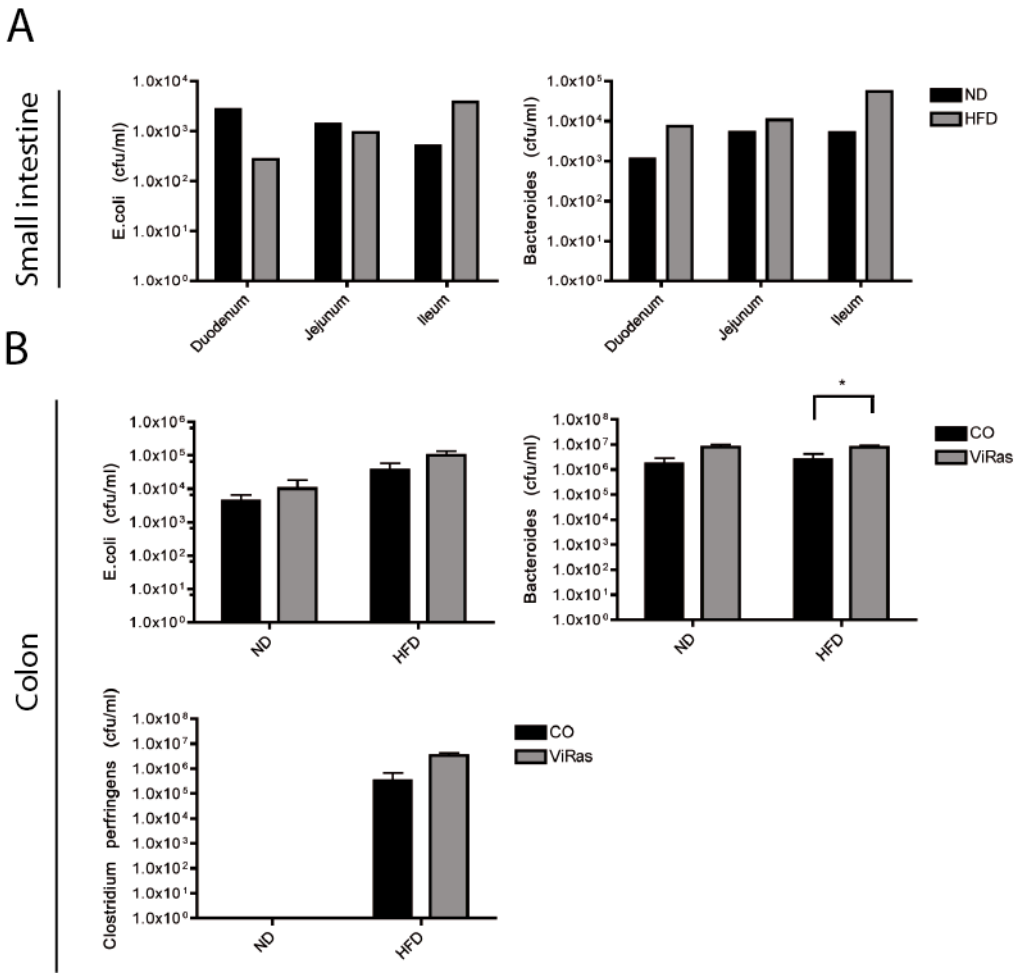

Figure 4.9: Bacterial colonization of small intestine and colon under different diet regimen. A: Colony forming unit (Cfu) of E.coli and Bacteroides in small intestinal stool samples of mice fed on either ND or HFD (n=1) **B:** Cfu of E.coli, Bacteroides and Clostridium perfringens in colonic stool samples of CO and ViRas mice on either ND or HFD (n=7) (statistical analysis made with robust method, *p<0,05).

However, due to limitations in *in vitro* culture system we defined the changes in microbiota in further details by 16S sequencing of stool samples from the small intestine and colon. The main phylums observed in the colon were Bacteroidetes, Firmicutes and Proteobacteria (Figure 4.10 A). Unlike *in vitro* cultures Bacteroidetes were decreased in the HFD mice, although percentage representation was still increased in the ViRas mice in comparison to the COs. Firmicutes, which constitutes Clostridia, were increased in HFD mice, although no difference could be detected between CO and ViRas mice. As for Proteobacteria, which E.coli belongs to, there was also an increase in the mice fed with HFD.

In accordance with decreased colonization in the small intestine, pyrosequenced amplicons also showed a very low species richness in the HFD group in comparison to the ND one. As for the species, they were mainly comprised of Bacteroidetes, Firmicutes and Proteobacteria, similar to that seen in the colonic samples (Figure 4.10 B). While there was no difference in Bacteroidetes during ND and HFD, Firmicutes seemed to be increased particularly after HFD. Interestingly a very high percentage of Proteobacteria (62 %) was detected in HFD ViRas mice, while CO mice showed only 5 %.

A

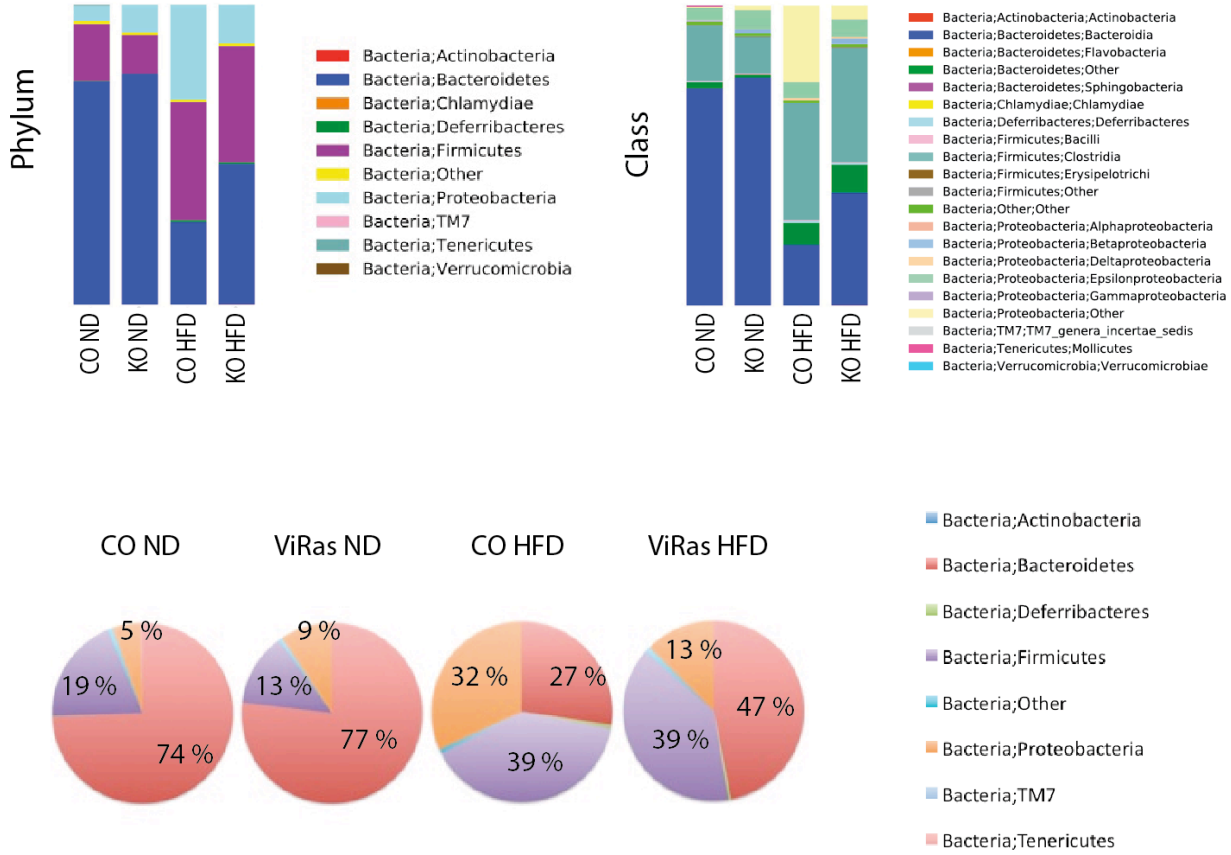
Phylum
CO ND
KO ND
CO HFD
KO HFD
Bacteria;Actinobacteria
Bacteria;Bacteroidetes
Bacteria;Chlamydiae
Bacteria;Deferribacteres
Bacteria;Firmicutes
Bacteria;Other
Bacteria;Proteobacteria
Bacteria;TM7
Bacteria;Tenericutes
Bacteria;Verrucomicrobia
Class
Bacteria;Actinobacteria;Actinobacteria
Bacteria;Bacteroidetes;Bacteroidia
Bacteria;Bacteroidetes;Flavobacteria
Bacteria;Bacteroidetes;Other
Bacteria;Bacteroidetes;Sphingobacteria
Bacteria;Chlamydiae;Chlamydiae
Bacteria;Deferribacteres;Deferribacteres
Bacteria;Firmicutes;Bacilli
Bacteria;Firmicutes;Clostridia
Bacteria;Firmicutes;Erysipelotrichi
Bacteria;Firmicutes;Other
Bacteria;Other;Other
Bacteria;Proteobacteria;Alphaproteobacteria
Bacteria;Proteobacteria;Betaproteobacteria
Bacteria;Proteobacteria;Deltaproteobacteria
Bacteria;Proteobacteria;Epsilonproteobacteria
Bacteria;Proteobacteria;Gammaproteobacteria
Bacteria;Proteobacteria;Other
Bacteria;TM7;TM7_genera_incertae_sedis
Bacteria;Tenericutes;Mollicutes
Bacteria;Verrucomicrobia;Verrucomicrobiae

CO ND
ViRas ND
CO HFD
ViRas HFD
5 %
19 %
74 %
9 %
13 %
77 %
32 %
27 %
39 %
13 %
47 %
39 %
Bacteria;Actinobacteria
Bacteria;Bacteroidetes
Bacteria;Deferribacteres
Bacteria;Firmicutes
Bacteria;Other
Bacteria;Proteobacteria
Bacteria;TM7
Bacteria;Tenericutes

B

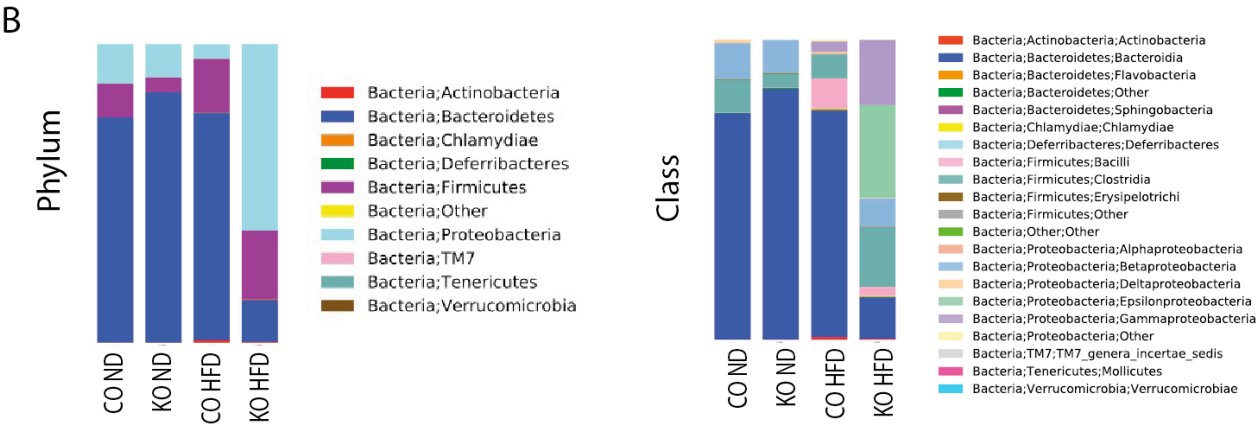
Phylum
CO ND
KO ND
CO HFD
KO HFD
Bacteria;Actinobacteria
Bacteria;Bacteroidetes
Bacteria;Chlamydiae
Bacteria;Deferribacteres
Bacteria;Firmicutes
Bacteria;Other
Bacteria;Proteobacteria
Bacteria;TM7
Bacteria;Tenericutes
Bacteria;Verrucomicrobia
Class
Bacteria;Actinobacteria;Actinobacteria
Bacteria;Bacteroidetes;Bacteroidia
Bacteria;Bacteroidetes;Flavobacteria
Bacteria;Bacteroidetes;Other
Bacteria;Bacteroidetes;Sphingobacteria
Bacteria;Chlamydiae;Chlamydiae
Bacteria;Deferribacteres;Deferribacteres
Bacteria;Firmicutes;Bacilli
Bacteria;Firmicutes;Clostridia
Bacteria;Firmicutes;Erysipelotrichi
Bacteria;Firmicutes;Other
Bacteria;Other;Other
Bacteria;Proteobacteria;Alphaproteobacteria
Bacteria;Proteobacteria;Betaproteobacteria
Bacteria;Proteobacteria;Deltaproteobacteria
Bacteria;Proteobacteria;Epsilonproteobacteria
Bacteria;Proteobacteria;Gammaproteobacteria
Bacteria;Proteobacteria;Other
Bacteria;TM7;TM7_genera_incertae_sedis
Bacteria;Tenericutes;Mollicutes
Bacteria;Verrucomicrobia;Verrucomicrobiae

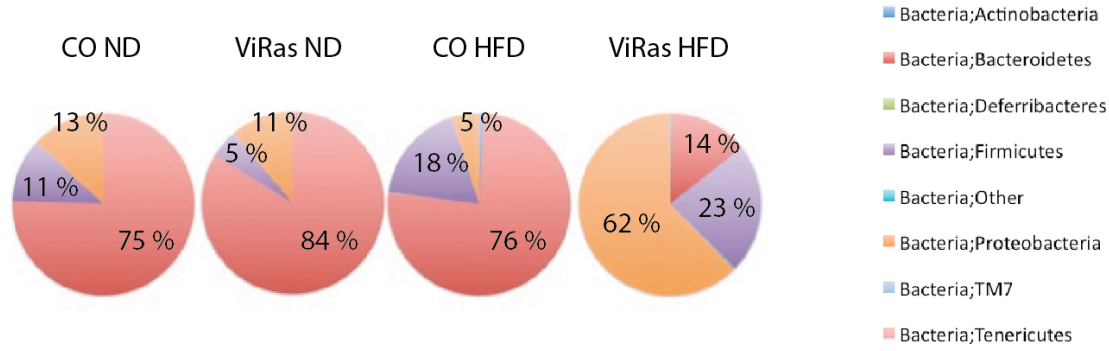
CO ND
ViRas ND
CO HFD
ViRas HFD
13 %
11 %
75 %
11 %
5 %
84 %
5 %
18 %
76 %
14 %
23 %
62 %
Bacteria;Actinobacteria
Bacteria;Bacteroidetes
Bacteria;Deferribacteres
Bacteria;Firmicutes
Bacteria;Other
Bacteria;Proteobacteria
Bacteria;TM7
Bacteria;Tenericutes

Figure 4.10: Mice show a shift of microbiota upon different diet conditions. A: Sequencing result of colonic stool samples of CO and ViRas mice collected between 18 and 23 weeks on either ND (n=3) or HFD (CO: n=5, ViRas: n=7). **B:** Sequencing results of small intestinal stool samples in CO and ViRas mice after 23 weeks on either ND (CO: n=2, ViRas: n=3) or HFD (CO: n=1, ViRas: n=4).

When analyzed deeper at the species level mainly two bacteria genera in the small intestine appeared to be increased in the ViRas HFD mice: Escherichia/Shigella (19 %) and Helicobacter (31 %), while these genera were hardly detectable in both the ND groups and CO mice on HFD (Figure 4.11).

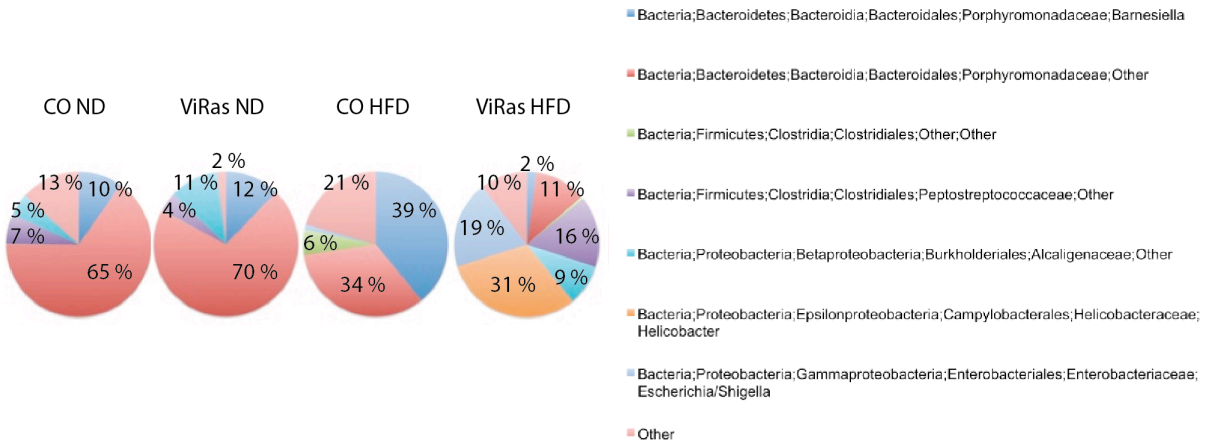

Figure 4.11: ViRas mice on HFD show and increase of Helicobacter and Escherichia/Shigella in the small intestine. Genus sequencing results of small intestinal stool samples in CO and ViRas mice after 23 weeks on either ND (CO: n=2, ViRas: n=3) or HFD (CO: n=1, ViRas: n=4).

Gram-negative bacteria, like E.coli, harbor lipopolysaccharides (LPS) in their outer membrane. Following a barrier defect endotoxin LPS is released in the circulation. Among others it is recognized by macrophages and B cells where it binds mainly to the Toll-like receptor 4 and activates the NF-$_k$B pathway. Thereby LPS is able to induce a strong pro-inflammatory immune response even resulting in septic shock [128].

Although the results were not significant, a trend towards increased LPS levels in the blood from the HFD mice in comparison to the ND group was observed (Figure 4.12). Although no difference between the genotypes was seen still these findings suggest a barrier defect in mice with HFD regimen.

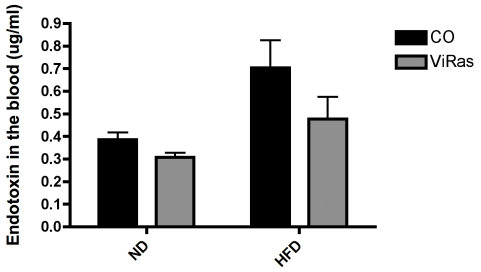

Figure 4.12: LPS levels in mice under ND and HFD conditions. Endotoxin levels measured in the serum of CO and ViRas mice (n=4) after 22 weeks on either ND or HFD.

These results suggest that HFD leads to a shift from Bacteroidetes to Firmicutes in the colon. However the particular community change observed in the small intestine appears remarkable since E.coli and Helicobacter have been shown to mask host immunity and furthermore have been suggested to play a role during pathogenesis in the intestine.

4.9. MyD88 deficiency confers protection during tumor development in ViRas mice

Bacteria and their products are mainly recognized by Toll-like receptors (TLRs). To elucidate whether there is a correlation between gut microbiota and the tumor development in the intestine the adaptor protein MyD88 that is downstream of many receptors such as TLRs and NODs was deleted in the whole body in ViRas animals. Resulting $MyD88^{-/-}$ ViRas mice as well as $MyD88^{-/-}$ CO mice were fed on HFD for about 23 weeks. $MyD88^{-/-}$ ViRas mice gained similar weight as their CO littermates (Figure 4.13 A). Blood counts were checked after 16 weeks on the diet. $MyD88^{-/-}$ ViRas mice did not show any difference in RBC counts, HGB levels and WBC counts in comparison to their $MyD88^{-/-}$ COs, suggesting neither anemia nor inflammation (Figure 4.13 B). Although $MyD88^{-/-}$ ViRas mice similar to ViRas animals continued to show elongation (Figure 4.13 C), serration and branching of the intestine (Figure 4.13 D, E), interestingly no tumors were detected (Figure 4.13 F) suggesting that MyD88 deficiency blocked tumor development in ViRas mice on HFD.

Indeed, MyD88 deletion had prominent effects on the phenotype of ViRas mice such as eliminating weight loss as well as the development of anemia and tumors seen in these animals.

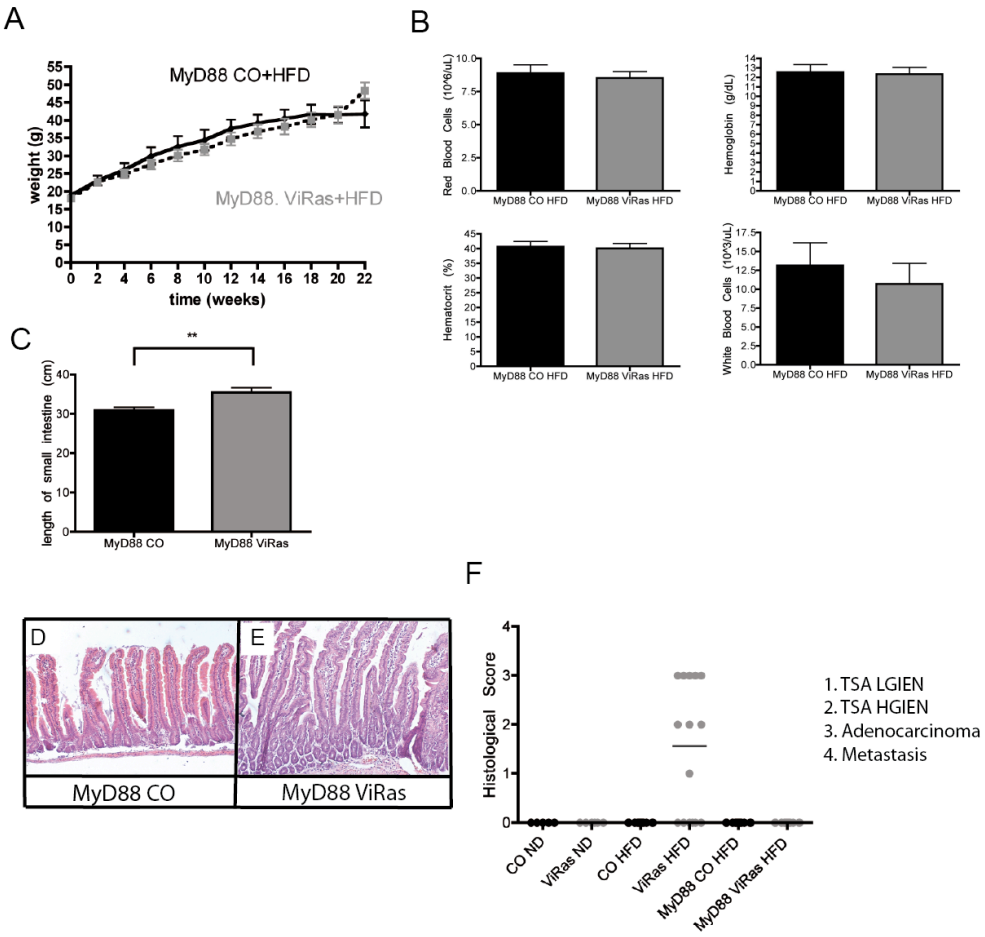

Figure 4.13: MyD88 deficiency protects against tumor development independent of the serrated phenotype in ViRas mice. A: Weight curve of MyD88$^{-/-}$ CO (n=8) and MyD88$^{-/-}$ ViRas (n=11) mice during 22 weeks on HFD. **B:** Blood count of MyD88$^{-/-}$ CO (n=6) and MyD88$^{-/-}$ ViRas (n=7) mice after 16 weeks on HFD. **C:** Length of the small intestine of MyD88$^{-/-}$ CO (n=10) and MyD88$^{-/-}$ ViRas (n=9) mice after 23 weeks on HFD (statistics made with t-test, **p<0,01). **D,E:** H&E staining of representative duodenum of a MyD88$^{-/-}$ CO **(D)** and a MyD88$^{-/-}$ ViRas **(E)** mouse (20x magnification). **F:** Histological score of MyD88$^{-/-}$ CO (n=19) and MyD88$^{-/-}$ ViRas (n=15) mice on HFD in comparison to ND (CO: n=5, ViRas: n=6) and HFD (CO: n=13, ViRas: n=15) groups.

To check if the protection against tumor development due to the MyD88 deletion also correlated with changes in the immune system FACS analysis were performed. Interestingly the decrease in population of MHC II on CD11c^{+} dendritic cells in LP and PP of the small intestine seen in ViRas mice in comparison to their COs after ND

and HFD was not seen in the mice with additional MyD88 deletion on HFD (Figure 4.14). However $CD11c^+$ dendritic cells and MHCII expression on this population showed a trend towards an increase following MyD88 deletion. These results may suggest a partial improvement on dendritic cell recruitment in the LP and PP upon MyD88 deficiency.

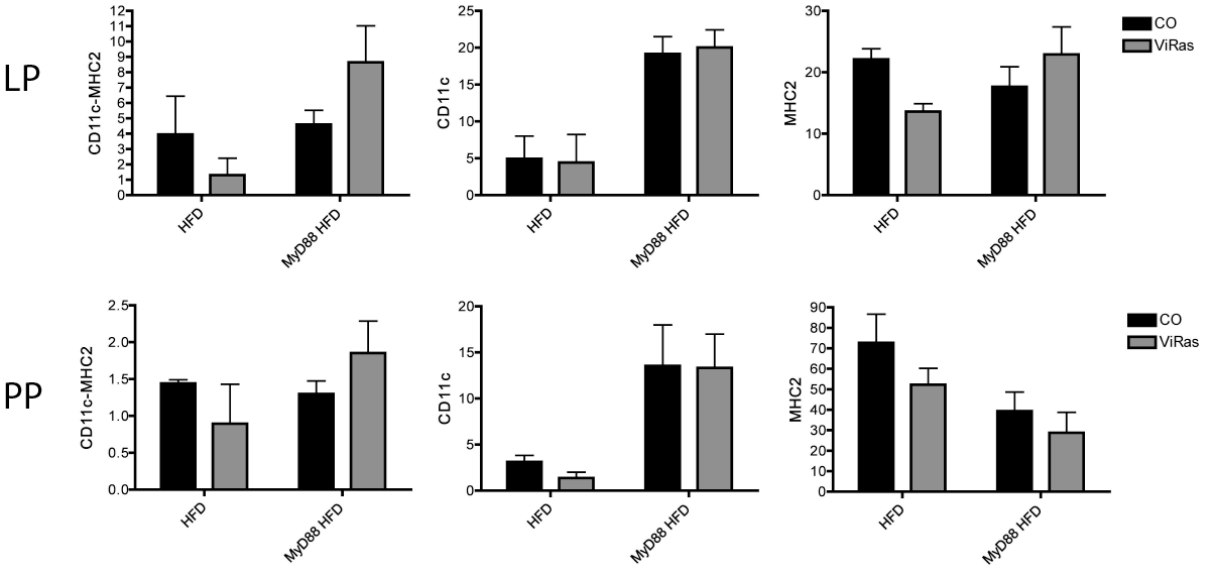

Figure 4.14: MyD88 deficiency confers partial improvement in immune response during HFD. FACS analysis using LP and PP from the small intestine of $MyD88^{-/-}$ CO (n=7) and ViRas (n=5) mice on HFD in comparison to CO and ViRas mice on HFD (n=2) for $CD11c^+$-$MHCII^+$, $CD11c^+$ and $MHCII^+$.

To examine whether MyD88 deficiency conferred protection against tumor development due to direct effect on the microbiota, stool samples from the colon and small intestine were sequenced (Figure 4.15 A). Importantly MyD88 deficiency caused a distinct shift in the bacterial communities found in the small intestine of ViRas mice on HFD suggesting that MyD88 deletion protected against adenocarcinoma development through decrease in the genera of Helicobacter and Escherichia/Shigella, in contrast to LPS levels that remained similar to HFD group (Figure 4.15 B).

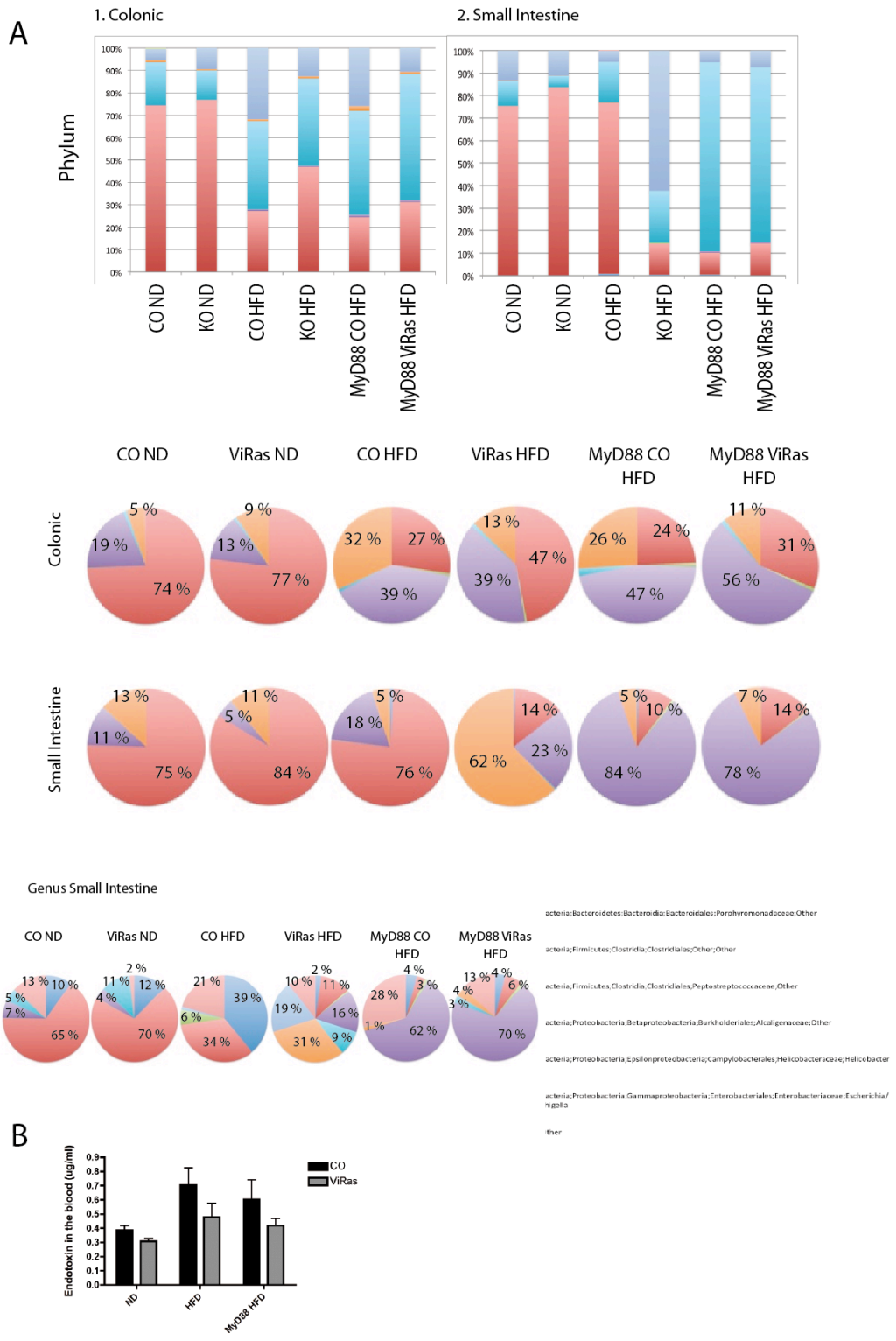

Figure 4.15: MyD88 deficiency causes a shift in microbiota decreasing proportion of opportunistic pathogens in the small intestine. A: Sequencing results of the colonic and small intestinal stool samples of CO and ViRas mice on either ND or HFD with or without MyD88 deletion (colonical samples: ND: n=3, CO HFD: n=5, ViRas HFD: n=7, MyD88 HFD: n=4; small intestinal samples: CO ND: n=2, ViRas ND: n=3, CO HFD: n=1, ViRas HFD: n=4, MyD88 HFD: n=4). **B:** Endotoxin levels measured in blood plasma of CO and ViRas mice on ND or HFD with or without MyD88 deletion (n=4).

4.10. ViRas mice with additional IL-1R, TLR-4 or TLR-2 deficiency continue to show neoplasia in the intestine but no invasive carcinoma

As MyD88 deficiency rescued against tumor development in ViRas mice we wanted to check which receptor conveyed signaling through this adapter protein. As many diverse receptors use MyD88 in common to activate the NF-$_K$B pathway [129], we checked IL-1R, TLR-4 and TLR-2 in particular. The knock out of IL-1R was important in order to prove whether bacteria played a direct role in the rescue of the phenotype due to MyD88 deficiency, as it responses to traditional IL-1 family ligands. TLR-4 and TLR-2 are two receptors that are mainly known to detect bacteria, the former especially lipopolysaccharide (LPS) from gram negative bacteria and the latter a broad spectrum of bacterial peptidoglycans. ViRas mice were crossed on IL-1R-, TLR-2- and TLR-4-deficient background and fed on HFD. There was no change in weight gain between CO and ViRas mice with additional TLR-2 and TLR-4 deletion (Figure 4.16 A). Although both TLR-2 and TLR-4 deletion corrected weight differences in ViRas mice on HFD, however IL-1R$^{-/-}$ ViRas animals continued to gain less weight than their littermate controls. Interestingly TLR-2$^{-/-}$ ViRas mice gained even more weight than their controls. After sacrifice, the histology of the intestine showed the same serration and branching of the crypts similar to that seen in ViRas mice on HFD (Figure 4.16 B-G). Further tumor development was also unaffected although none of them showed adenocarcinoma and metastasis (Figure 4.16 H).

In accordance, the blood counts in ViRas mice with additional TLR-2 deletion continued showing a significant decrease in RBC and for TLR-4 mice a significant decrease in HCT, which suggested anemia that is associated with tumor development in these animals (Figure 4.16 I).

These results suggest that TLR-2, TLR-4 and IL-1R were partially involved in conveying bacterial signals via MyD88 since whole body deletion of these receptors led to neoplasia despite the absence of invasive carcinoma in the small intestine.

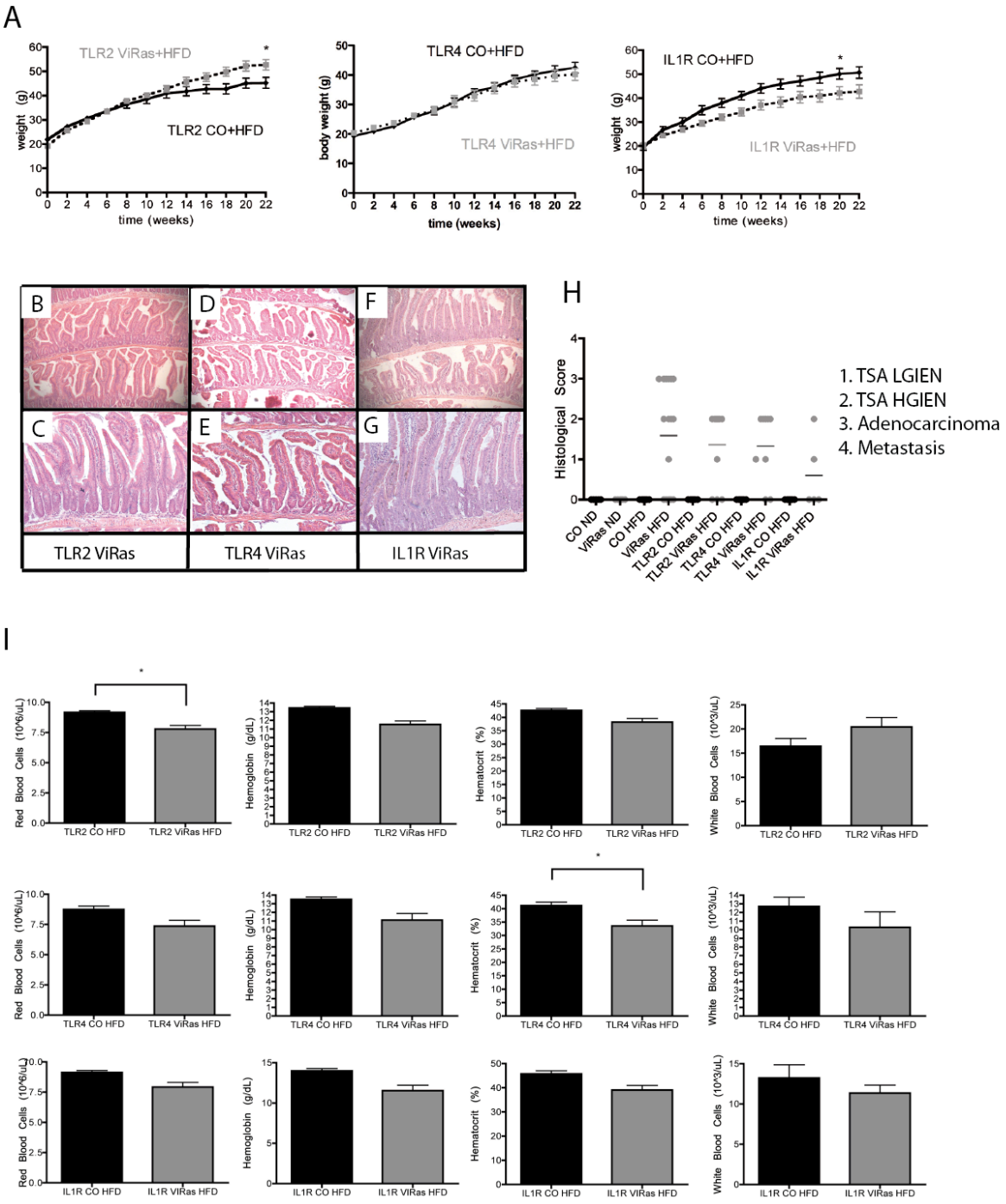

Figure 4.16: ViRas mice with additional knock out of TLR-2, TLR-4 or IL-1R show changes in weight gain but continue to show tumors. A: Weight curve of CO and ViRas mice with either TLR-2 (CO: n=11, ViRas: n=5), TLR-4 (CO: n=7, ViRas: n=6) or IL-1R (n=9) knock out fed over 22 weeks on HFD (statistical analysis made for multiple testing, *p<0,05). **B-G:** Representative histology of the duodenum of ViRas mice with TLR-2 **(B,C)**, TLR-4 **(D,E)** or IL-1R **(F,G)** deletion (B,D,F: 5x magnification, C,E,G: 10x magnification). **H:** Histological score of CO and ViRas mice on ND (CO: n=5, ViRas: n=6) or HFD (CO: n=13, ViRas: n=15) and CO and ViRas mice with TLR-2 (CO: n=9, ViRas: n=11), TLR-4 (n=9) or IL-1R (CO: n=10, ViRas: n=6) deficiency on HFD for 23 weeks. **I:** Blood counts of CO and ViRas mice with TLR-2 (CO: n=9, ViRas: n=15), TLR-4 (n=6) or IL-1R (CO: n=8, ViRas: n=10)

deletion after 16 weeks on HFD (statistics made with t-test, p-values adjusted for multiple testing, *p<0,05).

Furthermore, when GTTs were performed, hyperglycemia (Figure 4.17 A) and insulin sensitivity (Figure 4.17 B) in IL-1R$^{-/-}$ and TLR-2$^{-/-}$ CO mice in comparison to IL-1R$^{-/-}$ ViRas and TLR-2$^{-/-}$ ViRas double mutants were comparable to ViRas mice on HFD. However this difference was less visible in TLR-4$^{-/-}$ background. Importantly in accordance with previous publications TLR-4$^{-/-}$ conferred protection against diet-induced obesity and insulin resistance [130]. Although some other publications stand contradictory, still they suggest impairment in diet-induced metabolic diseases [131]. Although TLR-4$^{-/-}$ CO mice and TLR-4$^{-/-}$ ViRas mice gained equal weight on HFD (Figure 4.16 A), TLR-4 deletion increased glucose tolerance as it decreased insulin secretion during GTTs suggesting indeed TLR-4 deficiency conferred protection against diet-induced metabolic changes regardless of the genotype.

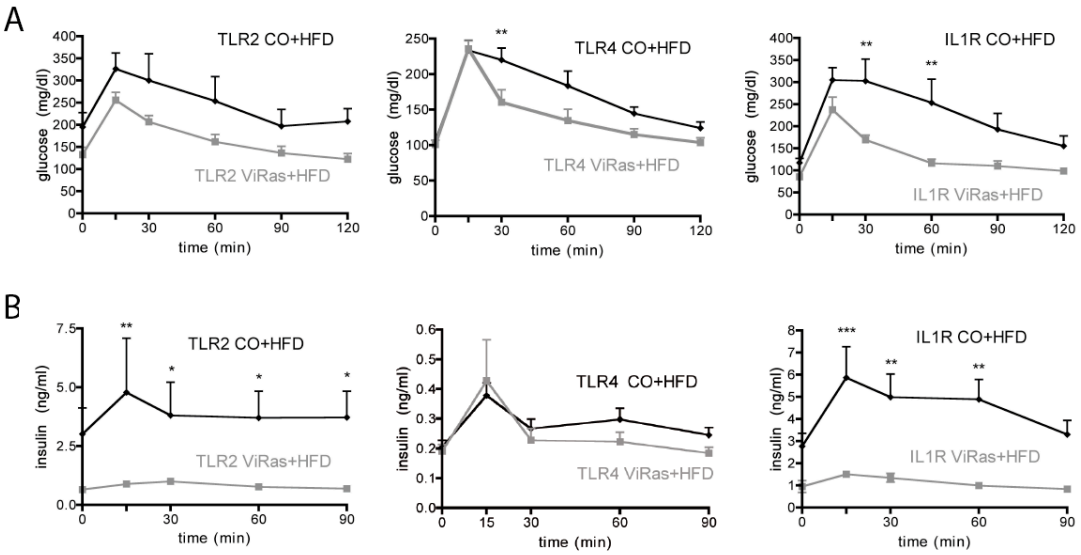

Figure 4.17: ViRas mice with additional knock out of TLR-2, TLR-4 or IL-1R still remain more insulin sensitive than their CO littermates on HFD. A: Glucose levels of the mice during GTT. **B:** Insulin levels during GTT. (TLR-2$^{-/-}$ CO: n=3, TLR-2$^{-/-}$ ViRas: n=5, TLR-4$^{-/-}$ CO: n=7, TLR-4$^{-/-}$ ViRas: n=6, IL-1R$^{-/-}$: n=5). (All statistical analysis made for multiple testing, *p<0,05, **p<0,01, ***p<0,001)

We further checked the microbiota by culturing colonic stool on selective agar plates. The main bacteria found in these mice were again E.coli, Bacteroides and Clostridium perfringens (Figure 4.18). There was similar increase in ViRas animals in comparison to controls, especially once TLR-4 alleles were knocked out. There was also a slight increase in Bacteroides in TLR-4$^{-/-}$ and IL-1R$^{-/-}$ ViRas mice in

comparison to their COs, however the difference was not significant. Further Clostridium perfringens was not detected in TLR-2$^{-/-}$ mice within the dilution checked.

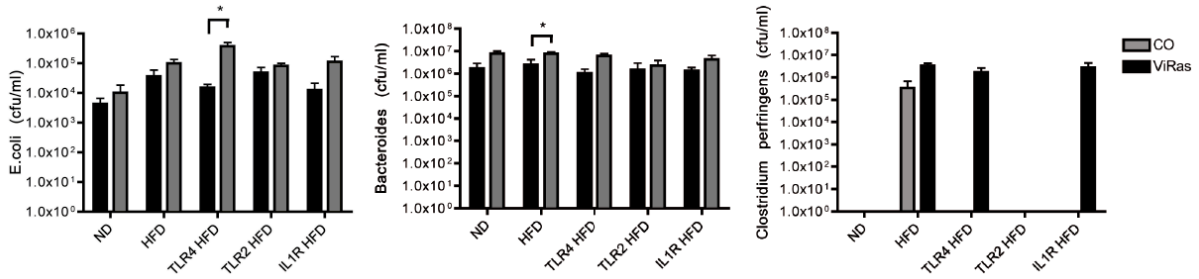

Figure 4.18: Bacterial counts of TLR2$^{-/-}$, TLR4$^{-/-}$ and IL1R$^{-/-}$ mice. Cfu of bacteria found in the colonic stool samples of CO and ViRas mice on ND or HFD and CO and ViRas mice on HFD with TLR-2, TLR-4 or IL-1R deficient background after 20 weeks on diet. (ND: n=7, HFD CO: n=7, TLR-4$^{-/-}$: n=17, TLR-2$^{-/-}$ CO: n=6, TLR-2$^{-/-}$ ViRas: n=10, IL-1R$^{-/-}$: n=5; statistical analysis made with robust method, *p<0,05).

Knocking out TLR-4 allele protected against diet-induced insulin resistance. Nevertheless neither IL-1R deficiency, nor TLR-4 or TLR-2 deletion resulted in the complete loss of tumor development we observed in MyD88 KOs. Still a partial but a clear protection was conferred during development of invasive carcinoma, suggesting at least some of the bacterial signals to be conveyed upstream of MyD88 via TLR-2, TLR-4 and IL-1R.

4.11. Deletion of MyD88 in hematopoietic cells confers no protection against tumor development

In order to detect which cell type MyD88-deficiency confered protection in the ViRas phenotype, bone marrow transplantation was performed, which restrict MyD88 deletion to the hematopoietic stem cells only. After irradiation mice were injected through the tail vein with either wild type (WT) or MyD88$^{-/-}$ bone marrow and fed on HFD for 22 weeks. Five out of seven mice transplanted with the WT bone marrow showed tumors (Figure 4.19 A), interestingly also in the colon, which was never observed in ViRas mice on HFD before. One mouse further developed in addition to a tumor in the duodenum (Figure 4.19 F) metastasis in colonic muscle (Figure 4.19 G) and in pancreas (Figure 4.19 H). In contrary four out of eight of the ViRas mice that received MyD88$^{-/-}$ bone marrow developed one tumor in the small intestine. As

for the histology of the small intestine itself, there was no visible difference between the two groups (Figure 4.19 B-E). Although there is a trend towards less tumor development in mice transplanted with MyD88$^{-/-}$ bone marrow in comparison to the ones with WT bone marrow they still showed tumor development comparable to ViRas mice on HFD (Figure 4.19 A). The restricted MyD88 deletion in hematopoietic cells seems not to be sufficient enough to reduce tumor incidence in ViRas mice on HFD.

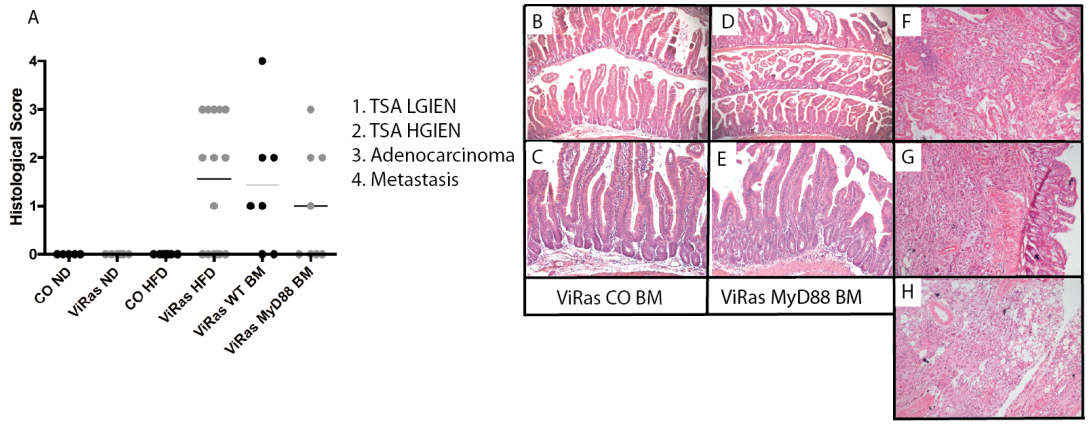

Figure 4.19: ViRas mice transplanted with WT BM or MyD88$^{-/-}$ BM continue to show increased tumor incidence. **A:** Histological score of tumors found in ViRas mice after BMT with either CO or MyD88$^{-/-}$ BM. (**B-E:** Representative pictures of the histology of the duodenum of ViRas mice transplanted with either WT (**B,C)** or MyD88$^{-/-}$ **(D,E)** BM. **F-H:** Representative pictures of the histology of tumor in ViRas mice after BMT with WT BM in duodenum **(F)**, colonic muscle **(G)** and pancreas **(H)**. (B,D: 5x magnification, C,E,F,G,H: 10x magnification)

4.12. ViRas mice with specific deletion of MyD88 in the intestinal epithelial cells continue to develop tumors

The loss of MyD88 in hematopoietic cells did not result in a rescue. In order to distinguish whether MyD88 deficiency in the intestinal epithelial cells is sufficient to block tumor development in ViRas mice, we crossed ViRas mice to floxed MyD88 (MyD88$^{fl/fl}$) animals and fed them on HFD. No differences in weight gain could be detected between MyD88$^{fl/fl}$ CO and MyD88$^{fl/fl}$ ViRas mice (Figure 4.20 A). However after sacrifice the length of the intestine in MyD88$^{fl/fl}$ ViRas mice was similarly increased as in ViRas animals, further the branching and serration of the villi were evident (Figure 4.20 C, D). Four out of seven MyD88$^{fl/fl}$ ViRas mice showed tumors in

the small intestine, TSA HGIEN and adenocarcinoma, whereas no metastasis were observed (Figure 4.20 B, E).

In order to check insulin sensitivity GTT was performed. Indeed similar to ViRas mice MyD88$^{fl/fl}$ ViRas animals showed a trend towards lower glucose levels than their CO littermates (Figure 4.20 F), although the results were not significant.

In summary, the loss of MyD88 in intestinal epithelial cells did not lead to a decrease in tumor development in ViRas animals.

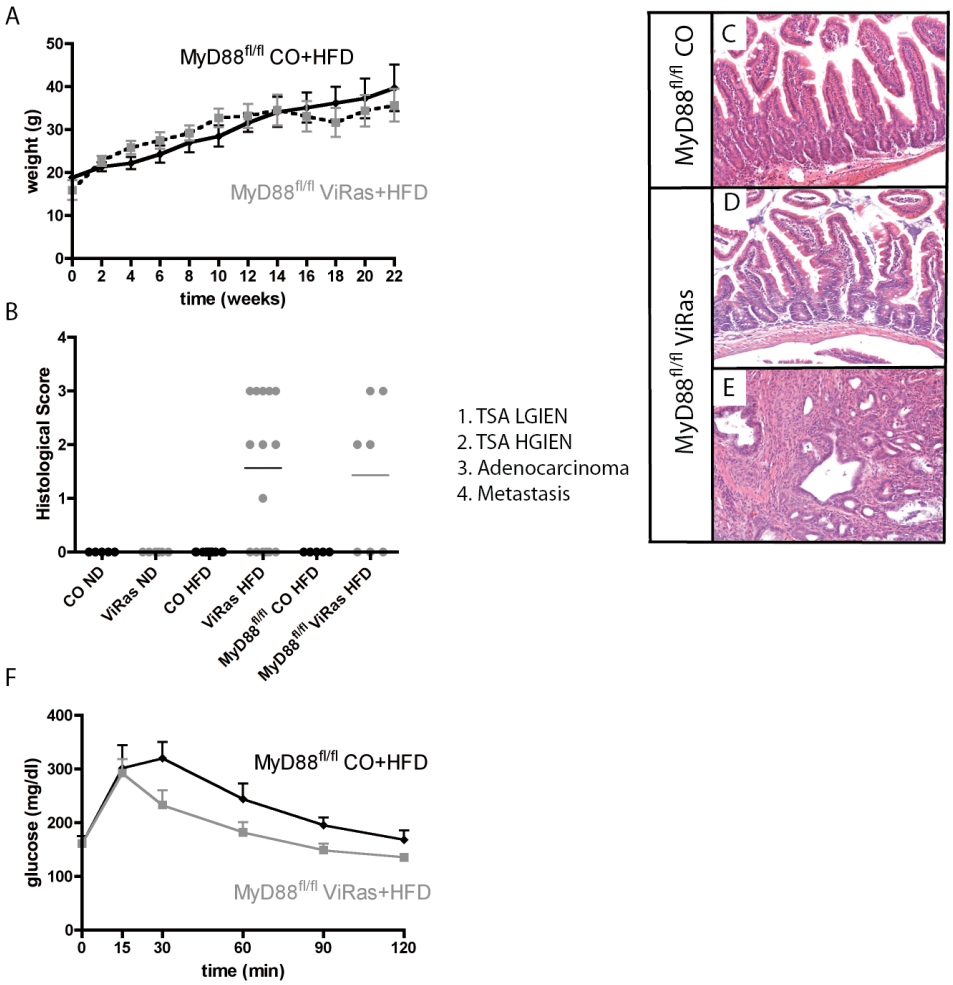

Figure 4.20: Additional specific knock out of MyD88 in intestinal epithelial cells do not rescue against tumor growth in ViRas mice. A: Weigh curve of MyD88$^{fl/fl}$ CO (n=4) and MyD88$^{fl/fl}$ ViRas (n=5) mice on HFD over 22 weeks. **B:** Histological score of MyD88$^{fl/fl}$ CO and MyD88$^{fl/fl}$ ViRas mice after 22 weeks on HFD in comparison to ND and HFD groups. **C-E:** Representative pictures of an H&E staining of duodenum of a MyD88$^{fl/fl}$ CO **(C)** and a MyD88$^{fl/fl}$ ViRas mouse **(D)** as well as an adenocarcinoma seen in the duodenum of a MyD88$^{fl/fl}$ ViRas mouse **(E)** (all 10x magnification). **F:** Glucose levels of the mice during GTT (n=3).

4.13. HFD leads to changes in bacterial fermentation end products

Since ViRas mice showed a shift in the microbiota in the small intestine and colon during tumor development and that this was completely abrogated following MyD88 deletion we checked short chain fatty acids (SCFA). SCFA, bacterial fermentation end products, are believed to have beneficial effects in host immunity. They are produced by different species of bacteria such as Lactobacillus or Bifidobacteria [132]. The main SCFA we analyzed were acetate, propionate, butyrate, valeric adid and iso-valeric acid. There was a significant decrease in acetate, propionate and butyrate in the HFD group compared to those on ND (Figure 4.21). Acetate levels were higher in ViRas mice compared to CO mice on HFD. Valeric acid and iso-valeric acid were increased after HFD. Indeed, in addition to a shift in the microbiota, also changes in the fermentation end products due to both diet and K-ras activation were observed, which could be indirectly linked to the tumor formation in the ViRas mice since SCFA, especially butyrate, have been shown to have immuno-regulatory effects.

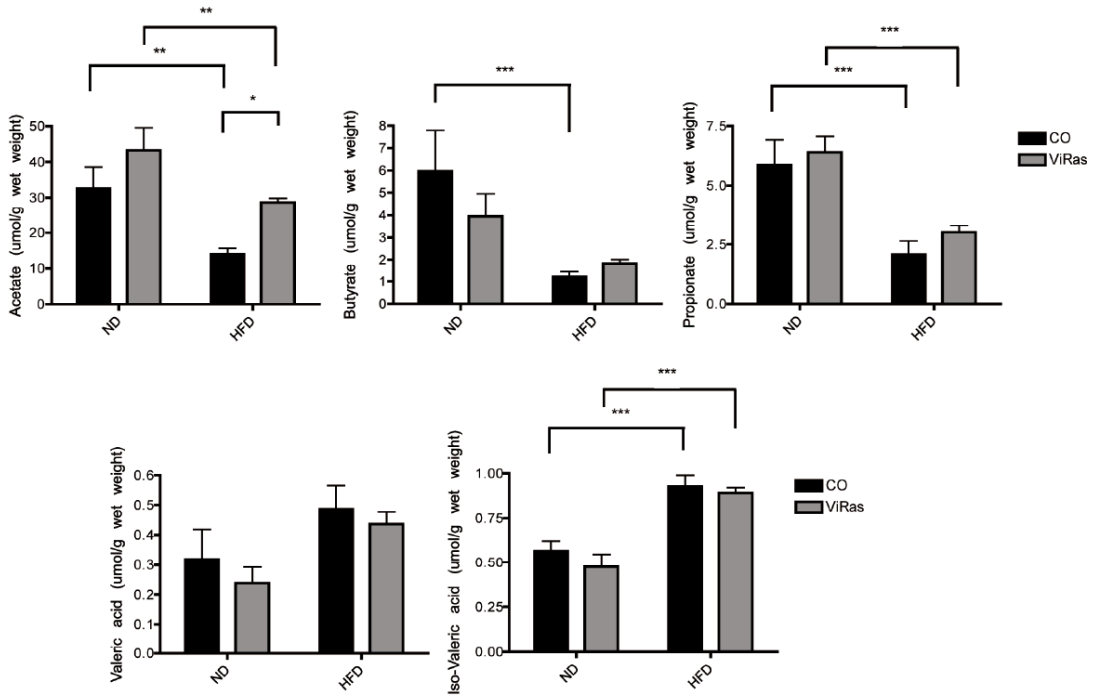

Figure 4.21: Mice show differences in SCFA levels after HFD. Measurement of SCFA in colonic stool samples of CO and ViRas mice after 16-22 weeks on ND and HFD. (ND CO: n=6, ND ViRas: n=8, HFD CO: n=7, HFD ViRas: n=11; statistical analysis were done for multiple testing, *p<0,05, **p<0,01, ***p<0,001).

4.14. Butyrate treatment significantly delays tumor development in ViRas mice following HFD

In addition to changes in the composition of bacteria in the small intestine and colon, we saw a decrease in SCFA in mice fed on HFD. It is known that SCFA play an important role in the regulation of the immune system. Of note butyrate is known to have beneficial properties [81] such as the inhibition of NF-$_k$B-dependent inflammatory pathway [80], anti-carcinogenic effects, the induction of apoptosis in tumor cells [79] or regulation of histone acetylase [133]. To unravel the effect of SCFA CO and ViRas mice fed on HFD were supplemented with butyrate.

Importantly no difference in weight gain was observed between the two genotypes (Figure 4.22 A). Furthermore the typical histology of the small intestine in ViRas mice with the elongation and branching of the villi was less apparent and only partially visible following butyrate treatment (Figure 4.22 B). Importantly tumor formation was significantly reduced in ViRas HFD mice. Only one out of seven mice developed TSA LGIEN in the duodenum (Figure 4.22 C) suggesting an anti-tumorigenic property for butyrate. As for the blood counts, mice did not show any difference between CO and ViRas mice (Figure 4.22 D).

During GTT butyrate treated ViRas mice showed significantly lower glucose (Figure 4.22 E) and insulin levels (Figure 4.22 F) than CO littermates, suggesting insulin sensitivity. Interestingly butyrate treatment decreased insulin secretion, suggesting anti-diabetic property during obesity.

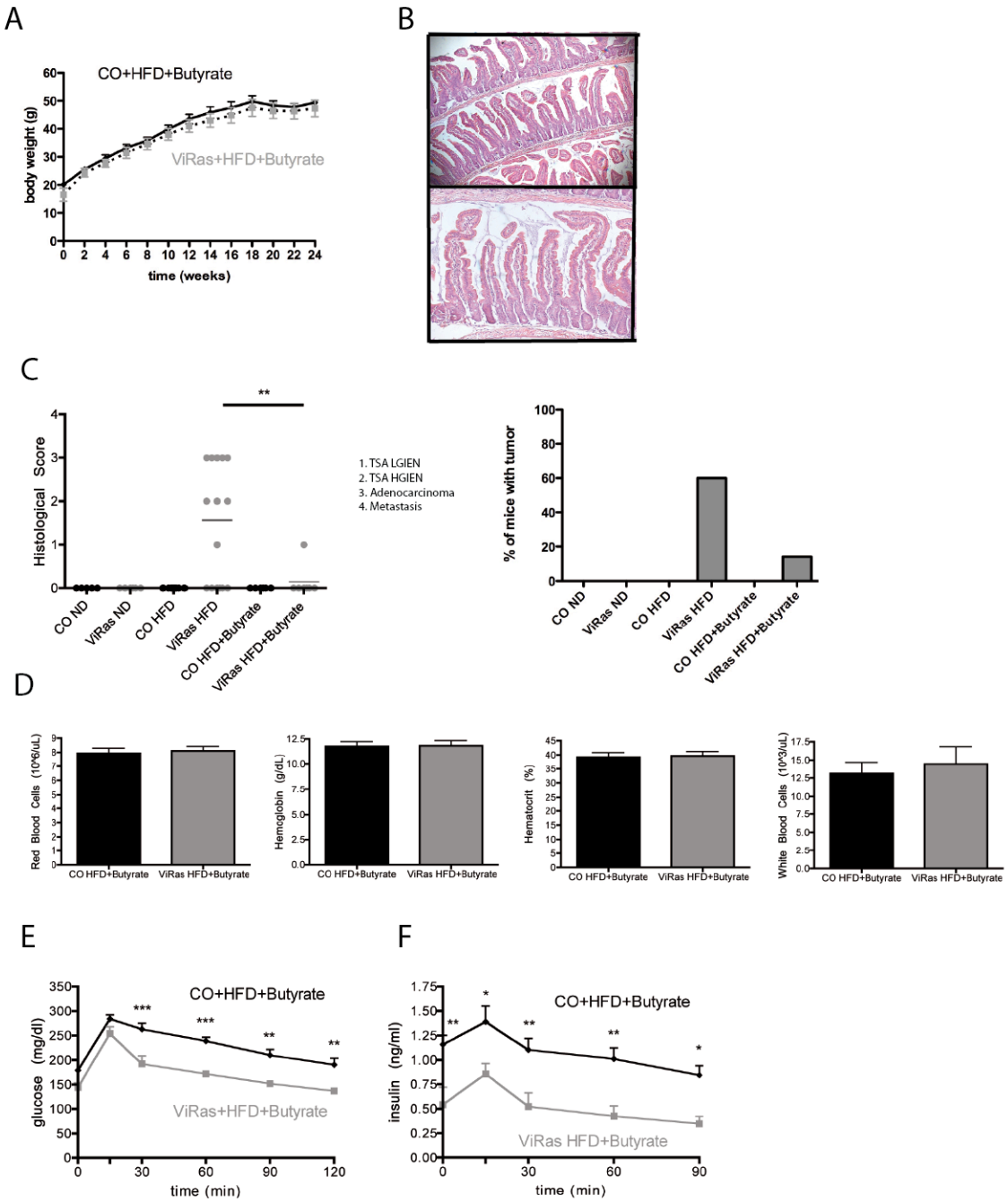

Figure 4.22: Butyrate treatment has beneficial effects on ViRas mice during HFD. A: Weight curves of CO (n=6) and ViRas (n=5) mice on HFD treated with butyrate for 24 weeks. **B:** Representative histology pictures of the duodenum of a ViRas mouse after 24 weeks on HFD with butyrate treatment (5x and 10x magnification). **C:** Histological score of CO and ViRas mice after 22-24 weeks on either ND, HFD treated with or without butyrate (statistical analysis made for mutiple testing, **p<0,01). **D:** Blood count of CO and ViRas mice after 16 weeks on HFD with butyrate (n=7). **E,F:** Glucose **(E)** and insulin **(F)** levels of mice during GTT (n=5) (statistical analysis made for multiple testing, *p<0,05, **p<0,01, ***p<0,001).

Further we elucidated the colonic microbiota in mice following butyrate treatment. Similarly to HFD group we saw an increase in E.coli counts in ViRas mice treated with butyrate in comparison to their COs (Figure 4.23 A). When colonic stool samples

were sequenced, the main bacteria found were Bacteroides, Firmicutes and Proteobacteria (Figure 4.23 B). The percentage proportion of bacteria after butyrate treatment did not differ significantly from those on HFD. Similarly, they showed the same percentage for Bacteroides (25 % in the CO, 42 % in the ViRas mice plus butyrate versus 27 % in CO, 47 % in ViRas mice after HFD) and slightly decreased for Proteobacteria (20 % in CO, 12 % in ViRas mice plus butyrate versus 32 % in CO, 13 % in ViRas mice after HFD). Firmicutes, in particularly Clostridia, were found at a slightly higher ratio in mice treated with Butyrate than those kept only on HFD (52 % in CO, 44 % in ViRas mice plus butyrate versus 39 % found in HFD mice). Interestingly MyD88-deficiency that also protected against tumor development showed increased Operational Taxonomic Units (OTUs) related to Clostridia in the colon. Furthermore there was a trend towards a decrease of endotoxin levels after butyrate treatment (Figure 4.23 C).

After having analyzed SCFA in the stool of these mice (Figure 4.23 D), interestingly no significant increase in the butyrate content was found. Although acetate, propionate, valeric acid and iso-valeric acid levels were similar to the HFD mice, there was a significant decrease in iso-valeric acid levels and an increase in valeric acid levels in the butyrate treated mice.

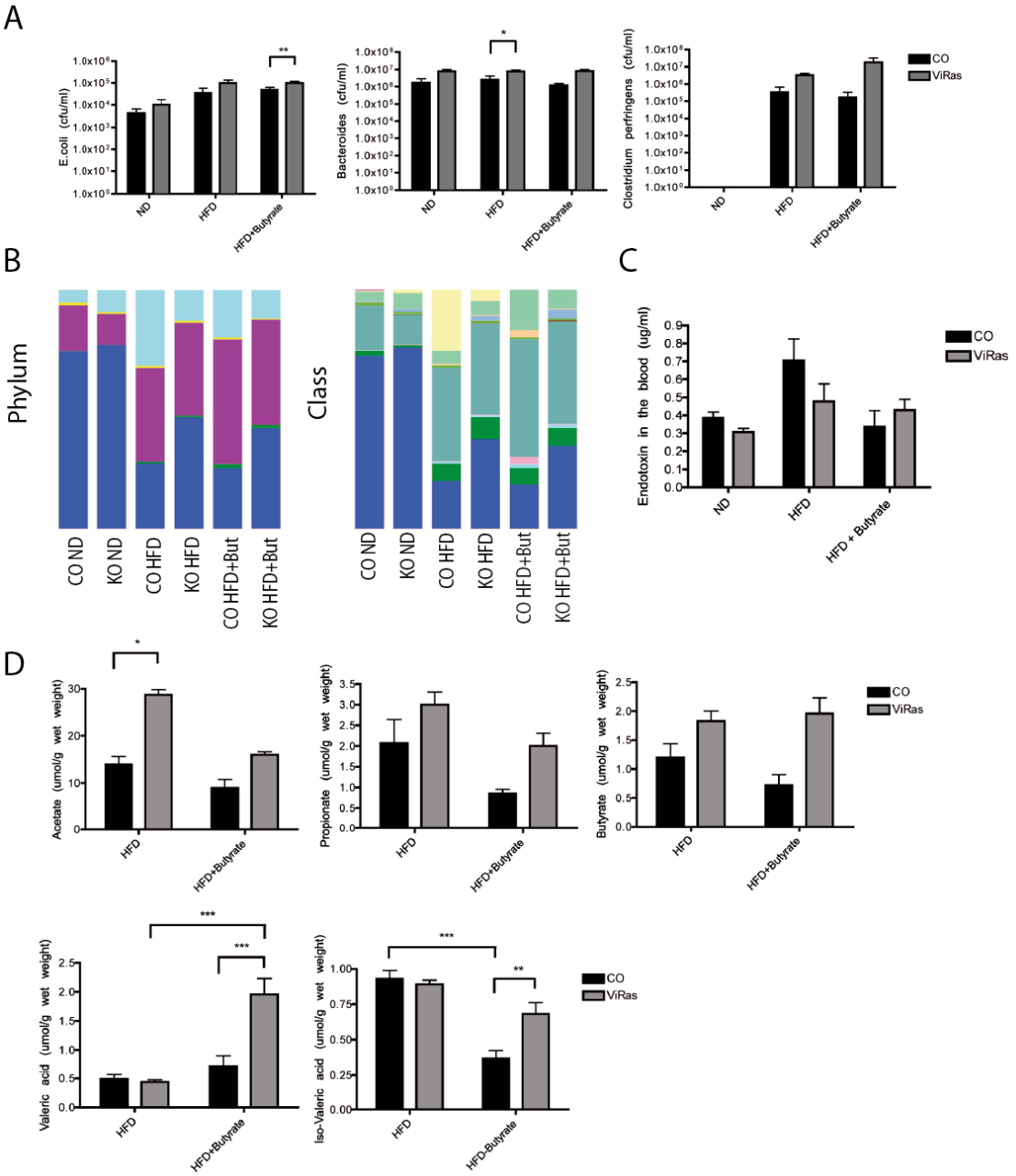

Figure 4.23: Butyrate treatment shows no effect on the composition of colonic microbiota. A: Cfu of bacteria found with selective agar plates in the colonic stool of mice after 20 weeks on ND (n=7), HFD with (n=20) or without (n=7) butyrate (Statistics made with robust method, *p<0,05, **p<0,01). **B:** Sequencing results of colonic stool samples of mice after 18-22 weeks on ND (n=3), HFD with (n=4) or without (CO: n=5, ViRas: n=7) butyrate. **C:** Endotoxin levels measured in the serum of CO and ViRas mice (n=4) after 22 weeks on ND, HFD with or without butyrate. **D:** Amount of SCFA found in colonic stool samples of mice after 16-22 on HFD with (CO: n=6, ViRas: n=5) or without (CO: n=7, ViRas: n=11) butyrate (statistical analysis made for multiple testing, *p<0,05, **p<0,01, ***p<0,001).

Another aspect was to investigate how butyrate treatment affects the immune system. As down-regulation of several parts of the immune system was seen in ViRas mice, which was boosted after HFD, duodenal gene expression in butyrate

treated mice was tested by microarray. Interestingly butyrate treated ViRas mice did not show decreased expression in those genes that were altered during ND and HFD without butyrate treatment (Figure 4.24). In terms of genes involved in binding and presentation of antigens to immune cells (Figure 4.24 A), no down-regulation for histocompatibility class II was seen. Genes related to Fc receptor were still decreased in ViRas mice in comparison to COs but over all higher in butyrate treated mice than in those without. Further expression of genes related to the immune system, like T-cell specific GTPase, immunoglobulin lambda chain and C-type lectins was not reduced in ViRas mice in comparison to COs after butyrate treatment (Figure 4.24 A). Furthermore during FACS analysis (Figure 4.24 B) no down-regulation of MHC II – $CD11c^+$ cells could be detected in LP and PP isolated from the small intestine of butyrate treated ViRas mice (Figure 4.24 B). Besides $CD11c^+$ dendritic cell recruitment was significantly improved in ViRas mice following butyrate treatment.

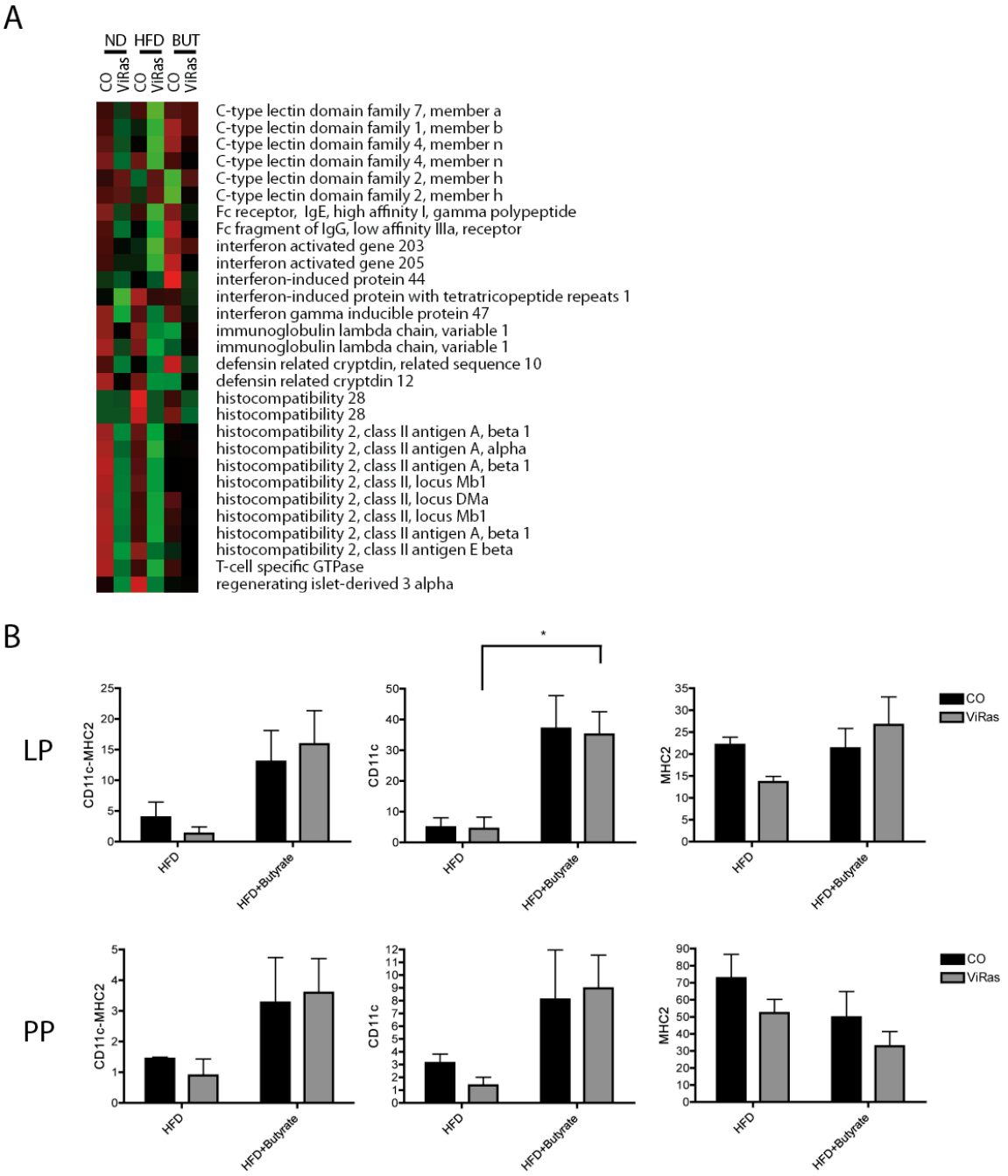

Figure 4.24: Butyrate treatment inhibits the genotype and diet related down-regulation of the immune system. A: Microarray using RNA from the duodenum of CO and ViRas mice after 23 weeks on ND (CO: n=2, ViRas: n=3) and HFD with (CO: n=1, ViRas: n=3) and without (n=2) butyrate, showing alterations in genes involved in pathogen recognition and host immune response. **B:** FACS analysis using LP and PP from butyrate treated CO (n=4) and ViRas (n=7) mice on HFD in comparison to CO and ViRas mice on HFD without butyrate treatment (n=2) for CD11c-MHCII, $CD11c^{+}$ and $MHCII^{+}$ cells (statistics made for multiple testing, *p<0,05).

Collectively butyrate supplementation caused a significant delay in tumor promotion and progression along with decreased tumor-associated anemia and inhibition of the K-ras and diet-associated down-regulation of the immune system. Furthermore it

ameliorated insulin sensitivity during HFD suggesting in addition to its anti-carcinogenic role also an anti-diabetogenic property.

4.15. Probiotics have partial beneficial effects on ViRas mice during HFD

Probiotics employ beneficial effects on health [134]. Indeed probiotic/prebiotic treatment is a common regimen for gastrointestinal diseases such as inflammatory bowel disease. As there was a shift in bacteria in the small intestine and colon and decreased fermentation end products as well as a protective effect of butyrate against tumor development, we observed the effect of probiotics in ViRas mice during HFD. Mice on probiotics did not show significant differences in weight gain between the genotypes, although ViRas mice seemed to gain less weight than their CO littermates (Figure 4.25 A). Further no difference in histology was observed when compared to ViRas mice fed on HFD alone (Figure 4.25 B). Mice continued to show TSA HGIEN however in the absence of invasive carcinoma (Figure 4.25 C) and displayed anemia (Figure 4.25 D).
During GTT ViRas mice treated with probiotics continued to show improved glucose tolerance and insulin sensitivity suggesting no beneficial effect of probiotics on metabolic parameters in ViRas mice (Figure 4.25 E,F).

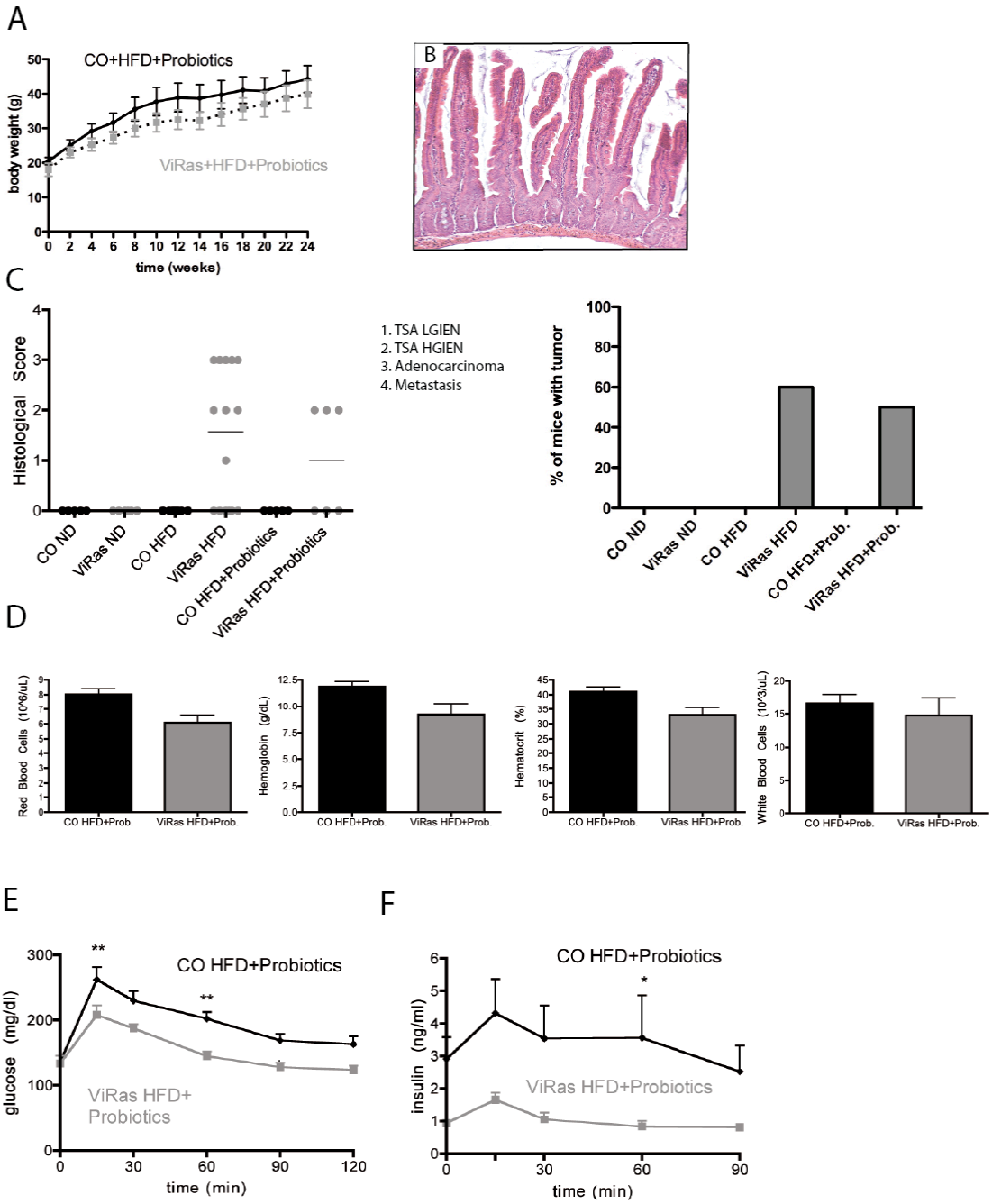

Figure 4.25: Probiotic treatment in ViRas mice protects against invasive cancer. A: Weight curve of CO (n=5) and ViRas (n=6) mice during 24 weeks on HFD plus probiotics. **B:** Representative picture of an H&E staining of the duodenum of a ViRas mouse after 24 weeks on HFD plus probiotics (10x magnification). **C:** Histological score of CO and ViRas mice after 22-24 weeks on ND or HFD with or without probiotics. **D:** Blood count of CO and ViRas mice after 16 weeks on HFD with probiotics (n=5). **E, F:** Glucose **(E)** and insulin **(F)** levels during GTT of CO and ViRas mice on HFD plus probiotics (n=5) (statistical analysis made for multiple testing, *p<0,05, **p<0,01).

Colonic stool samples were checked on selective agar plates (Figure 4.26 A). Following probiotic treatment, E.coli numbers were significantly increased in ViRas in comparison to CO mice. Although acetate and iso-valeric acid concentrations from

probiotic-treated mice were reduced as well as valeric acid levels increased in comparison to those on HFD alone (Figure 4.26 B) still the changes were comparable to that of HFD group without probiotic supplementation.

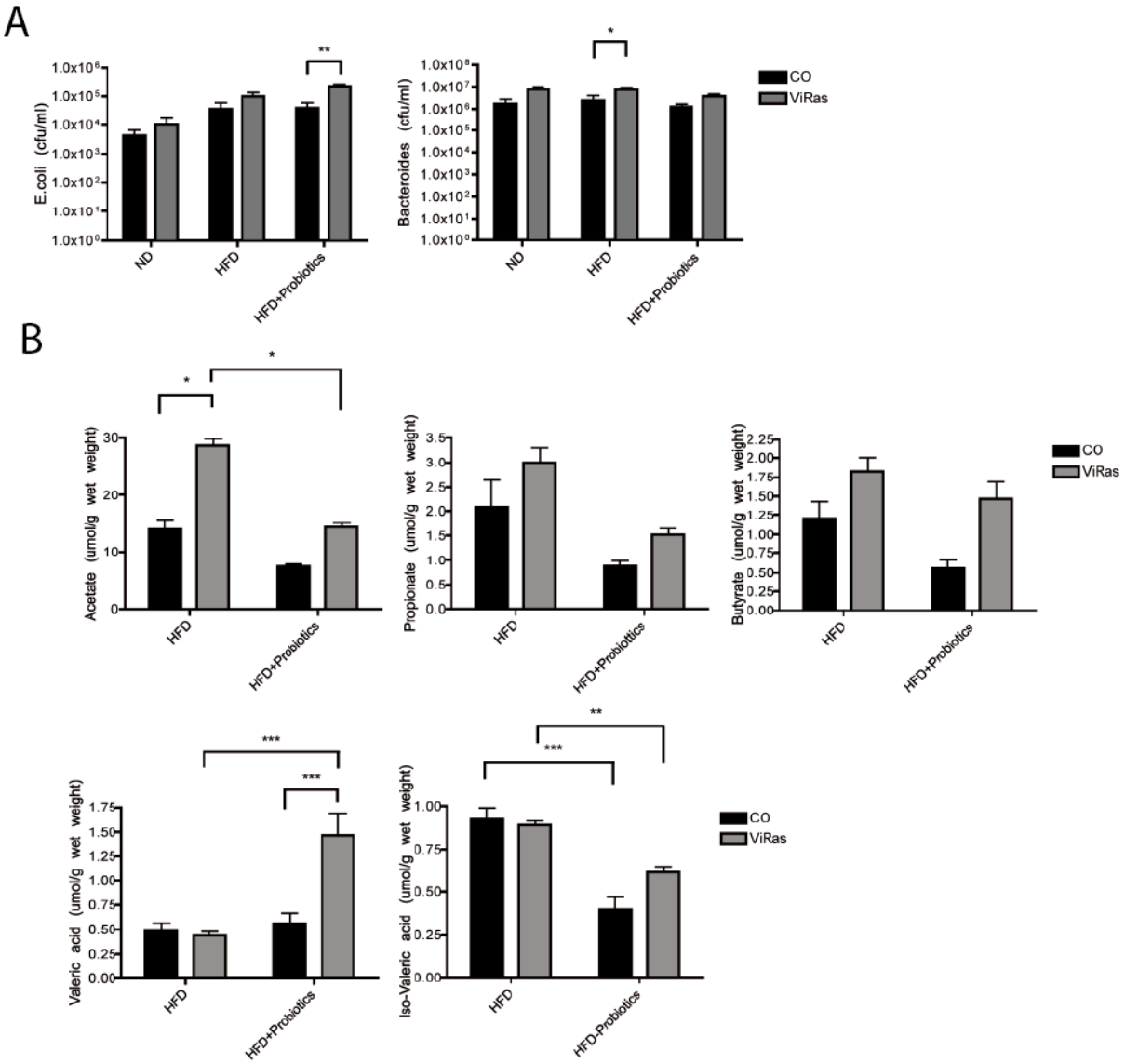

Figure 4.26: Bacterial counts and SCFA concentrations following probiotic treatment. A: Cfu of E.coli and Bacteroides in the colonic stool samples of mice after 20 weeks on ND (n=7), HFD (n=7) or HFD and probiotic treatment (n=16) (Statistics made with robust method, *p<0,05, **p<0,01). **B:** Amount of SCFA in the colonic stool samples of mice treated 16-22 weeks with HFD (CO: n=7, ViRas: n=11) or HFD plus probiotics (CO: n=5, ViRas: n=6) (statistical analysis made for multiple testing, *p<0,05, **p<0,01, ***p<0,001).

In summary, probiotic treatment did not provide fully beneficial effects as commonly believed but still provided a partial protection against invasive carcinoma in ViRas mice.

4.16. Treatment with arabinogalactan does not exert any beneficial effect in ViRas mice during HFD

Decreased fiber content of the diet is associated with increased tumor incidence [135, 136]. To exclude that tumor progression in ViRas mice was due to decreased fiber content of the HFD, mice were supplemented with arabinogalactan.

Arabinogalactan is a polysaccharide found in the cell walls of a variety of plants. It is an important source of dietary fiber and an essential part of the fermentation that result in the production of healthy compounds.

CO mice supplemented with arabinogalactan gained similar weight on HFD than the ViRas group (Figure 4.27 A). Interestingly mice continued to show invasive carcinoma (Figure 4.27 C) and associated anemia (Figure 4.27 D).

Colonic stool samples were analyzed on selective agar plates. Similarly, E.coli and Bacteroides counts were similar to HFD group alone (Figure 4.27 E). Collectively, the treatment with arabinogalactan did not impair tumor progression in ViRas mice on HFD suggesting that it is not the decreased fiber of the diet that increases tumor incidence in these animals.

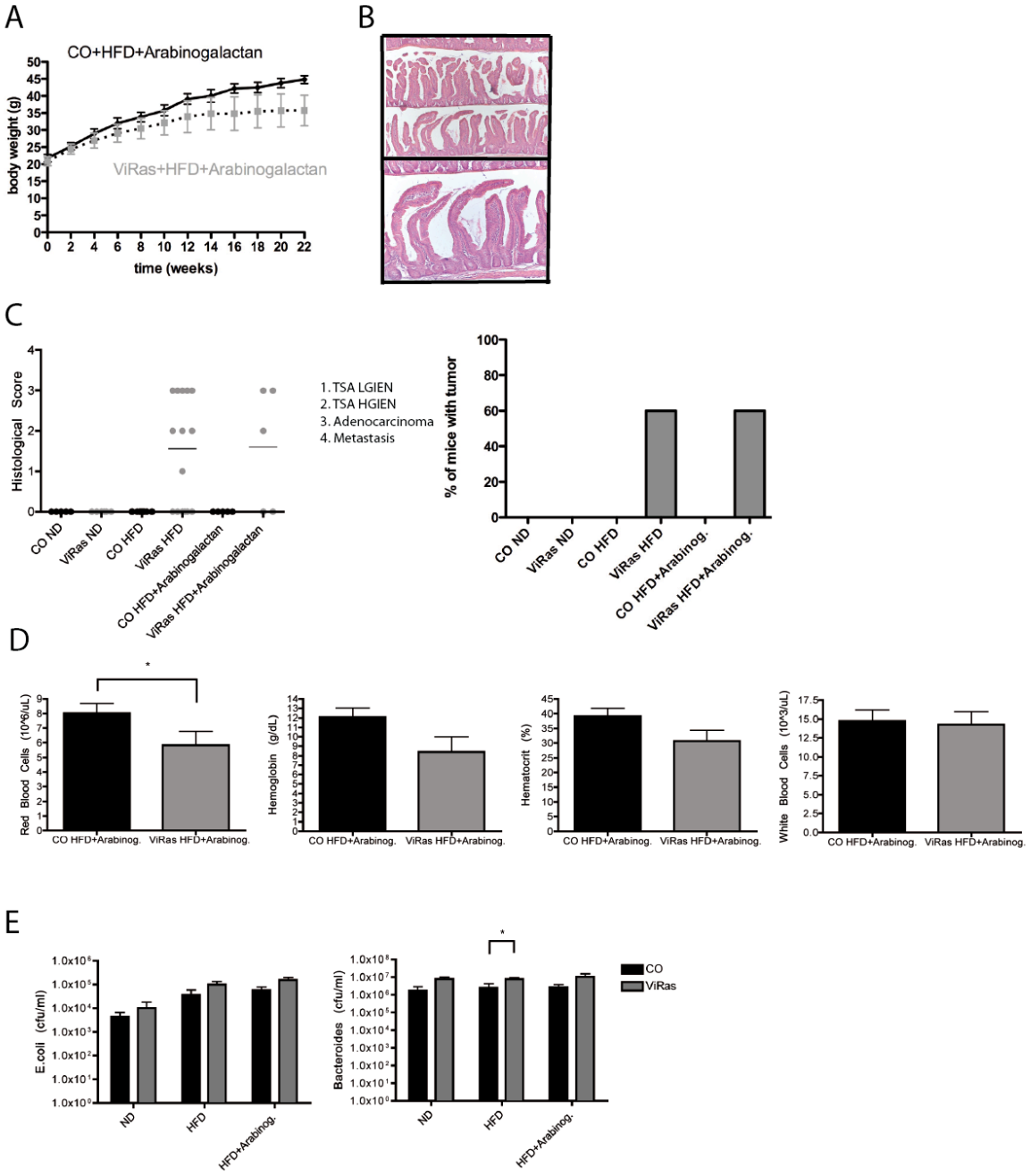

Figure 4.27: ViRas mice on HFD continue to show invasive carcinoma even though supplemented with arabinogalactan. A: Weight curves for CO and ViRas mice on HFD with arabinogalactan monitored over 22 weeks (n=5). **B:** Representative picture of the histology of the duodenum of ViRas mice on HFD with arabinogalactan (5x and 10x magnification). **C:** Histological score of the ND, HFD and HFD with arabinogalactan groups. **D:** Blood count of the mice after 16 weeks HFD with arabinogalactan (CO: n=4, ViRas: n=5, statistical analysis made with t-test, p-values adjusted for multiple testing, *p<0,05). **E:** Cfu of bacteria found in colonic stool samples of mice after 20 weeks on ND (n=7), HFD with (n=10) or without (n=7) arabinogalactan (statistical analysis made with robust method, *p<0,05).

4.17. Microbiota is directly involved in tumor progression

To prove the causal relationship between diet-induced changes in microbiota and intestinal cancer CO and ViRas mice on ND were colonized with fecal samples from HFD-fed ViRas donors. Remarkably, disease progression could be transmitted to otherwise healthy ViRas mice on ND but not to COs. These findings support that HFD-induced changes in bacterial community in the gut can cause tumor progression. Additionally, they provide further proof for a critical role of fat-diet shaped microbiota that cooperates with oncogenic kras activation during tumor progression in the small intestine yet independent of obesity.

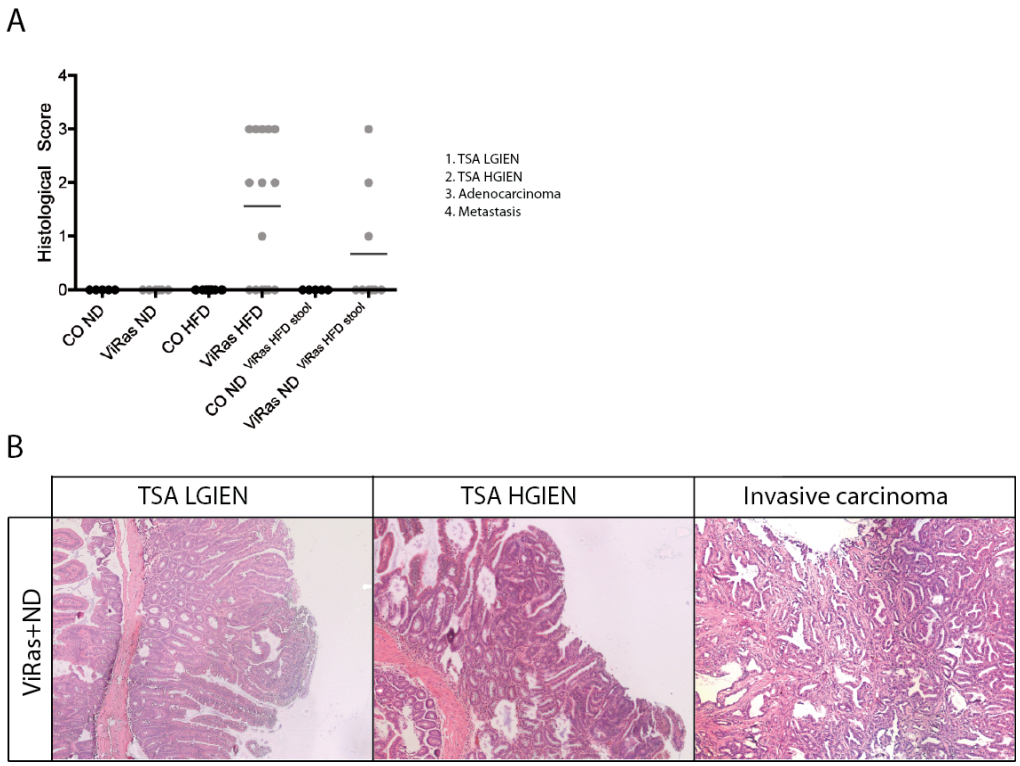

Figure 4.28: Invasive cancer can be transmitted to healthy ViRas mice on ND by microbiota transfer from HFD donors. A: Histological score of the ND (CO: n=5, ViRas: n=6), HFD (CO: n=13, ViRas: n=15) and ND transmitted with HFD microbiota (CO: n=5, ViRas: n=9) groups. **B:** H&E staining from 3 ViRas ND mice transmitted with HFD microbiota showing TSA LGIEN, TSA LGIEN as well as invasive carcinoma development (all 10x magnification).

5. Discussion

The incidence of obesity significantly increased by up to 30 % in the last 20 years. In the United States 1/3 of the population is classified as obese [137] and around 20 % in United Kingdom and Germany [138]. The state of obesity is a well-known risk factor not only for metabolic diseases such as diabetes, but also for cancer development as up to 20 % of all cancers have been attributed to obesity [18]. Obesity, overweight or physical inactivity accounts for 1/3 of the incidence for colorectal cancer although the mechanisms, how diet-induced obesity leads to the development of tumors remain still nebulous. In order to examine the mechanism that underlies diet-induced obesity-associated cancer development, the mice were treated with high fat diet (HFD) that consists 60 % of the calories from fat.

Colon cancer is one of the leading causes of death in the world and is mainly caused by mutations in proto-oncogenes or tumor-suppressor genes. One of the most common mutations in around 30 % of all cancer types and 50 % of intestinal cancer is in the K-ras oncogene [68]. Therefore oncogenic K-ras expression as a result of a selective mutation has been shown to serve as a mouse model for various types of cancer research. Conditional expression of oncogenic K-ras leads to enhanced proliferation [117]. As progression of uncontrolled cell growth is a certain way to initiate cell transformation but under normal conditions not sufficient for rapid growth, we chose this mouse model to examine the effect of diet-induced obesity and various treatments during cancer development. K-ras^{G12D} activation under the control of Villin-cre promoter (ViRas) gave us the possibility to examine the tumor growth in the intestine of the mice under different conditions. Oncogenic K-ras activation led to elongated intestine with serration and branching of the villi in the small intestine as well as in the crypts of the colon in mice.

Interestingly when fed on HFD mice developed next to anaemia invasive carcinoma in the small intestine, while no tumor development but only hyperplastic polyps were seen in the colon. Furthermore, when kept long enough on the fat-rich diet mice showed metastasis in pancreas, spleen and liver thereby providing a direct proof for a link between diet and tumorigenesis in the small intestine. In human, less than 3 % of the tumors in the digestive tract arise in the small bowel. Since cancer progression is restricted to small intestine in ViRas mice, one might question the relevance of this

model to human disease. However the current available genetic mouse models of colorectal cancer such as APC^{min} [139] or ß-catenin [140] mice all develop tumors in the small intestine as well. Whether the physiology and pathology of the mouse´s small intestine is comparable to human colonic disease remains to be answered. Still all these models have served in unravelling signalling nodes that so far had been instrumental in the diagnosis and therapy of colorectal cancer suggesting the use of such models to be crucial.

Obesity-induced insulin resistance has been closely associated with increased tumorigenesis. Interestingly ViRas mice on HFD kept lower glucose levels and remained insulin sensitive, meanwhile the control (CO) mice became hyperglycemic and highly insulin resistant. Although improved glucose clearance may be associated with decreased adiposity seen in these animals increased tumor incidence stands in contrast to what is commonly accepted. Our findings suggest high-fat diet can accelerate tumorigenesis in genetically susceptible mice yet independently of obesity.

Microbiota has a profound effect on host physiology. Recent evidence suggest altered composition of microbiota is associated to obesity [141]. Indeed germ-free mice were resistant to HFD-induced obesity [142] and the colonization with conventional mouse microbiota increased adiposity [86]. Recent studies implicate the composition of microbiota can predispose to the development of obesity through a switch towards growth of a distinct group of bacteria that are more efficient in harvesting nutrients [143]. Having said this we checked whether HFD employed any distinct changes in the composition of microbiota that could potentially be linked to the development of cancer in ViRas animals. In accordance with literature a clear decrease in Bacteroides and increase in Firmicutes was detected after high-fat feeding that was independent of K-ras activation. Although very little is known about the exact function of gut microbiota in terms of causing disease directly, the crosstalk between bacterial colonization and host during malignancy in the intestine is attracting more attention.

The small intestine is normally rarely colonized with low species richness in human and animals. Similar to colon mainly Bacteroides, Firmicutes and Proteobacteria are dominantly found in the small intestine. Interestingly however, an increase in Helicobacter and Escherichia/Shigella was observed in ViRas mice following HFD regimen. Escherichia/Shigella are gram-negative bacteria that harbour

lipopolysaccharides (LPS) in the membrane, an endotoxin that induces pro-inflammatory responses in the host that can further lead to septic shock. Helicobacter is known to be relevant in small intestinal diseases like chronic gastritis and it is known amongst others that it impairs the immune system by inhibiting the function of dendritic cells [144]. So far not much is known about the relationship between the state of obesity and the increase in Helicobacter in the small intestine [145], but it is clearly accepted that diet has a great impact on the bacteria in the intestine [146]. Whether microbial dysbiosis is a cause or a consequence of various diseases in the host is an ongoing debate. Interestingly HFD-induced dysbiosis in the small intestine of ViRas mice was closely associated to tumor progression in these animals. Our additional studies using prebiotic, probiotic, SCFA intervention as well as disruption of major signalling nodes that recognize bacteria or bacterial products implicate, that diet-induced distinct changes in microbiota may indeed be directly involved in disease progression.

First ViRas mice lacking MyD88 in the whole body were completely protected from the development of intestinal cancer. Furthermore this was associated with a shift in the bacterial community that showed a decrease in Helicobacter and Escherichia/Shigella in the small intestine. Indeed deleting MyD88 in hematopoietic cells or in the intestinal epithelial cells did not suffice to rescue the phenotype of ViRas mice as 50 % and 60 % of the mice continued to develop tumors in the small intestine, respectively. It seems that, despite the fact that there is a slight decrease of malignancy in $MyD88^{-/-}$ bone marrow transplanted mice the MyD88 deletion is required in more than one cell type in the intestine to get a complete rescue of cancer development. This indeed may be suggestive of the crosstalk between intestinal epithelium, the gut-associated lymphoid tissues and the microbiota during health and disease state of the host.

Second, although additional deletion of interleukin-1 receptor (IL-1R) or Toll-like receptors (TLRs) did not confer complete protection against tumor development, still they protected against the development of invasive cancer suggesting partial signals were conveyed through TLR-2, TLR-4 and IL-1R in ViRas mice.

Third, the shift in bacterial communities in the intestine of ViRas mice was further accompanied by a decrease in fermentation products like propionate, butyrate and acetate. Indeed supplementation with probiotics, the prebiotic arabinogalactan, the short chain fatty acid butyrate, that are all known to regulate microbiota, had diverse

effects on the tumor development in ViRas mice. Probiotics, well known as nutrient addition, have health promoting properties especially after the use of antibiotics. It has been shown that probiotics can be used as treatment against diseases as it can influence immune responses by regulating the function of immune cells [147]. Additional treatment of probiotics showed only partial beneficial effects as ViRas mice on HFD did not develop adenocarcinoma or metastasis but continued to show TSA HGIEN in the small intestine. On the contrary, no beneficial effects were seen using the prebiotic arabinogalactan supplementation in the ViRas mice during HFD. Arabinogalactan is a fibre that is not digested but fermented by commensal bacteria in the intestine, such as Lactobacilli and Bifidobacteria [148] that decrease significantly after HFD. The treatment with fibre results in increased growth of the "friendly" bacteria identifies it as a prebiotic [148, 149]. However no change in the tumor incidence was observed as ViRas mice on HFD supplemented with arabinogalactan continued to show TSA HGIEN and adenocarcinoma in 60 % of the cases. These results are suggestive of the fact that it is not the decreased fibre content of the HFD responsible for increased tumorigenesis in these mice. Moreover previous studies suggest arabinogalactan with significant increases in total faecal anaerobes and Lactobacillus spp. but with no other changes in pH or SCFA production [148]. Indeed the latter might be true since supplementation with a single SCFA, butyrate, conferred significant protection against tumor progression in ViRas mice. Butyrate has been previously shown that it has indeed immune-regulatory effects [78]. In cell culture experiments butyrate can inhibit proliferation and induce apoptosis [79]. In human colonic epithelial cells it was even observed that butyrate seems to have the ability to inhibit the activation of NF-$_k$B [80, 81]. Our findings demonstrate butyrate treatment significantly decreases tumor incidence in ViRas mice on HFD. Even the typical phenotype of the mice with K-ras activation in the intestine, that is the serration and branching in both small intestine and colon, was less apparent and only partially visible along the intestine in mice. Although the treatment did not show a distinct effect on the bacterial composition or the SCFA concentration in colonic stool of these mice however butyrate seems to have a crucial role during tumorigenesis in the small intestine.

Last but most important of all, the most direct proof that dysbiotic microbiota is associated with cancer progression, comes from our stool transplantation experiments. ViRas mice on ND did not show any tumors in the small intestine.

However only when these mice and control littermate animals were colonized with stool samples from ViRas donors that were on HFD, then the disease progression could be transmitted to healthy mutant mice. Interestingly the controls were free of tumors once again supporting the notion that diet-induced dysbiotic microbiota cooperated with oncogenic K-ras activation during tumor progression. Furthermore the tumors were similarly located in the small intestine indicating that distinct microbial shifts have a causal effect in inducing tumor development selectively in the small intestine but not in the colon.

The immune system plays an essential role in the development of cancer. On one hand it is known that inflammation with the release of certain pro-inflammatory cytokines, such as IL-6 and TNF-α, promotes the tumor growth [150]. On the other hand, the immune system is required for the recognition and elimination of tumor cells. We showed that K-ras activation dampens the immune system, which is further boosted after HFD feeding that could possibly explain the uncontrolled tumor growth in the small intestine. Especially MHC II were decreased in the ViRas mice, which are necessary for the recognition of antigens derived from pathogens and cancer cells. Indeed the activation of MHC II as well as MHC II on $CD11c^+$ dendritic cells were decreased in the LP of ViRas animals. Moreover further down-regulation of Fc receptors, T-cell specific GTPase and immunoglobulin chains as well as interferon related genes indicate not only a lack in the antigen-presentation but also a defect in the host immune response, thereby suggesting the immune system in these mice may remain refractory to recognize tumor cells and to fight against cancer.

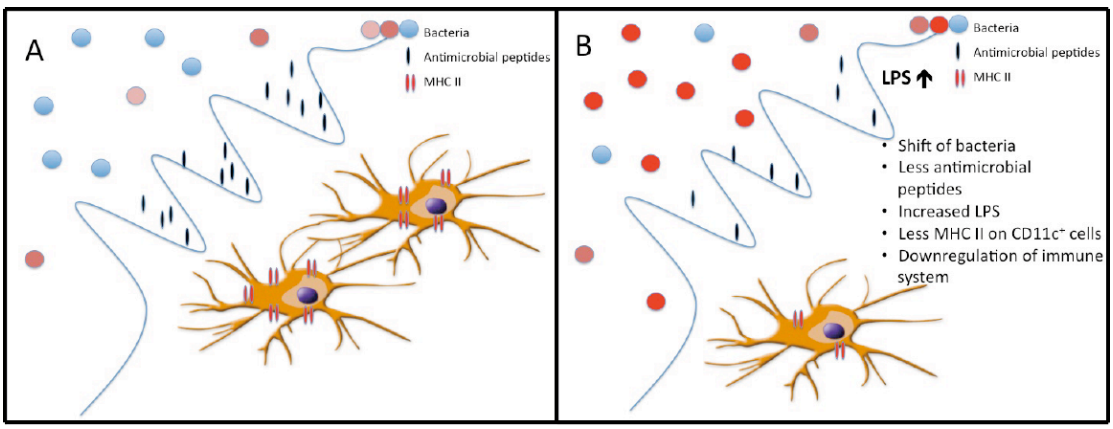

Figure 5.1: ViRas mice on HFD show changes in microbiota and immune system. Scheme of the situation in the intestine in normal mice (A) and ViRas mice on HFD (B). ViRas mice on HFD show a shift of microbiota and increased endotoxin

levels in the blood, decreased production of antimicrobial peptides as well as a decrease in MHC II on $CD11c^+$ dendritic cells.

It is still not known how tumor cells escape from immunity. Immune cells are continuously monitoring and eradicating modified cells thus representing an effective barrier against cancer cells and the formation of metastasis [17]. The prominence of the immune system has been shown in mice lacking parts of the immune system that develop tumors more rapidly and in a higher number than mice with intact immunity. Indeed immune cells in ViRas mice also seem to fail in detecting tumor cells in the intestine. Whether this is directly associated with the changes in microbiota is a relevant question. Since one of the major functions of microbiota is to help develop the lymphoid tissue in the gut, down-regulation of the host immune responses due to diet-shaped dysbiotic microbiota may possibly provide the working hypothesis. Indeed, partial increase in $CD11c^+$ dendritic cell recruitment in the LP or PP following butyrate supplementation and after MyD88 deletion stands in favour of this hypothesis.

It is still unclear how the immune system distinguishes between symbiotic and harmful bacteria. Pattern recognition receptors (PRRs) on antigen presenting immune cells, such as dendritic cells, can differ between pathogen-associated molecular patterns (PAMPs) of pathogenic bacteria and molecular patterns of commensal bacteria [151, 152]. The main PRRs, TLRs and Nucleotide-binding oligomerization domain-containing proteins (NODs) are recognizing bacterial components and they are assumed to be able to distinguish between the binding of microbe-associated molecular patterns (MAMPs) and PAMPs.

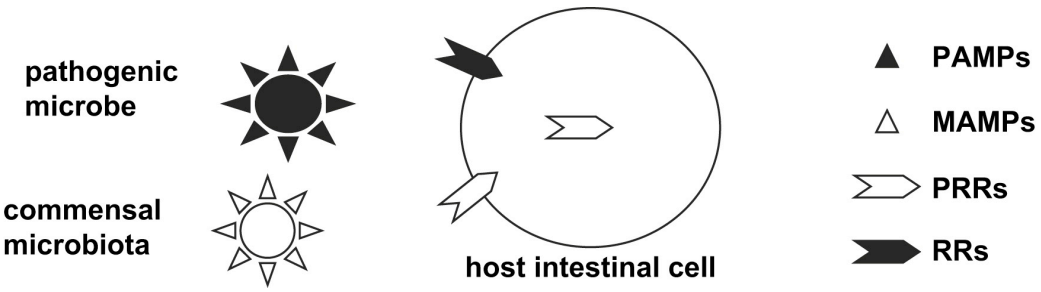

Figure 5.2: Pathogenic microbiota different patterns than symbiotic bacteria. Scheme showing the PAMPs of pathogenic bacteria and the MAMPs of commensal bacteria that are recognized mainly by transmembrane and cytoplasmic PPRs (TLRs and NODs). [152]

Potential hypothesis suggesting the PAMPs activate a pro-inflammatory immune response while commensals dampen the immune system could well be possible. It could well be that the epithelial cells could get refractory by the exposure to commensals. Alternatively commensals could be inducing other downstream signals then pathogens. Else PRRs could fail in the recognition of symbiotic bacteria through molecular changes in ligands of the bacteria [152].

Sansonetti et al. [153] disagreed with the hypothesis that PRRs recognize PAMPs, as symbiotic and pathogenic bacteria express extremely similar, if not identical prokaryote-specific motifs that are recognized. That makes it questionable how the PRRs are able to distinguish between PAMPs and MAMPs. Alternative hypothesis were that symbiotic bacteria express dedicated effectors that actively induce tolerance and that pathogenic microbes create, next to their sensing by PRRs, a particular level of stress that is perceived by the host as a danger signal [153].

Overall microbiota plays an enormous role in connection with obesity and intestinal cancer development. Indeed dysbiotic microbiota regulating immune functions is becoming increasingly recognized during immune-mediated diseases such as inflammatory bowel disease (IBD), rheumatoid arthritis, multiple sclerosis. Our study proposes another malignancy, cancer, that microbiota may play a causative role. It suggests diet-induced dysbiosis and active suppression of immune defence can be detrimental in the context of oncogenic K-ras activation. This indeed may have significant relevance to human disease and raise serious concerns for individuals with a family history of cancer. Whether altering gut microbiota through supplementation with probiotics, prebiotics or SCFAs could decrease tumor incidence in the intestine will be a major challenge that awaits to be answered.

6. Summary

Using a mouse model with oncogenic K-ras activation in the intestinal epithelial cells (ViRas mice) we could successfully demonstrate high fat feeding increased tumor incidence in mice. ViRas mice on a high fat diet (HFD) developed adenocarcinoma through the serrated route in the small intestine while no tumors, but only hyperplastic polyps were detected under normal diet (ND) condition.

We verified effectively that the tumor formation in ViRas mice under HFD regimen was associated with a distinct change in the microbiota and a down-regulation of the immune system in the gut. More precisely mice showed a shift in bacterial community favoring outgrowth of opportunistic pathogenic bacteria Helicobacter and Escherichia/Shigella especially in the small intestine.

We provided evidence that microbiota is directly involved in carcinogenesis as additional whole body knock out of MyD88 protected ViRas mice against tumor development. Indeed MyD88 deletion caused a shift in the bacterial composition in the small intestine of mice. However we could not detect one specific receptor that MyD88 dependent signals were conveyed, as the additional deletion of IL-1R, TLR-2 or TLR-4 did not confer protection against tumor promotion, although none of the mice developed adenocarcinoma. Moreover, deletion of MyD88 restricted to either hematopoietic cells or intestinal epithelial cells did not block tumor development, suggestive of a role for MyD88 signaling in multiple cell types together.

Further attempts in altering microbiota in favor of beneficial bacteria resulted in remarkable responses. Although prebiotic arabinogalactan supplementation did not affect tumor incidence, ViRas mice treated with probiotics continued to show adenoma formation however invasive carcinoma was completely blocked. Moreover, supplementation with a short chain fatty acid, butyrate, nearly completely conferred protection against tumorigenesis. Strikingly, transfer of stool samples from diseased donors to healthy ViRas mice was sufficient to enhance tumor progression in the absence of HFD, thereby suggesting a crucial role for dysbiotic microbiota in aggravating disease in the small intestine.

Although diet-induced low-grade inflammation has been recently shown in the context of diabetes and cancer and that inflammation has been widely accepted to play a significant role during intestinal tumorigenesis, pro-inflammatory cytokines

TNF-α and IL-6 were found to be slightly decreased in small intestine of ViRas mice after HFD. Moreover the recognition of antigens by the MHC II on dendritic cells as well as interferon related genes and the release of antimicrobial peptides were reduced in the small intestine of ViRas mice, which was further enhanced after high fat feeding.

Interestingly, after deletion of MyD88 or following butyrate treatment $CD11c^+$ dendritic cells recruitment was partially protected suggestive of a possible role of dysbiotic microbiota in down-regulation of host immune response. Collectively, these data implicate the interaction between host and environmental factors for the composition of microbiota that favors carcinogenesis and suggest tumor progression could be potentially transmitted in genetically predisposed individuals.

7. References

1. Boyle P, d'Onofrio A, Maisonneuve P, Severi G, Robertson C, Tubiana M, Veronesi U: **Measuring progress against cancer in Europe: has the 15% decline targeted for 2000 come about?** *Ann Oncol* 2003, **14**(8):1312-1325.
2. Ferlay J, Autier P, Boniol M, Heanue M, Colombet M, Boyle P: **Estimates of the cancer incidence and mortality in Europe in 2006**. *Ann Oncol* 2007, **18**(3):581-592.
3. Jemal A, Siegel R, Ward E, Hao Y, Xu J, Thun MJ: **Cancer statistics, 2009**. *CA Cancer J Clin* 2009, **59**(4):225-249.
4. Bilimoria KY, Bentrem DJ, Wayne JD, Ko CY, Bennett CL, Talamonti MS: **Small bowel cancer in the United States: changes in epidemiology, treatment, and survival over the last 20 years**. *Ann Surg* 2009, **249**(1):63-71.
5. Dabaja BS, Suki D, Pro B, Bonnen M, Ajani J: **Adenocarcinoma of the small bowel: presentation, prognostic factors, and outcome of 217 patients**. *Cancer* 2004, **101**(3):518-526.
6. Hatzaras I, Palesty JA, Abir F, Sullivan P, Kozol RA, Dudrick SJ, Longo WE: **Small-bowel tumors: epidemiologic and clinical characteristics of 1260 cases from the connecticut tumor registry**. *Arch Surg* 2007, **142**(3):229-235.
7. Neugut AI, Santos J: **The association between cancers of the small and large bowel**. *Cancer Epidemiol Biomarkers Prev* 1993, **2**(6):551-553.
8. Negri E, Bosetti C, La Vecchia C, Fioretti F, Conti E, Franceschi S: **Risk factors for adenocarcinoma of the small intestine**. *Int J Cancer* 1999, **82**(2):171-174.
9. Chow WH, Linet MS, McLaughlin JK, Hsing AW, Chien HT, Blot WJ: **Risk factors for small intestine cancer**. *Cancer Causes Control* 1993, **4**(2):163-169.
10. Gunter MJ, Leitzmann MF: **Obesity and colorectal cancer: epidemiology, mechanisms and candidate genes**. *J Nutr Biochem* 2006, **17**(3):145-156.
11. Balkwill F, Mantovani A: **Inflammation and cancer: back to Virchow?** *Lancet* 2001, **357**(9255):539-545.

12. Mantovani A, Allavena P, Sica A, Balkwill F: **Cancer-related inflammation**. *Nature* 2008, **454**(7203):436-444.
13. Federico A, Morgillo F, Tuccillo C, Ciardiello F, Loguercio C: **Chronic inflammation and oxidative stress in human carcinogenesis**. *Int J Cancer* 2007, **121**(11):2381-2386.
14. Hussain SP, Hofseth LJ, Harris CC: **Radical causes of cancer**. *Nat Rev Cancer* 2003, **3**(4):276-285.
15. Loftus EV, Jr.: **Clinical epidemiology of inflammatory bowel disease: Incidence, prevalence, and environmental influences**. *Gastroenterology* 2004, **126**(6):1504-1517.
16. Maloy KJ, Powrie F: **Intestinal homeostasis and its breakdown in inflammatory bowel disease**. *Nature* 2011, **474**(7351):298-306.
17. Hanahan D, Weinberg RA: **Hallmarks of cancer: the next generation**. *Cell* 2011, **144**(5):646-674.
18. Aggarwal BB, Vijayalekshmi RV, Sung B: **Targeting inflammatory pathways for prevention and therapy of cancer: short-term friend, long-term foe**. *Clin Cancer Res* 2009, **15**(2):425-430.
19. Moayyedi P: **The epidemiology of obesity and gastrointestinal and other diseases: an overview**. *Dig Dis Sci* 2008, **53**(9):2293-2299.
20. Jee SH, Kim HJ, Lee J: **Obesity, insulin resistance and cancer risk**. *Yonsei Med J* 2005, **46**(4):449-455.
21. Wild S, Roglic G, Green A, Sicree R, King H: **Global prevalence of diabetes: estimates for the year 2000 and projections for 2030**. *Diabetes Care* 2004, **27**(5):1047-1053.
22. King H, Aubert RE, Herman WH: **Global burden of diabetes, 1995-2025: prevalence, numerical estimates, and projections**. *Diabetes Care* 1998, **21**(9):1414-1431.
23. Das SK, Elbein SC: **The Genetic Basis of Type 2 Diabetes**. *Cellscience* 2006, **2**(4):100-131.
24. Kahn SE, Hull RL, Utzschneider KM: **Mechanisms linking obesity to insulin resistance and type 2 diabetes**. *Nature* 2006, **444**(7121):840-846.
25. Saini V: **Molecular mechanisms of insulin resistance in type 2 diabetes mellitus**. *World J Diabetes* 2010, **1**(3):68-75.

26. Roden M, Price TB, Perseghin G, Petersen KF, Rothman DL, Cline GW, Shulman GI: **Mechanism of free fatty acid-induced insulin resistance in humans**. *J Clin Invest* 1996, **97**(12):2859-2865.
27. Sundsten T, Ortsater H: **Proteomics in diabetes research**. *Mol Cell Endocrinol* 2009, **297**(1-2):93-103.
28. Taha C, Klip A: **The insulin signaling pathway**. *J Membr Biol* 1999, **169**(1):1-12.
29. Watson RT, Pessin JE: **Intracellular organization of insulin signaling and GLUT4 translocation**. *Recent Prog Horm Res* 2001, **56**:175-193.
30. Youngren JF: **Regulation of insulin receptor function**. *Cell Mol Life Sci* 2007, **64**(7-8):873-891.
31. Gregor MF, Hotamisligil GS: **Inflammatory mechanisms in obesity**. *Annu Rev Immunol* 2011, **29**:415-445.
32. Rocha VZ, Folco EJ: **Inflammatory concepts of obesity**. *Int J Inflam* 2011, **2011**:529061.
33. Tsatsanis C, Zacharioudaki V, Androulidaki A, Dermitzaki E, Charalampopoulos I, Minas V, Gravanis A, Margioris AN: **Adiponectin induces TNF-alpha and IL-6 in macrophages and promotes tolerance to itself and other pro-inflammatory stimuli**. *Biochem Biophys Res Commun* 2005, **335**(4):1254-1263.
34. Hummasti S, Hotamisligil GS: **Endoplasmic reticulum stress and inflammation in obesity and diabetes**. *Circ Res* 2010, **107**(5):579-591.
35. Sancho E, Batlle E, Clevers H: **Signaling pathways in intestinal development and cancer**. *Annu Rev Cell Dev Biol* 2004, **20**:695-723.
36. Elphick DA, Mahida YR: **Paneth cells: their role in innate immunity and inflammatory disease**. *Gut* 2005, **54**(12):1802-1809.
37. Mukherjee S, Vaishnava S, Hooper LV: **Multi-layered regulation of intestinal antimicrobial defense**. *Cell Mol Life Sci* 2008, **65**(19):3019-3027.
38. Hocker M, Wiedenmann B: **Molecular mechanisms of enteroendocrine differentiation**. *Ann N Y Acad Sci* 1998, **859**:160-174.
39. Vaishnava S, Behrendt CL, Ismail AS, Eckmann L, Hooper LV: **Paneth cells directly sense gut commensals and maintain homeostasis at the intestinal host-microbial interface**. *Proc Natl Acad Sci U S A* 2008, **105**(52):20858-20863.

40. Porter EM, Bevins CL, Ghosh D, Ganz T: **The multifaceted Paneth cell**. *Cell Mol Life Sci* 2002, **59**(1):156-170.
41. Brogden KA: **Antimicrobial peptides: pore formers or metabolic inhibitors in bacteria?** *Nat Rev Microbiol* 2005, **3**(3):238-250.
42. Biswas A, Petnicki-Ocwieja T, Kobayashi KS: **Nod2: a key regulator linking microbiota to intestinal mucosal immunity**. *J Mol Med (Berl)* 2011.
43. Delaunoit T, Neczyporenko F, Limburg PJ, Erlichman C: **Pathogenesis and risk factors of small bowel adenocarcinoma: a colorectal cancer sibling?** *Am J Gastroenterol* 2005, **100**(3):703-710.
44. Kennedy EP, Hamilton SR: **Genetics of colorectal cancer**. *Semin Surg Oncol* 1998, **15**(2):126-130.
45. Groden J, Thliveris A, Samowitz W, Carlson M, Gelbert L, Albertsen H, Joslyn G, Stevens J, Spirio L, Robertson M *et al*: **Identification and characterization of the familial adenomatous polyposis coli gene**. *Cell* 1991, **66**(3):589-600.
46. Powell SM, Zilz N, Beazer-Barclay Y, Bryan TM, Hamilton SR, Thibodeau SN, Vogelstein B, Kinzler KW: **APC mutations occur early during colorectal tumorigenesis**. *Nature* 1992, **359**(6392):235-237.
47. Su LK, Vogelstein B, Kinzler KW: **Association of the APC tumor suppressor protein with catenins**. *Science* 1993, **262**(5140):1734-1737.
48. de la Chapelle A, Peltomaki P: **Genetics of hereditary colon cancer**. *Annu Rev Genet* 1995, **29**:329-348.
49. Thompson E, Meldrum CJ, Crooks R, McPhillips M, Thomas L, Spigelman AD, Scott RJ: **Hereditary non-polyposis colorectal cancer and the role of hPMS2 and hEXO1 mutations**. *Clin Genet* 2004, **65**(3):215-225.
50. Papadopoulos N, Lindblom A: **Molecular basis of HNPCC: mutations of MMR genes**. *Hum Mutat* 1997, **10**(2):89-99.
51. Fearon ER, Vogelstein B: **A genetic model for colorectal tumorigenesis**. *Cell* 1990, **61**(5):759-767.
52. Vogelstein B, Fearon ER, Hamilton SR, Kern SE, Preisinger AC, Leppert M, Nakamura Y, White R, Smits AM, Bos JL: **Genetic alterations during colorectal-tumor development**. *N Engl J Med* 1988, **319**(9):525-532.
53. May P, May E: **Twenty years of p53 research: structural and functional aspects of the p53 protein**. *Oncogene* 1999, **18**(53):7621-7636.

54. Keino-Masu K, Masu M, Hinck L, Leonardo ED, Chan SS, Culotti JG, Tessier-Lavigne M: **Deleted in Colorectal Cancer (DCC) encodes a netrin receptor**. *Cell* 1996, **87**(2):175-185.
55. Knudson AG: **Two genetic hits (more or less) to cancer**. *Nat Rev Cancer* 2001, **1**(2):157-162.
56. Higuchi T, Sugihara K, Jass JR: **Demographic and pathological characteristics of serrated polyps of colorectum**. *Histopathology* 2005, **47**(1):32-40.
57. Snover DC, Jass JR, Fenoglio-Preiser C, Batts KP: **Serrated polyps of the large intestine: a morphologic and molecular review of an evolving concept**. *Am J Clin Pathol* 2005, **124**(3):380-391.
58. Kambara T, Simms LA, Whitehall VL, Spring KJ, Wynter CV, Walsh MD, Barker MA, Arnold S, McGivern A, Matsubara N *et al*: **BRAF mutation is associated with DNA methylation in serrated polyps and cancers of the colorectum**. *Gut* 2004, **53**(8):1137-1144.
59. Jass JR: **Serrated adenoma and colorectal cancer**. *J Pathol* 1999, **187**(5):499-502.
60. Snover DC: **Serrated polyps of the large intestine**. *Semin Diagn Pathol* 2005, **22**(4):301-308.
61. Fogt F, Rahemtulla A, Jian B: **Colonic serrated pathway lesions: Molecular and histologic changes in serrated colonic proliferations (Review)**. *Mol Med Report* 2008, **1**(1):21-26.
62. Ponz de Leon M, Di Gregorio C: **Pathology of colorectal cancer**. *Dig Liver Dis* 2001, **33**(4):372-388.
63. Li SC, Burgart L: **Histopathology of serrated adenoma, its variants, and differentiation from conventional adenomatous and hyperplastic polyps**. *Arch Pathol Lab Med* 2007, **131**(3):440-445.
64. Tanaka T: **Colorectal carcinogenesis: Review of human and experimental animal studies**. *J Carcinog* 2009, **8**:5.
65. Molina JR, Adjei AA: **The Ras/Raf/MAPK pathway**. *J Thorac Oncol* 2006, **1**(1):7-9.
66. Mitin N, Rossman KL, Der CJ: **Signaling interplay in Ras superfamily function**. *Curr Biol* 2005, **15**(14):R563-574.

67. Mor A, Philips MR: **Compartmentalized Ras/MAPK signaling**. *Annu Rev Immunol* 2006, **24**:771-800.

68. Schubbert S, Shannon K, Bollag G: **Hyperactive Ras in developmental disorders and cancer**. *Nat Rev Cancer* 2007, **7**(4):295-308.

69. Lowy DR, Willumsen BM: **Function and regulation of ras**. *Annu Rev Biochem* 1993, **62**:851-891.

70. Johnson L, Mercer K, Greenbaum D, Bronson RT, Crowley D, Tuveson DA, Jacks T: **Somatic activation of the K-ras oncogene causes early onset lung cancer in mice**. *Nature* 2001, **410**(6832):1111-1116.

71. Costello EK, Lauber CL, Hamady M, Fierer N, Gordon JI, Knight R: **Bacterial community variation in human body habitats across space and time**. *Science* 2009, **326**(5960):1694-1697.

72. Whitman WB, Coleman DC, Wiebe WJ: **Prokaryotes: the unseen majority**. *Proc Natl Acad Sci U S A* 1998, **95**(12):6578-6583.

73. **Structure, function and diversity of the healthy human microbiome**. *Nature* 2012, **486**(7402):207-214.

74. Yatsunenko T, Rey FE, Manary MJ, Trehan I, Dominguez-Bello MG, Contreras M, Magris M, Hidalgo G, Baldassano RN, Anokhin AP *et al*: **Human gut microbiome viewed across age and geography**. *Nature* 2012, **486**(7402):222-227.

75. Guarner F: **Enteric flora in health and disease**. *Digestion* 2006, **73 Suppl 1**:5-12.

76. Hooper LV, Midtvedt T, Gordon JI: **How host-microbial interactions shape the nutrient environment of the mammalian intestine**. *Annu Rev Nutr* 2002, **22**:283-307.

77. Wolin MJ: **Fermentation in the rumen and human large intestine**. *Science* 1981, **213**(4515):1463-1468.

78. Jass JR: **Diet, butyric acid and differentiation of gastrointestinal tract tumours**. *Med Hypotheses* 1985, **18**(2):113-118.

79. Comalada M, Bailon E, de Haro O, Lara-Villoslada F, Xaus J, Zarzuelo A, Galvez J: **The effects of short-chain fatty acids on colon epithelial proliferation and survival depend on the cellular phenotype**. *J Cancer Res Clin Oncol* 2006, **132**(8):487-497.

80. Inan MS, Rasoulpour RJ, Yin L, Hubbard AK, Rosenberg DW, Giardina C: **The luminal short-chain fatty acid butyrate modulates NF-kappaB activity in a human colonic epithelial cell line**. *Gastroenterology* 2000, **118**(4):724-734.

81. Canani RB, Costanzo MD, Leone L, Pedata M, Meli R, Calignano A: **Potential beneficial effects of butyrate in intestinal and extraintestinal diseases**. *World J Gastroenterol* 2011, **17**(12):1519-1528.

82. Corthesy B, Gaskins HR, Mercenier A: **Cross-talk between probiotic bacteria and the host immune system**. *J Nutr* 2007, **137**(3 Suppl 2):781S-790S.

83. Turnbaugh PJ, Hamady M, Yatsunenko T, Cantarel BL, Duncan A, Ley RE, Sogin ML, Jones WJ, Roe BA, Affourtit JP *et al*: **A core gut microbiome in obese and lean twins**. *Nature* 2009, **457**(7228):480-484.

84. Flint HJ, Duncan SH, Scott KP, Louis P: **Interactions and competition within the microbial community of the human colon: links between diet and health**. *Environ Microbiol* 2007, **9**(5):1101-1111.

85. Tsukumo DM, Carvalho BM, Carvalho-Filho MA, Saad MJ: **Translational research into gut microbiota: new horizons in obesity treatment**. *Arq Bras Endocrinol Metabol* 2009, **53**(2):139-144.

86. Turnbaugh PJ, Ley RE, Mahowald MA, Magrini V, Mardis ER, Gordon JI: **An obesity-associated gut microbiome with increased capacity for energy harvest**. *Nature* 2006, **444**(7122):1027-1031.

87. Cani PD, Amar J, Iglesias MA, Poggi M, Knauf C, Bastelica D, Neyrinck AM, Fava F, Tuohy KM, Chabo C *et al*: **Metabolic endotoxemia initiates obesity and insulin resistance**. *Diabetes* 2007, **56**(7):1761-1772.

88. Uemura N, Okamoto S, Yamamoto S, Matsumura N, Yamaguchi S, Yamakido M, Taniyama K, Sasaki N, Schlemper RJ: **Helicobacter pylori infection and the development of gastric cancer**. *N Engl J Med* 2001, **345**(11):784-789.

89. Wu S, Rhee KJ, Albesiano E, Rabizadeh S, Wu X, Yen HR, Huso DL, Brancati FL, Wick E, McAllister F *et al*: **A human colonic commensal promotes colon tumorigenesis via activation of T helper type 17 T cell responses**. *Nat Med* 2009, **15**(9):1016-1022.

90. Frank DN, St Amand AL, Feldman RA, Boedeker EC, Harpaz N, Pace NR: **Molecular-phylogenetic characterization of microbial community**

imbalances in human inflammatory bowel diseases. *Proc Natl Acad Sci U S A* 2007, **104**(34):13780-13785.

91. Sears CL, Pardoll DM: **Perspective: alpha-bugs, their microbial partners, and the link to colon cancer**. *J Infect Dis* 2011, **203**(3):306-311.
92. Wells JM, Rossi O, Meijerink M, van Baarlen P: **Epithelial crosstalk at the microbiota-mucosal interface**. *Proc Natl Acad Sci U S A* 2011, **108 Suppl 1**:4607-4614.
93. Ng SC, Kamm MA, Stagg AJ, Knight SC: **Intestinal dendritic cells: their role in bacterial recognition, lymphocyte homing, and intestinal inflammation**. *Inflamm Bowel Dis* 2010, **16**(10):1787-1807.
94. Fukata M, Abreu MT: **Role of Toll-like receptors in gastrointestinal malignancies**. *Oncogene* 2008, **27**(2):234-243.
95. Chen K, Huang J, Gong W, Iribarren P, Dunlop NM, Wang JM: **Toll-like receptors in inflammation, infection and cancer**. *Int Immunopharmacol* 2007, **7**(10):1271-1285.
96. Kawai T, Akira S: **TLR signaling**. *Semin Immunol* 2007, **19**(1):24-32.
97. MacKichan ML: **Toll bridge to immunity. Immune molecules hold promise for vaccine adjuvant discovery**. *IAVI Rep* 2005, **9**(4):1-5.
98. Bonizzi G, Karin M: **The two NF-kappaB activation pathways and their role in innate and adaptive immunity**. *Trends Immunol* 2004, **25**(6):280-288.
99. Ghosh S, May MJ, Kopp EB: **NF-kappa B and Rel proteins: evolutionarily conserved mediators of immune responses**. *Annu Rev Immunol* 1998, **16**:225-260.
100. Karin M, Greten FR: **NF-kappaB: linking inflammation and immunity to cancer development and progression**. *Nat Rev Immunol* 2005, **5**(10):749-759.
101. Luo JL, Kamata H, Karin M: **IKK/NF-kappaB signaling: balancing life and death--a new approach to cancer therapy**. *J Clin Invest* 2005, **115**(10):2625-2632.
102. Yuan M, Konstantopoulos N, Lee J, Hansen L, Li ZW, Karin M, Shoelson SE: **Reversal of obesity- and diet-induced insulin resistance with salicylates or targeted disruption of Ikkbeta**. *Science* 2001, **293**(5535):1673-1677.

103. Arkan MC, Hevener AL, Greten FR, Maeda S, Li ZW, Long JM, Wynshaw-Boris A, Poli G, Olefsky J, Karin M: **IKK-beta links inflammation to obesity-induced insulin resistance**. *Nat Med* 2005, **11**(2):191-198.

104. Xu H, Barnes GT, Yang Q, Tan G, Yang D, Chou CJ, Sole J, Nichols A, Ross JS, Tartaglia LA *et al*: **Chronic inflammation in fat plays a crucial role in the development of obesity-related insulin resistance**. *J Clin Invest* 2003, **112**(12):1821-1830.

105. Grivennikov SI, Greten FR, Karin M: **Immunity, inflammation, and cancer**. *Cell* 2010, **140**(6):883-899.

106. Karin M, Cao Y, Greten FR, Li ZW: **NF-kappaB in cancer: from innocent bystander to major culprit**. *Nat Rev Cancer* 2002, **2**(4):301-310.

107. Karin M: **NF-kappaB as a critical link between inflammation and cancer**. *Cold Spring Harb Perspect Biol* 2009, **1**(5):a000141.

108. Medzhitov R: **Recognition of microorganisms and activation of the immune response**. *Nature* 2007, **449**(7164):819-826.

109. Johansson C, Kelsall BL: **Phenotype and function of intestinal dendritic cells**. *Semin Immunol* 2005, **17**(4):284-294.

110. Macpherson AJ, Harris NL: **Interactions between commensal intestinal bacteria and the immune system**. *Nat Rev Immunol* 2004, **4**(6):478-485.

111. Madison BB, Dunbar L, Qiao XT, Braunstein K, Braunstein E, Gumucio DL: **Cis elements of the villin gene control expression in restricted domains of the vertical (crypt) and horizontal (duodenum, cecum) axes of the intestine**. *J Biol Chem* 2002, **277**(36):33275-33283.

112. Glaccum: **Phenotypic and functional characterization of mice that lack the type I receptor for IL-1**. *J Immunol* 1997, **159(7)**:3364-3371.

113. Hou B, Reizis B, DeFranco AL: **Toll-like receptors activate innate and adaptive immunity by using dendritic cell-intrinsic and -extrinsic mechanisms**. *Immunity* 2008, **29**(2):272-282.

114. Adachi: **Targeted Disruption of the MyD88 Gene Results in Loss of IL-1- and IL-18-Mediated Function**. *Immunity* 1998, **9**:143-150.

115. Hoshino: **Cutting Edge: Toll-Like Receptor 4 (TLR4)-Deficient Mice Are Hyporesponsive to Lipopolysaccharide: Evidence for TLR4 as the Lps Gene Product1**. *J Immunol* 1999, **162**:3749-3752.

116. Takeuchi: **Differential Roles of TLR2 and TLR4 in Recognition of Gram-Negative and Gram-Positive Bacterial Cell Wall Components**. *Immunity* 1999, **11**:443-451.

117. Tuveson DA: **Endogenous oncogenic K-ras(G12D) stimulates proliferation and widespread neoplastic and developmental defects.** *Cancer Cell* 2004, **5**:375-387.

118. Quince C, Lanzen A, Curtis TP, Davenport RJ, Hall N, Head IM, Read LF, Sloan WT: **Accurate determination of microbial diversity from 454 pyrosequencing data**. *Nat Methods* 2009, **6**(9):639-641.

119. Quince C, Lanzen A, Davenport RJ, Turnbaugh PJ: **Removing noise from pyrosequenced amplicons**. *BMC Bioinformatics* 2011, **12**:38.

120. Gentleman RC, Carey VJ, Bates DM, Bolstad B, Dettling M, Dudoit S, Ellis B, Gautier L, Ge Y, Gentry J *et al*: **Bioconductor: open software development for computational biology and bioinformatics**. *Genome Biol* 2004, **5**(10):R80.

121. Tusher VG, Tibshirani R, Chu G: **Significance analysis of microarrays applied to the ionizing radiation response**. *Proc Natl Acad Sci U S A* 2001, **98**(9):5116-5121.

122. Hothorn T, Bretz F, Westfall P: **Simultaneous inference in general parametric models**. *Biom J* 2008, **50**(3):346-363.

123. Bretz F, Hothorn, T., Westfall, P.: **Multiple Comparisons Using R**; 2010.

124. Maronna RA, Yohai, V.J.: **Robust regression with both continuous and categorical predictors**. *Journal of Statistical Planning and Inference* 2000, **89**:197-214.

125. Bennecke M, Kriegl L, Bajbouj M, Retzlaff K, Robine S, Jung A, Arkan MC, Kirchner T, Greten FR: **Ink4a/Arf and oncogene-induced senescence prevent tumor progression during alternative colorectal tumorigenesis**. *Cancer Cell* 2010, **18**(2):135-146.

126. Zhu P, Tan MJ, Huang RL, Tan CK, Chong HC, Pal M, Lam CR, Boukamp P, Pan JY, Tan SH *et al*: **Angiopoietin-like 4 protein elevates the prosurvival intracellular O2(-):H2O2 ratio and confers anoikis resistance to tumors**. *Cancer Cell* 2011, **19**(3):401-415.

127. Ley RE, Turnbaugh PJ, Klein S, Gordon JI: **Microbial ecology: human gut microbes associated with obesity**. *Nature* 2006, **444**(7122):1022-1023.

128. Zhang G, Ghosh S: **Molecular mechanisms of NF-kappaB activation induced by bacterial lipopolysaccharide through Toll-like receptors**. *J Endotoxin Res* 2000, **6**(6):453-457.

129. Janssens S, Beyaert R: **A universal role for MyD88 in TLR/IL-1R-mediated signaling**. *Trends Biochem Sci* 2002, **27**(9):474-482.

130. Tsukumo DM, Carvalho-Filho MA, Carvalheira JB, Prada PO, Hirabara SM, Schenka AA, Araujo EP, Vassallo J, Curi R, Velloso LA *et al*: **Loss-of-function mutation in Toll-like receptor 4 prevents diet-induced obesity and insulin resistance**. *Diabetes* 2007, **56**(8):1986-1998.

131. Vijay-Kumar M, Aitken JD, Carvalho FA, Ziegler TR, Gewirtz AT, Ganji V: **Loss of function mutation in toll-like receptor-4 does not offer protection against obesity and insulin resistance induced by a diet high in trans fat in mice**. *J Inflamm (Lond)* 2011, **8**(1):2.

132. Floch MH: **The effect of probiotics on host metabolism: the microbiota and fermentation**. *J Clin Gastroenterol* 2010, **44 Suppl 1**:S19-21.

133. Chen JS, Faller DV, Spanjaard RA: **Short-chain fatty acid inhibitors of histone deacetylases: promising anticancer therapeutics?** *Curr Cancer Drug Targets* 2003, **3**(3):219-236.

134. Quigley EM: **Gut microbiota and the role of probiotics in therapy**. *Curr Opin Pharmacol* 2011.

135. Bingham SA: **Epidemiology of dietary fibre and colorectal cancer: current status of the hypothesis**. *Nutr Health* 1985, **4**(1):17-23.

136. Qasim A, O'Morain C: **Primary prevention of colorectal cancer: are we closer to reality?** *Eur J Gastroenterol Hepatol* 2010, **22**(1):9-17.

137. McGuire S: **Shields M., Carroll M.D., Ogden C.L. adult obesity prevalence in Canada and the United States. NCHS data brief no. 56, Hyattsville, MD: National Center for Health Statistics, 2011**. *Adv Nutr* 2011, **2**(4):368-369.

138. Berghofer A, Pischon T, Reinhold T, Apovian CM, Sharma AM, Willich SN: **Obesity prevalence from a European perspective: a systematic review**. *BMC Public Health* 2008, **8**:200.

139. Hinoi T, Akyol A, Theisen BK, Ferguson DO, Greenson JK, Williams BO, Cho KR, Fearon ER: **Mouse model of colonic adenoma-carcinoma progression based on somatic Apc inactivation**. *Cancer Res* 2007, **67**(20):9721-9730.

140. Harada N, Tamai Y, Ishikawa T, Sauer B, Takaku K, Oshima M, Taketo MM: **Intestinal polyposis in mice with a dominant stable mutation of the beta-catenin gene**. *EMBO J* 1999, **18**(21):5931-5942.

141. Flint HJ: **Obesity and the gut microbiota**. *J Clin Gastroenterol* 2011, **45 Suppl**:S128-132.

142. Backhed F, Manchester JK, Semenkovich CF, Gordon JI: **Mechanisms underlying the resistance to diet-induced obesity in germ-free mice**. *Proc Natl Acad Sci U S A* 2007, **104**(3):979-984.

143. Ley RE, Backhed F, Turnbaugh P, Lozupone CA, Knight RD, Gordon JI: **Obesity alters gut microbial ecology**. *Proc Natl Acad Sci U S A* 2005, **102**(31):11070-11075.

144. Wang YH, Gorvel JP, Chu YT, Wu JJ, Lei HY: **Helicobacter pylori impairs murine dendritic cell responses to infection**. *PLoS One* 2010, **5**(5):e10844.

145. Ioannou GN, Weiss NS, Kearney DJ: **Is Helicobacter pylori seropositivity related to body mass index in the United States?** *Aliment Pharmacol Ther* 2005, **21**(6):765-772.

146. Hildebrandt MA, Hoffmann C, Sherrill-Mix SA, Keilbaugh SA, Hamady M, Chen YY, Knight R, Ahima RS, Bushman F, Wu GD: **High-fat diet determines the composition of the murine gut microbiome independently of obesity**. *Gastroenterology* 2009, **137**(5):1716-1724 e1711-1712.

147. Yan F, Polk DB: **Probiotics and immune health**. *Curr Opin Gastroenterol* 2011, **27**(6):496-501.

148. Robinson RR, Feirtag J, Slavin JL: **Effects of dietary arabinogalactan on gastrointestinal and blood parameters in healthy human subjects**. *J Am Coll Nutr* 2001, **20**(4):279-285.

149. Grieshop CM, Flickinger EA, Fahey GC, Jr.: **Oral administration of arabinogalactan affects immune status and fecal microbial populations in dogs**. *J Nutr* 2002, **132**(3):478-482.

150. Zamarron BF, Chen W: **Dual roles of immune cells and their factors in cancer development and progression**. *Int J Biol Sci* 2011, **7**(5):651-658.

151. Medzhitov R, Janeway CA, Jr.: **Innate immunity: the virtues of a nonclonal system of recognition**. *Cell* 1997, **91**(3):295-298.

152. Hsiao WW, Metz C, Singh DP, Roth J: **The microbes of the intestine: an introduction to their metabolic and signaling capabilities**. *Endocrinol Metab Clin North Am* 2008, **37**(4):857-871.

153. Sansonetti PJ: **To be or not to be a pathogen: that is the mucosally relevant question**. *Mucosal Immunol* 2011, **4**(1):8-14.

Danksagung

Ich möchte mich in erster Linie bei Frau Dr. Arkan für die exzellente und oft sehr zeitaufwendige Betreuung bedanken. Sie hat mich seit der Aufnahme in ihre Arbeitsgruppe sehr unterstützt sowohl was mein Erlernen von neuen Arbeitstechniken, als auch das Anreichern von Wissen angeht und sie war auch stets bei persönlichen Gesprächen eine große Hilfe. Mein weiterer Dank geht an Prof. Dr. Greten für die Kooperation und Unterstützung während der ganzen Zeit, ohne ihn wäre einiges Organisatorische nicht möglich gewesen. Ich bedanke mich bei Prof. Dr. Schemann für die externe Betreuung meiner Doktorarbeit, sowie bei Prof. Dr. Schmid für die Seminare und die Ausflüge der 2. Medizinischen Klinik. Auch bedanke ich mich bei der Deutschen Krebshilfe für die Finanzierung und das Ermöglichen meiner Doktorarbeit.

Ein besonderer Dank gilt allen Mitarbeitern des Labors für die guten zwischenmenschlichen Kontakte und die Unterstützung in allen Lebenslagen, vor allem natürlich meiner Arbeitsgruppe, Cigdem Atay, Franziska Romrig und Jessica Heringer. Vor allem auch danke ich Sarah Schwitalla und Paul Ziegler für die Zusammenarbeit bei Knochenmarkstransplantation und FACS.

Bei Andreas Böck möchte ich mich ganz herzlich für die große und zeitaufwendige Hilfe bei den statistischen Analysen bedanken.

Ich danke unseren Kooperationspartnern, im Klinikum rechts der Isar Dr. Reindl für die Hilfe und Unterstützung beim FACS und Frau da Costa für die Analyse des Microarray und die Zeit, die sie sich nahm, mir die Methode näher zu erklären. Prof. Dr. Kirchner und Dr. Kriegl von der Pathologie der LMU danke ich für die Analyse der vielen Histologien, Dr. Alpert im Deutschen Institut für Ernährungsforschung Potsdam-Rehbrücke für die Analyse der SCFA, sowie Prof. Dr. Polson vom Biotechnologischen Institut Delaware in den USA für die Analyse der Sequenzierung und die fruchtbare Zusammenarbeit.

Auch möchte ich den Tierpflegern danken, die mit viel Einsatz für das Wohl unserer Tiere gesorgt haben.

Zum Schluss bedanke ich mich ganz herzlich bei meiner Familie sowie meinen Freunden für die Unterstützung und Geduld, die sie zeitweise aufbringen mussten.